LOW AFFINITY, HIGH-AVIDITY LECTIN-CARBOHYDRATE INTERACTIONS:

STRUCTURE-FUNCTION STUDIES ON THE CORTICAL GRANULE LECTIN FROM

XENOPUS LAEVIS.

by

ALEXANDER STANDISH TRACY

Under the Direction of Dr. Michael Pierce

ABSTRACT

The *Xenopus laevis* cortical granule lectin, termed XL35, is an oligomeric, Ca^{2+}-dependent lectin that is exocytosed from the oocyte at fertilization and forms the permanent block to polyspermy by crosslinking its mucin-like ligand present in the jellycoat of *Xenopus* eggs. Structural characterization studies have been performed using dynamic light scattering and sedimentation equilibrium measurements, and the results suggest that XL35 as purified from oocytes consists of a homo-oligomer composed of 12 monomers. The region of the polypeptide responsible for the formation of oligomers most likely resides in a hydrophobic domain at the C-terminus of the lectin. SDS-PAGE analysis of denatured XL35 in the presence or absence of reducing agents indicates that XL35 oligomers are formed through a combination of hydrophobic contacts and intermolecular disulfide bonds. MALDI-TOF mass spectrometry analysis of reduced and carboxymethylated (RCM) XL35 treated with N-glycanase indicates that only a limited amount of secreted XL35 is processed by signal peptidase: the majority of XL35 is secreted as the full-length polypeptide. The limited processing of the XL35 putative signal sequence and the localization of XL35 in the cortical granules suggests that XL35 transits the intracellular regulated secretion pathway as it becomes packaged in the cortical granules. Molecular mass determinations before and after N-glycanase treatment suggest that at least 2 of the 3 potential N-linked glycosylation sites are utilized. Based on the chemical modification of selected amino acids, tryptophan and a carboxylic acid moiety appear to be involved in ligand binding. XL35 binds to a wide variety of galactose-terminating oligosaccharides and recognizes both the α- and β-anomers of galactose, although α-anomers are preferred. XL35 binds poorly or not at all to sugars other than galactose. The monovalent dissociation constants that XL35 exhibits for monovalent ligands were determined to be in the millimolar range, but XL35 creates a highly stable complex with multivalent ligands, both native and synthetic, that exhibits little, if any, dissociation, as assessed by surface plasmon resonance measurements.

The ability of XL35 to efficiently form the block to polyspermy is intimately linked to its intrinsically low monovalent affinity along with the high-avidity multivalent interactions that are a result of its oligomeric structure. XL35 has also shown Ca^{2+}-dependent binding to *Cryptococcus neoformans* and *Candida albicans*, and its localization to the epidermis in the *Xenopus* tailbud-stage embryos suggests that it may have a role in innate immunity.

INDEX WORDS: Ca^{2+}-dependent lectin, fertilization, *Xenopus laevis*, multivalent interaction, inhibition assay, surface plasmon resonance

LOW AFFINITY, HIGH-AVIDITY LECTIN-CARBOHYDRATE INTERACTIONS: STRUCTURE-FUNCTION STUDIES ON THE CORTICAL GRANULE LECTIN FROM *XENOPUS LAEVIS*

By

ALEXANDER STANDISH TRACY

B.S., The College of William and Mary, 1989

M.S., George Mason University, 1997

A Dissertation Submitted to the Graduate Faculty of The University of Georgia in Partial Fulfillment of the Requirements for the Degree

DOCTOR OF PHILOSOPHY

ATHENS, GEORGIA

2002

LOW AFFINITY, HIGH-AVIDITY LECTIN-CARBOHYDRATE INTERACTIONS: STRUCTURE-FUNCTION STUDIES ON THE CORTICAL GRANULE LECTIN FROM *XENOPUS LAEVIS*

by

ALEXANDER STANDISH TRACY

Approved:

Major Professor: Michael Pierce

Committee: Kojo Mensa-Wilmot
James Prestegard
J. David Puett
Robert Woods

Electronic Version Approved:

Gordhan L. Patel
Dean of the Graduate School
The University of Georgia
May 2002

DEDICATION

To my wife, who has always encouraged me as a scientist and has helped me to grow as a husband and father. To our children, who help us to rediscover the world that we thought we knew so well.

ACKNOWLEDGMENTS

I would like to thank Dr. Michael Pierce for many years of support and encouragment: he has acted both as a mentor and friend and I am very grateful for all of his contributions to my training. In addition, I would also like to thank my committee members for their insight and guidance as my project developed.

Thanks also to the members of the Pierce lab who have helped me in many ways during graduate career: Trisha Sheahan, Gerardo Alvarez-Manilla, Maria Kamar, Intaek Lee, and Jin-Kyu Lee.

TABLE OF CONTENTS

Page

ACKNOWLEDGMENTS v

LIST OF TABLES viii

LIST OF FIGURES ix

LIST OF ABBREVIATIONS xii

CHAPTER 1 – LITERATURE REVIEW 1

Introduction 1

Mannose Binding Protein 5

XL35 13

Jellycoat Protein (JCP) 21

Homologues of XL35 27

CHAPTER 2 – MATERIALS AND METHODS 30

Purification of XL35 30

SDS-PAGE Analyses 30

Dynamic Light Scatttering 31

Sedimentation Equilibrium Analysis 31

MALDI-TOF 32

Chemical Modification Studies 32

Preparation of JCP-Alkaline Phosphatase Conjugate - Thiolation of JCP 33

Preparation of JCP-Alkaline Phosphatase Conjugate - Derivatization of BAP 33

Biotinylation of XL35 34

ELISA Inhibition Assay 34
Capture Inhibition Assay..... 35
Saturation Binding Assays..... 35
Surface Plasmon Resonance (SPR) Analyses..... 36
Characterization of the Glycopolymers and JCP 37
Phenol-Sulfuric Assay..... 37
CHAPTER 3 - RESULTS..... 39
Structural Studies – Mechanism of XL35 Oligomerization..... 39
Structural Studies – Size of Oligomer as Determined by Sedimentation Equilibrium.. 42
Structural Studies – Size of Oligomer as Determined by Light Scattering..... 46
Studies on Monomer - Signal Sequence and Molecular Weight of XL35 Monomer.... 48
Ligand Binding Properties of XL35 - Residues involved in ligand binding 54
Ligand Binding – ELISA Assay Development and Characterization 56
CHAPTER 4 - DISCUSSION 80
Structure and Organization of XL35..... 80
XL35 Ligand Binding Properties..... 85
REFERENCES..... 94

LIST OF TABLES

TABLE 3-1: DYNAMIC LIGHT SCATTERING RESULTS FOR XL35 46

TABLE 3-2: INHIBITION DATA FOR MONOVALENT COMPOUNDS..... 61

TABLE 3-3: INHIBITION DATA FOR MULTIVALENT LIGANDS 64

TABLE 3-4 : DIFFERENCES IN APPARENT K_{OFF} AS A FUNCTION OF ASSOCIATION TIME 74

LIST OF FIGURES

FIGURE 1-1: STRUCTURAL ORGANIZATION OF SOME MEMBERS OF THE C-TYPE LECTIN SUPERFAMILY 4

FIGURE 1-2: THE ROLE OF MBP IN COMPLEMENT ACTIVATION..... 6

FIGURE 1-3: STRUCTURE OF MBP TRIMER..... 8

FIGURE 1-4: STRUCTURAL MOTIF FOR C-TYPE LECTINS..... 9

FIGURE 1-5: THE CORTICAL GRANULE REACTION AT VARIOUS TIME POINTS... 14

FIGURE 1-6: EXOCYTOSIS OF THE CORTICAL GRANULES: SCHEMATIC OF THE EVENTS FOLLOWING FERTILIZATION 17

FIGURE 1-7: FORMATION OF THE FERTILIZATION LAYER IN X. LAEVIS..... 18

FIGURE 1-8: BINDING OF XL35 TO SELECTED MICROBES..... 20

FIGURE 1-9: CUTAWAY DIAGRAM SHOWING AN EGG DURING FERTILIZATION .. 22

FIGURE 1-10: ELECTRON MICROGRAPH OF THE J_1 LAYER OF THE *XENOPUS* JELLYCOAT 23

FIGURE 1-11: OLIGOSACCHARIDES FROM THE JCP OF *X. LAEVIS*..... 25

FIGURE 3-1: PRIMARY SEQUENCE AND DOMAINS OF XL35..... 40

FIGURE 3-2: XL35 OLIGOMERIZES THROUGH A COMBINATION OF HYDROPHOBIC CONTACTS AND DISULFIDE BONDS..... 41

FIGURE 3-3: XL35 SUBJECTED TO A LIMITED ACID DIGEST IS NOT AN OLIGOMER 42

FIGURE 3-4: SEDIMENTATION EQUILIBRIUM ANALYSIS OF XL35..... 44

FIGURE 3-5: APPARENT MOLECULAR WEIGHT OF XL35 AT DIFFERENT CONCENTRATIONS..... 45

FIGURE 3-6: PREDICTED SIGNAL SEQUENCE FOR XL35 51
FIGURE 3-7: MALDI-TOF OF REDUCED AND CARBOXYMETHYLATED (RCM) XL35 52
FIGURE 3-8: MALDI OF RCM XL35 TREATED WITH N-GLYCANASE 53
FIGURE 3-9: A WIDE VARIETY OF CHEMICAL TREATMENTS DO NOT ELIMINATE XL35 BINDING 55
FIGURE 3-11: CHEMICAL TREATMENTS THAT MODIFY TRP OR ASP/GLU ELIMINATE BINDING ACTIVITY 56
FIGURE 3-12: EFFECT OF MELIBIOSE ON BINDING OF XL35 TO JCP 57
FIGURE 3-13: SATURATION BINDING CURVE USING JCP-BAP CONJUGATE 59
FIGURE 3-14: HOMOLOGOUS INHIBITION AND NEGATIVE CONTROLS 60
FIGURE 3-15: SYNTHETIC CORE FOR TRIMERIC CLUSTERS 63
FIGURE 3-16: POLYACRYLAMIDE BACKBONE USED FOR GLYCOPOLYMER 63
FIGURE 3-17: COMPARISON OF MONOVALENT AND MULTIVALENT LIGANDS FOR XL35 65
FIGURE 3-18: SENSORGRAM OF MONOVALENT LIGAND (LACTOSE) 67
FIGURE 3-19: OVERLAY OF SPR ANALYSES SHOWING THE EFFECT MULTIVALENCY HAS ON THE KINETICS OF THE INTERACTION 70
FIGURE 3-20: A SERIES OF KINETIC SENSORGRAMS USING MELIBIOSE POLYMER 72
FIGURE 3-21: EVALUATION OF MASS TRANSPORT AT LOW CONCENTRATIONS OF MELIBIOSE POLYMER 73
FIGURE 3-22: USING SPR TO ASSESS THE FORMATION OF A IRREVERSIBLE COMPLEX 73

FIGURE 3-23: EQUILIBRIUM SPR ANALYSIS USING MELIBIOSE GLYCOPOLYMER 77
FIGURE 3-24: SENSORGRAM OF INTERACTION BETWEEN XL35 AND SOLUBILIZED JCP 78

LIST OF ABBREVIATIONS

BAP	bacterial alkaline phosphatase
CRD	carbohydrate-recognition domain
DMSO	dimethyl sulfoxide
DTT	dithiothreitol
ECM	extracellular matrix
EDC	1-ethyl-3-(3-dimethylaminopropyl)-carbodiimide hydrochloride
HCS	hepes-buffered saline with 10 mM $CaCl_2$, pH 7.4
HNBB	2-hydroxy-5-nitrobenzyl bromide
HL-1	human lectin-1
HL-2	human lectin-2
HRP	horseradish peroxidase
JCP	jellycoat protein
JCP-BAP	jellycoat protein-bacterial alkaline phosphatase conjugate
JCP-SATA	jellycoat protein – S-acetylmercaptosuccinic anhydride (SATA) intermediate
MAC	membrane attack complex
MALDI-TOF	matrix-assisted laser desorption ionization-time of flight mass spectrometry
MBL	mannose-binding lectin (also mannose-binding protein)
MBP	mannose-binding protein (also mannose-binding lectin)
NHS	N-hydroxysuccinimide
NP40	nonidet P-40

PBS	phosphate-buffered saline
RCM	reduced and carboxymethylated
SATA	S-acetylmercaptosuccinic anhydride
SDS	sodium dodecyl sulfate
SDS-PAGE	sodium dodecyl sulfate-polyacrylamide gel electrophoresis
SMCC	succinimidyl 4-(N-maleimidomethyl)cyclohexane-1-carboxylate
SPR	surface plasmon resonance
TCS	tris-buffered saline with 10 mM $CaCl_2$, pH 7.4
TRE	trypsinized rabbit erythrocytes
XL35	*X. laevis* cortical granule lectin

CHAPTER 1 – LITERATURE REVIEW

Introduction

Although lectins were first isolated from plants over 100 years ago, the discovery of animal lectins is much more recent, with the first conclusive evidence coming from the work of Ashwell et al.[1-6] who discovered that the removal of sialic acids from secretory glycoproteins dramatically shortened their half-life in serum. Animal lectins have been found to perform a diverse set of functions, from the trafficking of leukocytes during their recirculation to the quality control of newly-synthesized secretory glycoproteins in the endoplasmic reticulum. Many of the structures of these lectins reflect their diverse function, although it is now generally accepted that most animal lectins can be categorized into several groups based on sequence homology or the presence of a particular structural motif. These include the C-type lectins, which are characterized by their requirement for calcium, S-type lectins that require a free thiol for activity, mannose-6-phosphate or P-type lectins, as well as the I-type lectins such as the Siglecs which share homology with the immunoglobulin superfamily.

S-type lectins, also known as galectins, are small, monomeric or divalent β-galactoside-binding proteins that do not require a divalent cation to bind their ligands but must be maintained in a reduced state in order to remain active. Although this absolute requirement for a reducing environment would suggest that galectins function solely in the cytosol, they have been shown to be secreted via a non-classical secretory mechanism and can remain active in the ECM provided they have access to high-affinity carbohydrate ligands[7-12]. Galectins bind with high affinity to polylactosamine-containing structures[13], and recent studies[14] have demonstrated a direct role

in cell adhesion for a sponge galectin that was found to crosslink sponge cells and an extracellular aggregation factor. Galectin-1 has also been shown to induce apoptosis in activated T-cells as well as T-cell leukemic cell lines[15, 16].

Lectins that recognize mannose-6-phosphate, also termed P-type lectins, are involved in the targeting of specific acid hydrolases to the lysosome, where these enzymes function to degrade cellular macromolecules. Fibroblasts derived from patients deficient in the GlcNAc-1-phosphotransferase capable of synthesizing the mannose-6-phosphate epitope contain large inclusion bodies filled with undegraded cellular waste[17-20]. Two distinct mannose-6-phosphate receptors have been identified that bind glycans containing mannose-6-phosphate epitopes in either a cation-dependent or independent fashion[21-30]. Both are capable of binding to glycans containing two mannose-6-phosphate epitopes with dissociation constants in the nanomolar range and typically function in the trans-Golgi network (TGN) or late endosome to divert lysosomal enzymes from the secretory pathway to the lysosome[31-35].

I-type lectins are similar to immunoglobulins in that they are type I transmembrane proteins that contain an amino-terminal variable (V) domain followed by a series of C2 repeats (V_1-$C2_n$) which serve to extend the CRD above the glycocalyx. This family includes lectins such as sialoadhesin, CD22, CD33, myelin associated glycoprotein (MAG) and the Schwann cell myelin protein. Sialoadhesin (Siglec-1) was identified as a receptor expressed on a subset of murine macrophages which mediated the sialic acid-dependent binding to sheep erythrocytes and although its K_D for α(2-3) sialyllactose is 0.5 mM, its apparent avidity for macrophages is increased, presumably through multivalency[36-45]. CD22 (Siglec-2) is expressed on B cells and has been shown to form a noncovalent dimer that can be chemically cross linked. In addition to its ability to form multimers, CD22 is known to be associated with the B cell immunoglobulin receptor complex and its cytoplasmic tail is phosphorylated upon immunoglobulin

receptor stimulation[46, 47]. Phosphorylated CD22 then recruits SHP, a protein typrosine phosphatase that down-regulates that signal mediated through the B cell receptor complex[48-50]. This hypothesis is supported by the finding that CD22 -/- mice exhibit aberrant B cell responses following stimulation through the B cell immunoglobulin receptor[51].

C-type, or Ca^{2+}-dependent, lectins were the first family of lectins identified based on a common structural motif and represent the most diverse lectin family both in terms of their structures and the ligands that they recognize[52-54]. The organization of several members of the C-type lectin superfamily is shown in Figure 1-1. As can be inferred from Figure 1-1, C-type lectins are involved in many biological processes, including endocytosis, innate immunity and leukocyte trafficking. The work in this dissertation will focus on XL35, an oligomeric lectin from the cortical granules of *Xenopus* oocytes and eggs that forms the permanent block to polyspermy and likely functions in the developing embryo. Although XL35 does not contain the specific Ca^{2+}-binding motif that defines the C-type lectin superfamily, it has been shown to be Ca^{2+}-dependent and appears to have structural similarities with members of the C-type lectins. A detailed description of mannose-binding protein (MBP), another member of the C-type lectin superfamily, will be presented as part of this review.

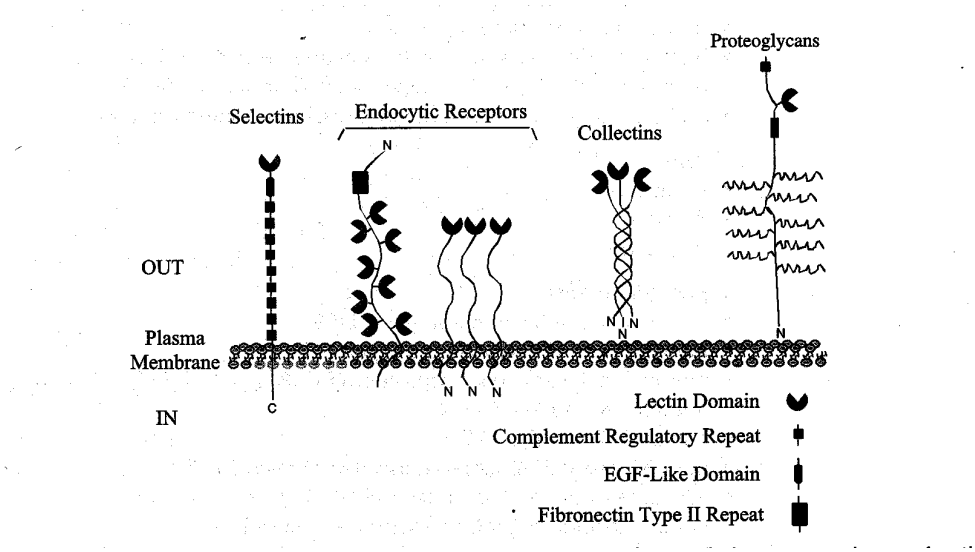

Figure 1-1: Structural Organization of Some Members of the C-type Lectin Superfamily

Organization of the carbohydrate recognition domain (CRD) for several members of the C-type lectin superfamily.

From [54]

The cDNA for XL35 was isolated in 1997 and recombinant XL35 was expressed in *E. coli* and found to be active by an agglutination assay. Southern blot analysis using a portion of the coding sequence showed the existence of a single band, which argued against the existence of multiple genes in *Xenopus*. Northern blot analysis was also performed using a portion of the sequence for XL35 and the XL35 mRNA was found to be highly expressed through gastrulation, confirming previous studies that had suggested XL35 has a role in development. Using the primary sequence for XL35, two human homologues were isolated from a human small intestine library that showed 60% identity to the XL35 sequence at the amino acid level and may have a role in innate immunity based on their tissue distribution, subcellular localization and binding specificity. Additional homologues have subsequently been identified in mouse and rat,[55, 56] suggesting that these lectins represent a novel family of lectins that require calcium but lack the traditional C-type lectin motif[57]. Because the primary sequence of

XL35 is very unique, and does not display significant homology to known proteins other than the putative lectins previously described, the experiments in this thesis focused on the structural and ligand-binding properties of XL35 that are important for its biological function. The structural model chosen for comparison to XL35 is that of the mannose binding protein (MBP), a C-type serum lectin that functions in pathogen surveillance by binding to the cell wall oligosacharides of pathogens and targeting them for destruction. A review of the biology and structure of MBP will be presented to highlight the similarities between MBP and XL35.

Mannose Binding Protein

Mannose binding protein (MBP) is a well-characterized serum lectin with homologues in many species[58-65], including man, that plays an important role in innate immunity. MBP binds to the surfaces of pathogens and can target them for destruction using either the lectin pathway of the complement system[66-68] or by directly mediating phagocytosis without the deposition of C3 and C4 fragments[69, 70]. MBP's role in complement activation is shown in detail in Figure 1-2. There are three pathways that converge to initiate assembly of the Membrane Attack Complex (MAC), which forms pores in the pathogen's membrane and results in the lysis of the target cell.

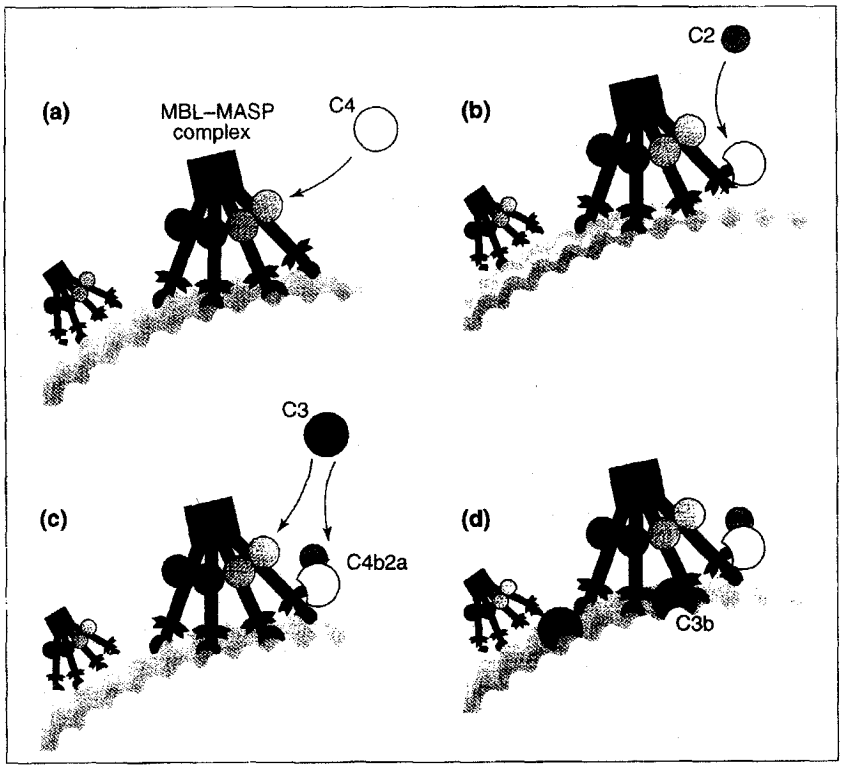

Figure 1-2: The Role of MBP in Complement Activation

The mannose-binding lectin (mannose-binding protein) pathway of complement activation. MBP circulates in serum as a complex with Mannose-Associated Serine Proteases (MASPs, grey spheres on stalk of MBP). (a) Binding to a microbial surface activates the MASPs and they, in turn, activate C4. (b) Activated C4 fragments bind to microbial surfaces or MBP complex and activate C2. (c) Activated C4/C2 complex (C4b2a, also known as C3 convertase) cleaves C3, which binds to nearby surface and recruits components for membrane attack complex (MAC) as well as receptors for phagocytosis.

From [71]

As is the case with many lectins, MBP is an oligomeric protein composed of identical 32 kDa polypeptides that initially associate through hydrophobic contacts to form trimers (also known as the “structural unit” of MBP); after formation of the structural unit the trimers form higher-order structures through disulfide bonds. The polypeptide for MBP can be organized into four structural domains: an N-terminal region responsible for interchain disulfide bonding, a neck region responsible for the initial association of the individual peptides, a collagenous domain, and a C-type lectin domain based on the motif identified by Drickamer[52, 58, 72, 73]. The ability of MBP to form trimers has been attributed to the collagenous domains of the MBP peptide, but several studies[74-76] have shown that the neck region is sufficient to form trimers through a triple α-helical coiled coil. These trimers, however, fail to activate complement,[75] suggesting that the collagenous region is necessary to activate the complement cascade.

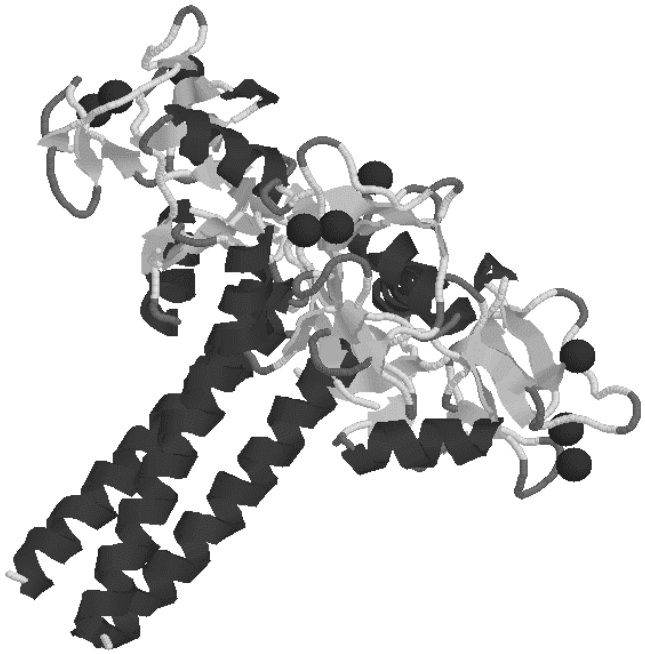

Figure 1-3: Structure of MBP Trimer

The crystal structure of the rat MBP-A trimer as determined by Weis et al.

From [73]

The amino acid sequence that defines C-type lectins is shown in Figure 1-4 and contains a number of highly conserved amino acids that need to be spaced appropriately, along with a combination of aliphatic and aromatic residues that are also conserved to form the full motif. The CRD of MBP is composed primarily of loops and extended structures, with the balance of the secondary structure in this region being short α-helices and β-strands[77]. The Ca^{2+} that is chelated by C-type lectins stabilizes local secondary structure which imparts protease resistance[78-85] and ensures that the CRD is folded correctly for ligand binding.

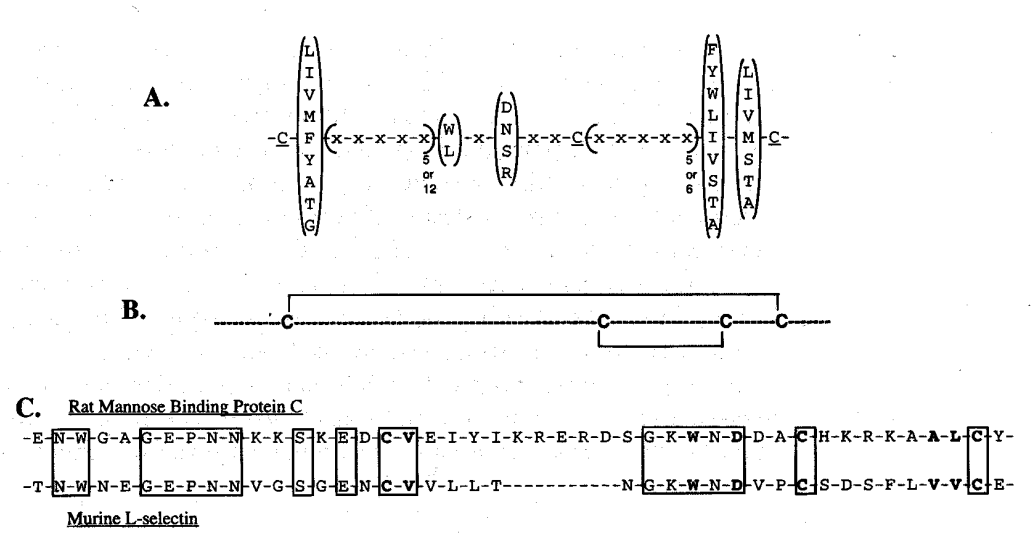

Figure 1-4: Structural Motif for C-type Lectins

A) The structural motif found in the CRD of C-type lectins. Invariant cysteine residues are underlined, conserved residues are in parentheses, and the spacing between residues is shown by the Xs in parentheses. B) Disulfide bonding within the same region for C-type lectins. C) An alignment of rat MBP and murine L-selectin. Identical residues are boxed and residues shown in boldface type are within the C-type lectin CRD.

From [57]

Ng et al.[86] crystallized native, one-ion, or apo-MBP and the resulting structures showed that, although the core of the CRD did not show substantial changes in the absence of Ca^{2+}, crystal structures of rat liver MBP lacking either one or both of the Ca^{2+} ions show large changes in the loop structures of the CRD that are directly involved in ligand binding. The relative rigidity of the CRD core was attributed to its stabilization through hydrophobic packing and disulfide bonds, but a critical proline was shown to undergo a transition from the cis to the trans-isomer as Ca^{2+} was removed. Even in structurally distinct proteins such as the legume lecins, Ca^{2+} has been shown to orient a critical acid-amide pair (Glu185 and Asn187 in MBP) within the protein binding site so the side chains from those residues will be correctly oriented to bind ligand[87]. In C-type lectins such as MBP, the role of Ca^{2+} appears to be even more critical: in the crystal

structure of MBP complexed with an oligosaccharide,[73] the Ca^{2+} in site 2 was shown to directly chelate the ligand via the C3 and 4 hydroxyl groups and actually orients the sugar within the binding site. The complex formed by C-type lectins and their ligands, therefore, should actually be considered a ternary complex where the Ca^{2+} serves as a bridge between an acid/amide pair on the protein and vicinal hydroxyls in the sugar ligand. The orientation of a hydrophobic group (His^{189} in MBP), along with the constraints imposed upon the sugar ligand by the Ca^{2+}-protein complex, provides the specificity that permits C-type lectins to discriminate between monosaccharides that may differ only in the arrangement around a single chiral carbon.

The pattern of hydrogen bonding between the protein and hydroxyl groups on the ligand is thought to give lectins their specificity and ability to discriminate between different carbohydrates. [88] A very common hydrogen-bonding pattern involves an acid-amide pair from the protein complexing to an individual hydroxyl in the following fashion: (N-H)n$\rightarrow$O-H$\rightarrow$O=C. The amide functionality is usually provided by a main-chain amide or an Asn or Gln while the acceptor is generally an acidic side chain. Although oligosaccharides are very polar and highly solvated in comparison to typical small-molecule ligands, there is usually at least one nonpolar region in the sugar based on the distribution of axial and equatorial hydroxyl groups around the ring. For galactose, this region is fairly extensive due to the axial arrangement of the C4 hydroxyl that results in an apolar region extending from C3 through C6. The biological consequence of this physical phenomena is seen in all of the (known) crystal structures of galactose-binding lectins, each of which contains an aromatic amino acid in the ligand binding site which packs against the apolar face of the galactose[89]. The apolar region of mannose is less extensive, and although MBP contains His^{189} that makes Van der Waals contacts with mannose, crystal structures of MBP co-crystallized with its ligand show that those contacts are more limited[73].

The structural elements in the CRD that give MBP its specificity were directly examined using site-directed mutagenesis to determine the selectivity and specificity of the mutants[90, 91]. By substituting Gln for Glu^{185} and Asp for Asn^{187}, a weak preference for galactose was established in a mutant form of rat MBP-A which was then enhanced through the substitution of Trp for His^{189}. The resulting mutant exhibited galactose-binding affinity similar to the rat asiologlycoprotein receptor but the specificity was poor; therefore a glycine-rich loop was introduced that resulted in an MBP mutant which exhibited affinity and specificity for galactose-terminating oligosaccharides that were comparable to galactose-binding lectins. Structural studies[92] with the MBP mutants confirmed that the glycine-rich loop served to hold Trp^{189} (His in wild-type MBP) in a configuration that would prevent mannose from binding through a steric effect.

Although native MBP does not bind to structures terminating in galactose, it has a fairly broad specificity for a lectin and can bind N-acetylglucosamine, fucose and mannose. This promiscuity gives MBP the capability to bind to a large variety of human pathogens, but since it binds free sugars with millimolar dissociation constants, it is unlikely that glycoproteins can be bound avidly because the interaction is usually not multivalent and would not possess the correct geometry for high avidity binding. When those carbohydrates are presented multivalently, however, as is the case for the cell walls of many pathogens, binding constants as high as 10^{-9} M have been reported[93]. In this way, multivalency and ligand presentation act as important molecular determinants that prevent the non-specific activation of complement that would be directed against endogenous glycoproteins.

The “neck” region of MBP is sufficient to form the trimeric structural unit that subsequently associates into higher-order structures via cysteines in the N-terminus[74, 94]. The α-helical region has a typical heptad repeat where hydrophobic residues occupy positions *a* and *d*, but additional interactions were observed between

hydrophobic residues found on the outside of the α-helical bundle and on the CRD. Interestingly, although truncated forms of both the rat and human forms of serum MBP could bind to the surface of mannose-rich cells and were capable of forming trimers, these truncation mutants were unable to fix complement. These data suggest that the higher-order oligomers formed through the collagenous domains are essential for complement activation[75, 76].

Although levels of MBP present in serum can vary widely, several studies[95, 96] noted an association between abnormally low levels of MBP in children and severe recurring infections or diarrhea in a condition that had been previously described as “failure to thrive”[97-100]. There are three point mutations within the collagenous domain that have been associated[101-103] with low serum levels of MBP and result in the following amino acid changes: R52C, G54D and G57Q. There appear to be two physiological effects of these mutations, the first being an impaired rate of secretion of the mutant forms of MBP while the second relates to the inability of the smaller mutant forms of MBP to fix complement. Using the rat MBP-A as a model system, Heise et al.[104] re-created several of the common human mutations in the collagenous domain and studied the rate of secretion using a series of pulse-chase experiments. The R→C mutant exhibited nearly normal secretion rates, but the additional Cys resulted in non-native disulfide bonds that limited the assembly of higher-order oligomers[105]. Two of the G→D mutants, however, showed a rate of secretion that was reduced by more than 5-fold. Additionally, several Lys residues in the collagenous domain that were shown to be either hydroxylated or glycosylated were also mutated. Although individual mutations to these residues did not show an effect in either secretion or oligomerization state, the double mutants showed a rate of secretion that was 3-fold slower than wild-type and could not form oligomers containing greater than 6 CRDs. Several studies have

confirmed that mutants of both the human[106, 107] and rat[75, 76] mannose-binding proteins are unable to fix complement. Lipscombe et al.[108] showed that the frequency of the genetic defect was approximately 5-7% in otherwise healthy populations. More recent studies have shown that several novel serine proteases called MBP-associated serine proteases (MASPs) associate with MBP through its collagenous domain, and these proteases are responsible for initiating the lectin-mediated pathway of complement activation[109].

Taken together, the structural and clinical studies on MBP offer insights into the structural elements of the MBP polypeptide required for proper biological function. Ligand binding, although promiscuous and weak, is mediated through a specific series of hydrogen bonds and hydrophobic contacts that are stabilized in part through the chelation of a divalent cation. As is the case with many lectins, there are separate domains responsible for carbohydrate binding activity and for oligomerization. Mutations in the oligomerization domain have demonstrated the role of multivalency in transforming a weak monovalent interaction into a highly stable multivalent interaction with an apparent dissociation constant in the nanomolar range. Although MBP and innate immunity appear to be very removed from XL35 and the formation of the fertilization layer, the body of literature surrounding MBP has provided direction to identify the regions of XL35 responsible for its monovalent specificity and affinity as well as the basis for its multivalent avidity.

XL35

All organisms that undergo sexual reproduction invest a substantial amount of energy to ensure that each egg is fertilized by a single sperm. There are several systems in place to prevent polyspermy, since embryos fertilized by multiple sperm either die or show serious developmental abnormalities. The first block to polyspermy is

a transient membrane depolarization that typically occurs within 1-3 seconds of the binding of the first sperm and lasts approximately a minute. Subsequent sperm cannot fuse with the plasma membrane of the egg; this temporarily prevents polyspermy until the cortical granule reaction can occur. In addition to the membrane depolarization that occurs following fertilization, the fertilization event also results in the release of Ca^{2+} from the endoplasmic reticulum, which increases in the concentration of intracellular Ca^{2+} 3-fold. The released Ca^{2+} travels around the surface of the egg at a rate of approximately 10 μm/sec[110] and triggers the cortical granule reaction which results in the formation of the permanent block to polyspermy.

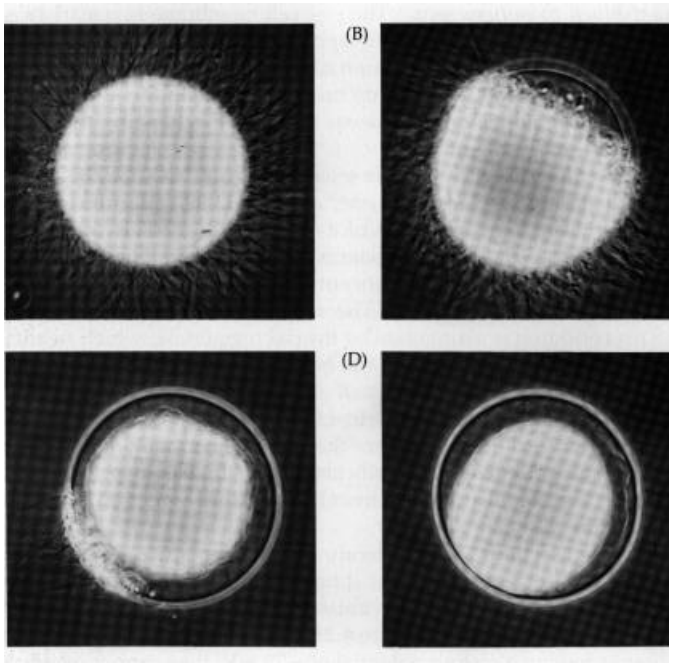

Figure 1-5: The Cortical Granule Reaction at Various Time Points

From [111]

The cortical granule reaction is a permanent remodeling of the surface of the newly fertilized egg and its extracellular matrix to make the egg refractory to supernumerary sperm that may have the potential to fuse with the plasma membrane. In response to the rise in intracellular Ca^{2+} that accompanies fertilization, the cortical

granules exocytose their contents into the perivitelline space[112, 113], and once XL35 is released into the jellycoat, the lectin cross-links its ligand, a high molecular mass mucin that is found in the J_1 layer of jellycoat. This forms the F, or fertilization layer that can be seen as an electron dense layer in the newly fertilized egg by electron microscopy. The fertilization layer blocks additional sperm from fertilizing the egg but also prevents cortical granule macromolecules from escaping: the build up of these macromolecules results in a increase in osmotic pressure within the perivitilline space that causes the raising of the fertilization layer[114]. XL35 represents approximately 77% of the total protein in the cortical granules[115] and the additional proteins include proteases and glycosidases[116-118] presumably involved in the modification of the surface of the fertilized egg.

XL35 was purified and characterized by the Hedrick and Barondes laboratories[115, 119] and was described as an homo-oligomeric glycoprotein of approximately 500 kDa composed of 43-45 kDa monomers. Hemagglutination studies using XL35 showed that agglutination of trypsinized rabbit erythrocytes could be inhibited using millimolar concentrations of EDTA or α- or β-galactosides, suggesting that XL35 was a lectin that recognized oligosaccharides terminating in galactose and that it required a divalent cation for activity. Radioiodinated XL35 that had been cross-linked using gluteraldehyde gave a characteristic ladder pattern and based on the relative migration the highest molecular-weight band [120] it was estimated that XL35 is composed of 10-12 similar or identical subunits. Treatment of the denatured protein with N-glycanase efficiently removed the carbohydrate and eliminated the heterogeneity typically observed by reducing SDS-PAGE, which suggests that XL35 contains only N-linked oligosaccharides.

In addition to its known function in preventing polyspermy, several lines of evidence suggest that XL35 may have a function during zygotic development as well.

Immunohistochemical studies of developing *Xenopus* embryos localized XL35 to the cleavage furrows of the blastula[121] and to the neural fold in stage 15 embryos[122], suggesting that it has an active role in cell migration or in the formation of the embryonic extracellular matrix. Northern blot analysis[123] of total RNA from oocytes or embryos at various stages strongly suggests that XL35 has a role in development since XL35 is highly expressed during gastrulation, a time when many embryonic genes that regulate cell migration and differentiation are expressed.

Prior to fertilization: the microvilli are intact and the cortical granules have not been activated.

Immediately following fertilization: the cortical granules begin to fuse with the plasma membrane.

Formation of the fertilization layer: causes a difference in osmotic pressure (raising of the fertilization envelope).

Completion of the fertilization layer: excess sperm have been released.

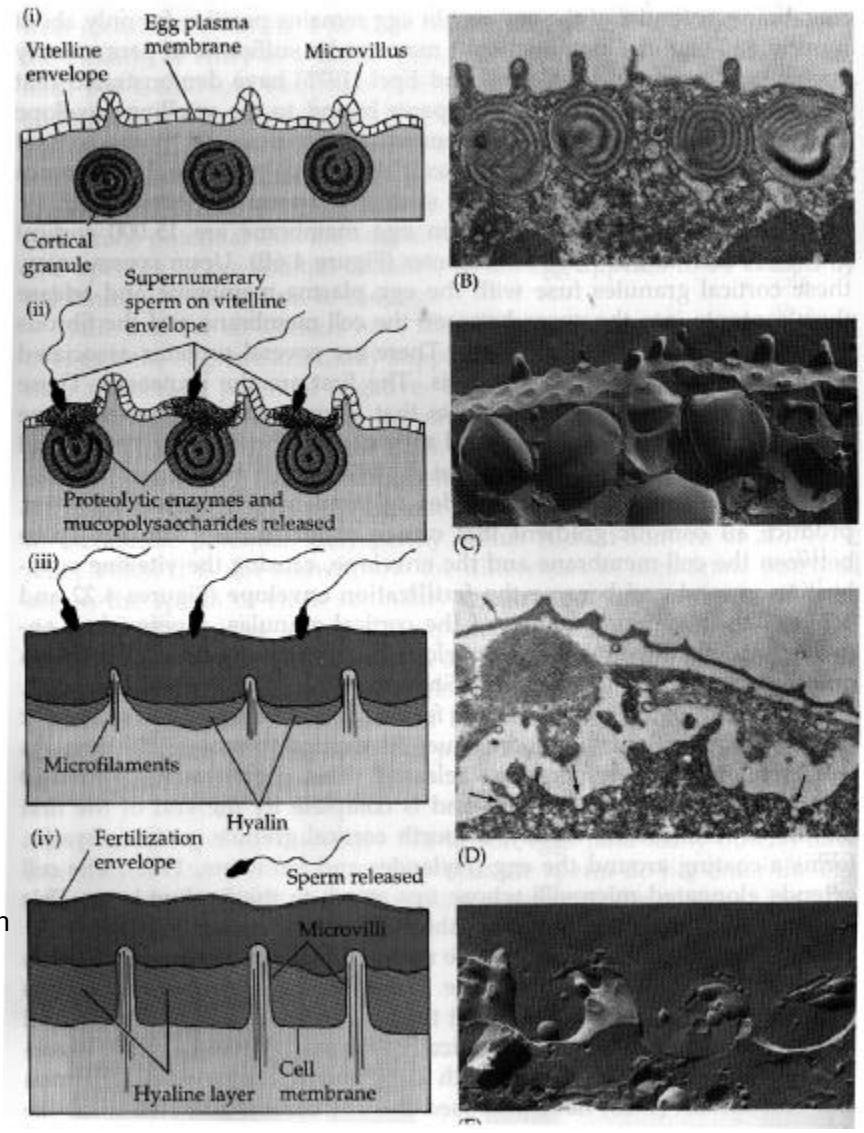

Figure 1-6: Exocytosis of the Cortical Granules: Schematic of the events following fertilization

From [124] From [125]

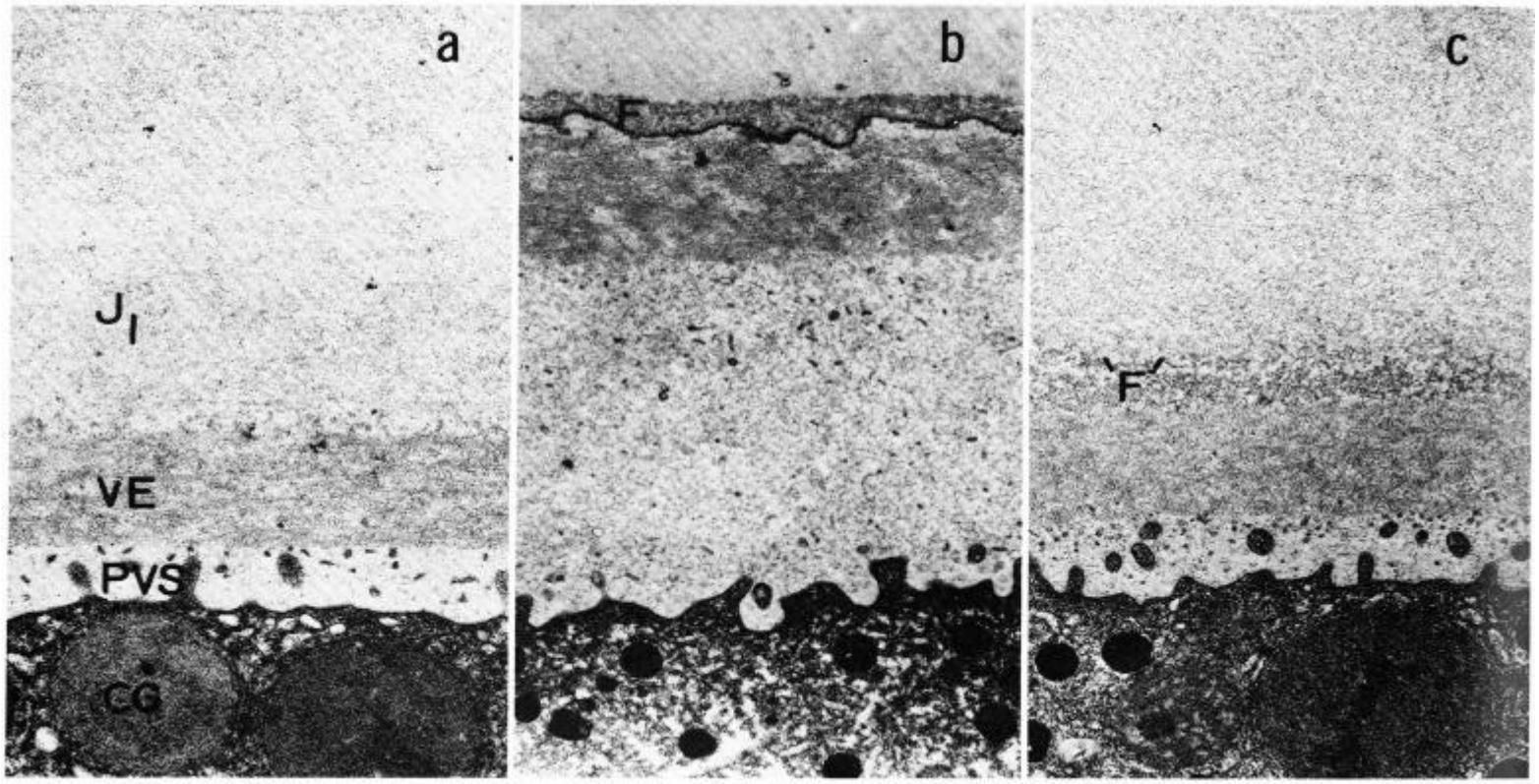

Figure 1-7: Formation of the Fertilization Layer in X. laevis

Electron micrograph of Xenopus laevis eggs (a) prior to fertilization, (b) following fertilization, and (c) an unfertilized egg treated with cortical granule exudate that contains XL35. Abbreviations J_1: innermost jellycoat layer, VE: vitelline envelope, PVS: perivitelline space, CG: cortical granule, F: fertilization layer, 'F: F-like layer.

From [112]

Although the potential ligand for XL35 during development is unknown, there have been reports of blood group-B active glycolipids being expressed in Xenopus blastulae that appear to be involved in Ca^{2+}-dependant cell-cell adhesion[126]. Finally, Gawantka et al.[127] performed in-situ hybridization for approximately 1700 randomly selected cDNAs using *Xenopus* gastrula-, neurula-, and tailbud-stage embryos in conjunction with a limited set of major tissues. XL35 was one of the mRNAs detected, and they localized XL35 to the epidermis in the neurula and tailbud-stage embryo. Although the study by Gawantka offered no details as to the potential function of the XL35 that was detected in the epidermis of the tailbud-stage embryo, it is possible that in adult frogs, XL35 is involved in innate immunity. XL35's broad specificity would make it ideally suited for this purpose and the skin appeared to contain relatively high levels of XL35 mRNA. Amphibian skin is a secretory organ that has previously been shown to be an excellent source of antimicrobial agents[128-132]. The best-characterized class of antimicrobial peptides from *Xenopus* are termed the magainins, [128, 133-136] which have been shown to be present in both the gastrointestinal tract as well as the skin[132, 137-139]. Expression of the magainins in the skin also appears to be developmentally regulated and peaks during metamorphosis[140].

Additional studies that tested XL35 against panels of Gram-negative and positive bacteria as well as against selected fungi showed that XL35 was capable of specifically agglutinating *Corynebacterium sp.*, a Gram-positive mycobacterium and that the binding was calcium-dependent[141]. Reports on the cell wall polysaccharides from several mycobacteria, including corynebacteria, indicated they are composed of an arabinogalactan-repeating unit[142, 143].

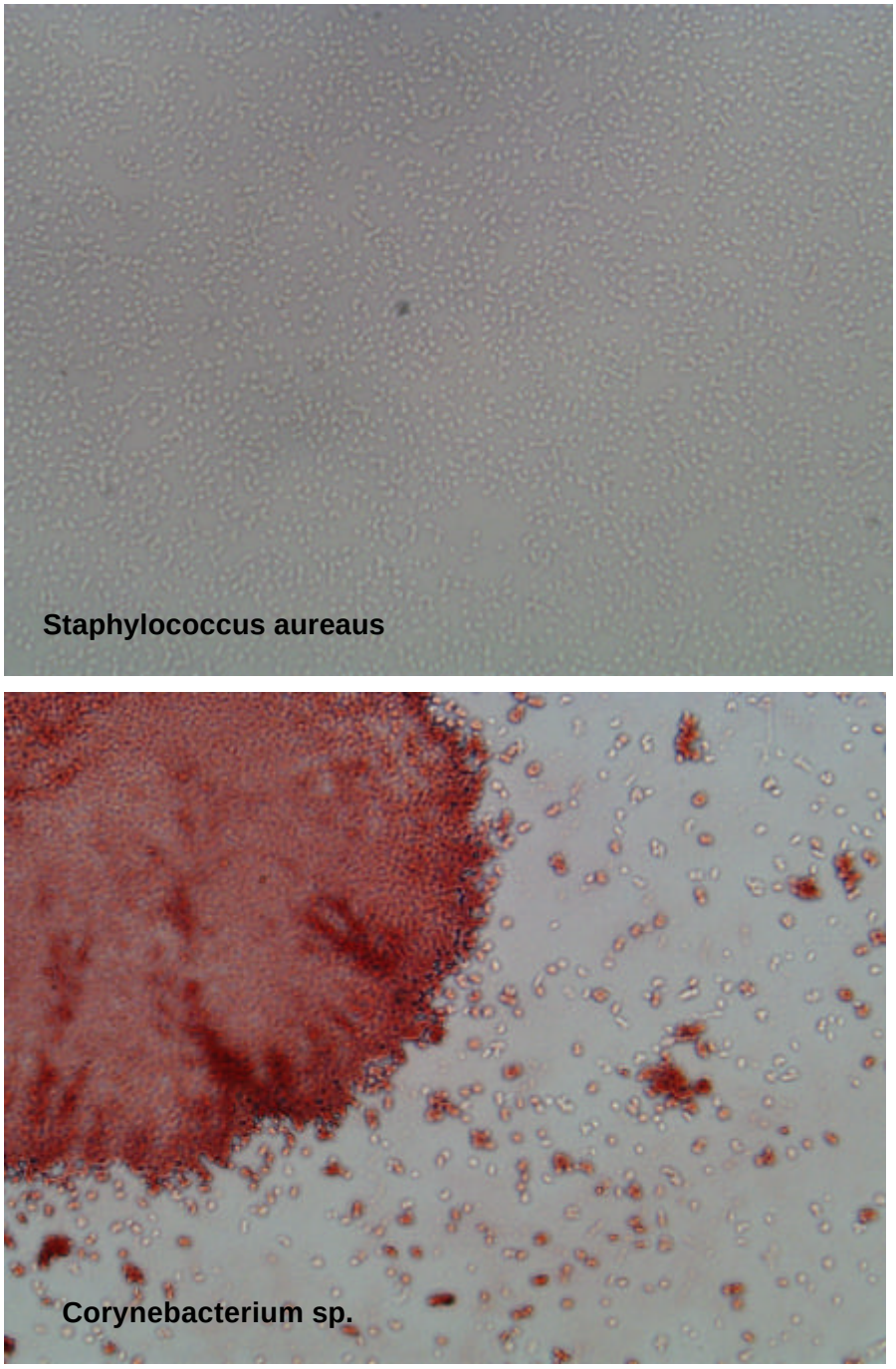

Figure 1-8: Binding of XL35 to Selected Microbes

Jellycoat Protein (JCP)

The glycoprotein ligand for XL35 is contained in the *Xenopus* jellycoat, which is a thick gelatinous matrix composed of several morphologically distinct layers that are species-specific and are layered around the egg as it travels down the oviduct. The JCP has been shown to be critical for successful fertilization, since dejellied eggs cannot be fertilized, but the addition of UV-solubilized jelly to the dejellied eggs permitted 52% of the dejellied eggs to be fertilized[144]. Additionally, the formation of the fertilization layer, which is critical for the viability of the embryo, occurs through an agglutination reaction that involves both JCP components and XL35[112]. A review by Hedrick and Nishihara summarized some of the biological processes in which the JCP appears to play an integral role: binding of sperm to the egg, the induction of the acrosome reaction, the formation of the block to polyspermy and the hardening of the envelope to protect the growing embryo[145].

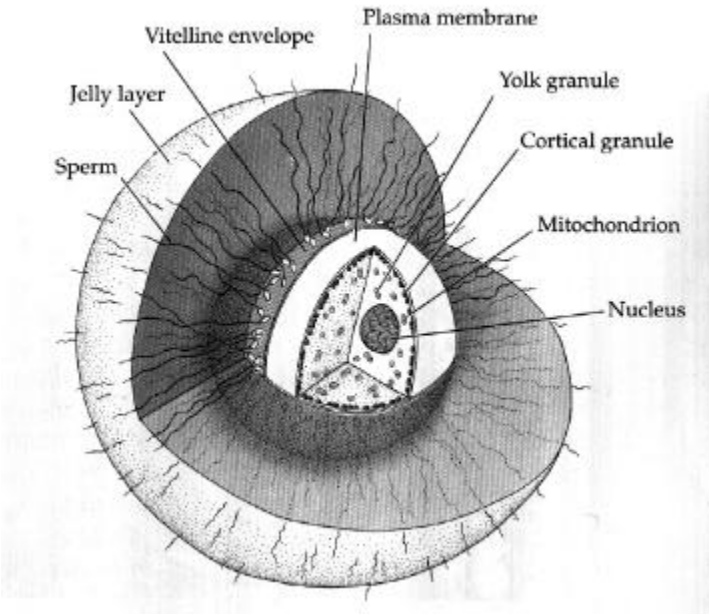

Figure 1-9: Cutaway Diagram Showing an Egg During Fertilization

From [146]

In *X. laevis*, the JCP layer that XL35 encounters upon exocytosis from the cortical granules is a structurally complex matrix composed of three to four distinct layers (J_1-J_4). As opposed to the deposition of the JCP in *B. japonicus*, each layer of the *X. laevis* JCP is individually layered around the oocyte as it travels down the oviduct. Several studies used biotinylated XL35 to demonstrate that the principal ligand for XL35 resides in the innermost or J_1 layer of the JCP[147, 148]. This innermost jellycoat layer is known to be highly charged and can be stained using Alcian blue, but because the jellycoat as a whole has a relatively low level of sialic acid and because $^{35}SO_4$ is readily incorporated into the J_1 layer, it was hypothesized that the acidic moieties in this layer are glycans substituted with sulfate esters[149]. This hypothesis has recently been confirmed by the NMR analysis of β-eliminated alditols from the JCP[150].

The jellycoat is composed of 50-60% carbohydrate by weight[151], and each layer contains a scaffold of linear, high-molecular mass mucins to which are bound smaller globular proteins[152]. Subtle ultrastructural differences in the distribution of linear versus globular components are observed between the jellycoat layers, which permit the identification each layer in the extracellular matrix by rotary shadowing and electron microscopy. The J_1 layer that contains the ligand for XL35 is characterized by predominantly linear structures with a very few globular proteins. In contrast, the J_2 layer contains linear filaments along with what appears to be particulate material while the J_3 layer is composed of branched fibrous material with individual globular proteins spaced along the filaments.

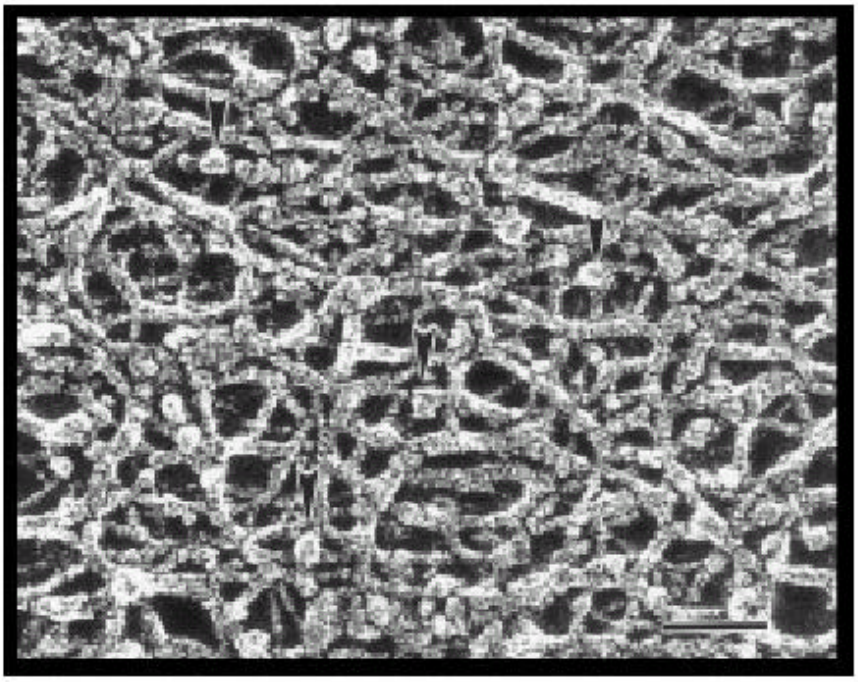

Figure 1-10: Electron Micrograph of the J_1 Layer of the *Xenopus* Jellycoat

The J_1 layer of Xenopus laevis egg jelly consists of an interconnected fibrillogranular matrix. Network fibers are decorated with numerous globular components (shown with arrowheads). Bar = 55 nm

From [152]

The ultrastructural observations of the JCP correlate well with what is known about the structural organization of mucins: typcially, mucins are arranged as tandem repeats of a domain that contains a high percentage of serine or threonine residues and nearly all of these serine or threonine residues are substituted with oligosaccharides through an O-glycosidic bond[153]. These tandem repeat domains are flanked on either side with regions that are rich in cysteines and contribute to the formation of multimers in vivo. The high degree of glycosylation imparts some unique physical properties to mucins, making them linear molecules with no secondary structure. Unlike most proteins composed of random coils, the large number of oligosaccharides along the peptide make mucins very rigid structures that are often compared to bottle-brushes. In addition to the steric constraints imposed by the presence of so many oligosaccharides along the peptide backbone, charge repulsion through sialation or sulfation of mucin glycans ensures that the protein retains the linear conformation which is energetically most favorable[154]. These factors combine to form a protein that is highly solvated in solution, occupies a large hydrodynamic volume, and is capable of forming gels.

The neutral glycans of the JCP have been characterized in a series of studies using either nuclear magnetic resonance or mass spectrometry[155, 156] and several of the structures identified were novel, including a dimeric H antigen and a blood group A antigen terminated with an additional N-acetylglycosamine. Several acidic oligosaccharides were also identified from the JCP of *X. laevis* and were shown to contain either N-acetylneuraminic acid (NeuAc) or 2-keto-3-deoxy-D-glycero-D-galacto-nononic aicd (Kdn). Interestingly, the authors noted a high degree of glycan variability from different spawnings, so much so that some clutches of eggs showed no NeuAc or Kdn in the JCP[157]. The most recent study identified 23 unique O-linked oligosaccharides from six individual *Xenopii*[150]. Six of the structures were sulfated at either the 3- or 6-position, confirming the previous studies using $^{35}SO_4$.

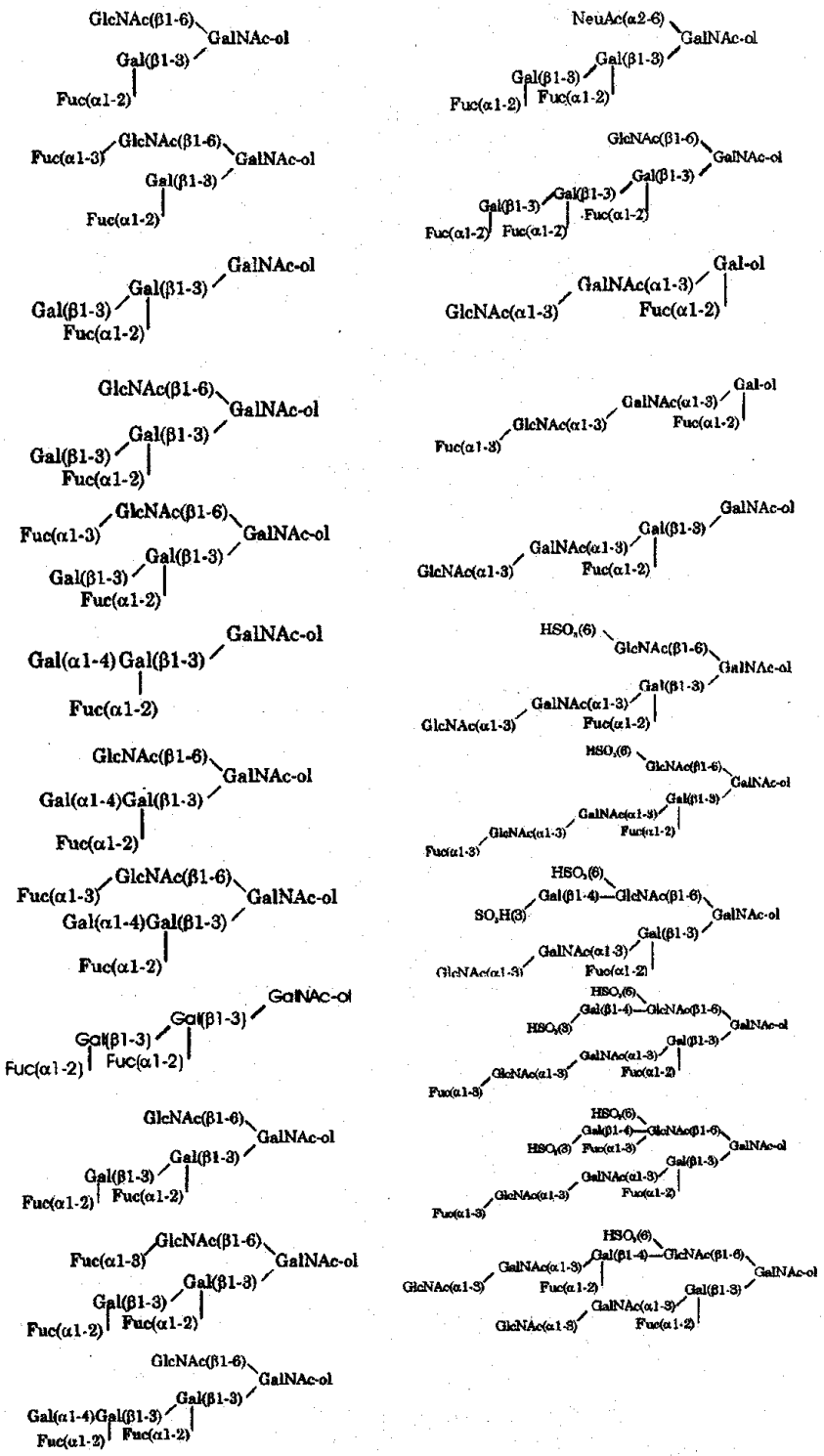

Figure 1-11: Oligosaccharides from the JCP of *X. laevis*

Adapted from [150]

Surprisingly, the terminal carbohydrates of the isolated oligosaccharides displayed a remarkable amount of heterogeneity. Based on the heterogeneity observed, the authors described four phenotypes characterized by at least two different glycosyltransferase activities responsible for the synthesis of oligosaccharides terminated in α1,4-Gal or α1,3-Fuc (denoted as G±, F±). While the majority of the *Xenopus* specimens studied presented the (G+, F±) phenotype which signifies the JCP of these specimens contained the putative ligand for XL35, the lack of this epitope on the remaining specimens had no impact on development following fertilization. The authors found this result surprising because XL35 is known to form the block to polyspermy and these specimens lacked the putative ligand required to form that layer and maintain the viability of the embryo. Several previous studies using hemagglutination of trypsinized rabbit erythrocytes (TRE) suggested XL35 could recognize both α- and β-galactosides, [115, 119] because the addition of either α- or β-galactosides inhibited the agglutination of a mixture containing TRE and XL35. At the time of publication, however, these studies appeared to contradict each other and the discrepancy was attributed to the variability associated with agglutination assays. Using a more quantitative series of assays, the experiments in this thesis have established that XL35 has very broad specificity and is capable of recognizing both α- and β-galactosides. The results presented here reconcile both the apparently contradictory agglutination results and XL35's ability to form the block to polyspermy despite the heterogeneity of the JCP.

Although the exact function of sulfate esters present in the *Xenopus* JCP is not known, studies[158] in *B. japonicus* suggest that the jellycoat may chelate divalent cations such as Ca^{2+} and Mg^{2+}, thereby providing the required chemical environment for the induction of the acrosome reaction and for the penetration of the vitelline envelope. Here again, my results suggest that although sulfated galactosides are not better ligands

for XL35 as compared to their neutral counterparts, XL35 can tolerate sulfation at selected positions: this has the effect of broadening its potential ligand pool within the JCP.

Homologues of XL35

The recently identified human[56] and mouse[55] homologues of XL35 have been termed Human Lectins-1 and 2 (HL-1 and 2) and intelectin, respectively. Based on amino acid sequence, HL-1 and 2 were found to be 80% similar and 60% identical to XL35 and all contained a small fibinogen-like motif that is found in the Ficolin/Opsonin/p35 lectin family. Using genomic clones for HL-1 and 2, fluorescence *in situ* hybridization (FISH) localized both of the genes to chromosome 1q 22-23.5, which is within the chromosomal locus (1q22 to 1q25) previously identified for the selectin family of lectins[159]. Based on Northern blot analysis, the tissue distribution of HL-1 and 2 is distinct, since HL-1 is expressed at high levels in heart, small intestine, colon, thymus, ovary and testis while HL-2 and the mouse homologue intelectin are found only in the small intestine. Insight into potential functions for HL-2 and intelectin have been gleaned from immunocytochemistry, since both intelectin and HL-2 are localized to Paneth cells, which are cells in the small intestinal thought to be involved in microbial defense. HL-1 expression, however, appears to be restricted to endothelial cells, including endothelial cells lining the hepatic veins and arteries within the portal tract, the vessels of the thymus and tonsils as well as several sections obtained from human heart.

Since the XL35 oligomer is too large to study using typical structural techniques, the purpose of this study is to understand the structural elements of XL35 that allow it to fulfill its biological function in lieu of complete structural characterization. The XL35 peptide may be divided into three domains based on its predicted secondary structure:

an N-terminal domain containing the signal sequence, a central region that probably contains the CRD and is rich in turns and loop structures, and a C-terminal domain that is predicted to be α-helical and is likely involved in the formation of XL35 oligomers.as discussed in Chapter 3. The tentative assignment of functions to different regions of XL35 is based on the known structural elements of galactose-binding lectins that suggest the CRD will contain a large amount of loops and turns; additionally, the selective modification of specific amino acid residues in XL35 support this hypothesis. Like MBP, XL35 appears to be able to oligomerize through a combination of hydrophobic contacts and disulfide bonds, and the C-terminal domain is most likely responsible for this function, since it is predicted to be α-helical and contains 4 of the 9 cysteines found in the XL35 sequence.

To study the mechanism and specificity of ligand binding, equilibrium ELISA and surface plasmon resonance (SPR) ligand binding assays were developed using commercial oligosaccharides and synthetic oligosaccharides selected based on recurring glycans found in the *Xenopus* JCP. Kinetic SPR assays were employed to understand the effect of multivalency on the avidity of the interaction, and synthetic glycopolymers were synthesized and tested as mimics for the native JCP ligand. The size of the oligomer was studied using sedimentation equilibrium analysis and dynamic light scattering, and the mechanism of oligomerization was characterized using SDS-PAGE and gel filtration.

These data show that although XL35 is not a C-type lectin, it requires calcium and very closely resembles MBP and other pattern-recognition lectins in that it has a fairly broad specifity and appears to use several of the same amino acids typically involved in galactose-binding lectin CRDs. As is the case for MBP, oligomerization appears to be critical for XL35's function since multivalent lectin-ligand complexes show very high avidity despite the low intrinsic affinity of monovalent lectin-oligosaccharide interactions.

CHAPTER 2 – MATERIALS AND METHODS

Purification of XL35

XL35 was purified from oocytes as previously described, except that an anion exchange step was added prior to melibiose affinity chromatography. Briefly, mature female *Xenopii* were anesthetized using ethyl m-aminobenzoate (Tricaine, MS-222), and the oocytes were obtained surgically and homogenized in ice-cold TCS (10 mM Tris, 10 mM $CaCl_2$, 150 mM NaCl, pH 7.4). Nine volumes of cold acetone was added to the initial homogenate, the pellet was captured by filtration and then washed three times with cold acetone to remove residual lipids. The de-lipidated pellet was resuspended in TCS+0.3 M Galactose and centrifuged at 10,000g for 20 minutes. The clarified supernatant was dialyzed against 50 mM Tris, pH 8.5 prior to being applied to a 2.6×10 cm DEAE-650M column (TosoHaas) equilibrated in the same buffer. XL35 was eluted using a buffer containing 50 mM Tris, 1.2 M NaCl, pH 8.5, and the protein fractions were pooled and applied to a 3 mL melibiose affinity column equilibrated in TCS. The melibiose column was washed extensively with TCS, and XL35 eluted with TBS+50 mM EDTA. Purified XL35 was then dialyzed against TCS for storage. Typical yields were approximately 2-3 mg of purified XL35 from 15 mL of surgically removed oocytes as the starting material.

SDS-PAGE Analyses

Three aliquots of purified XL35 (10 μg each) were mixed with Laemmli loading buffer: two of the aliquots were added to loading buffer without reducing agent and the third contained 5% β-mercaptoethanol. The first sample was loaded onto a 4-20% Tris-glycine mini-gel (Bio-Rad) without further preparation, while the remaining two samples

were boiled at 95^{o}C for 10 minutes and cooled prior to being loaded on non-adjacent lanes on the gel to prevent the diffusion of β-mercaptoethanol between samples. Samples were electrophoresed at 80V until sample stacking was complete, and then the voltage was increased to 120V for the duration of the run. The gel was stained with colloidal coomassie (Novex) according to the manufacturer's instructions, and the image was acquired and analyzed using a FluorS imaging station and Quantity One™ software (Bio-Rad).

Dynamic Light Scatttering

Prior to the introduction of samples, cuvettes were cleaned with 0.8 M HCL, then rinsed with deionized water and ethanol before being dried with nitrogen. To establish a baseline and verify that the cuvette was properly cleaned, the scattering intensity of deionized water filtered through a 0.02 micron Whitman anodisc filter was recorded. Purified XL35 (approximately 38 μM) in TCS was either filtered using a 0.1 μm ceramic filter according to the manufacturer's instructions (Protein Solutions) or centrifuged at 15,000 g for 10 minutes prior to analysis by dynamic light scattering. At least ten separate measurements were conducted for each analysis and the results were analyzed using the DynaPro software (Protein Solutions).

Sedimentation Equilibrium Analysis

Three separate samples of purified XL35 were reconstituted in TCS to yield absorbances of approximately 0.6, 0.4 and 0.2 AU, which correspond to concentrations of 10.00, 6.67 and 3.33 μM. These samples as well as a TCS blank were loaded into a Beckman Optima XLA analytical ultracentrifuge and centrifuged at 3500 rpm at 20^{o}C for approximately 16 hours. After equilibrium was reached, the concentration along the length of each cell was determined by taking the absorbance at 280 nm. Results were

expressed as a plot of dln A versus r^2 to obtain the molecular weight. All sedimentation equilibrium analyses were performed by Dr. John Brewer.

MALDI-TOF

The size of the XL35 monomer was determined by MALDI-TOF analysis. Purified XL35 was reduced using 10 mM DTT and alkylated with 50 mM iodoacetamide in the presence of 50 mM Tris, 8 M Urea, pH 8.0. The reduced and alkylated protein was purified by RP-HPLC using a C4 column (Brownlee aquapore) with a gradient of 0.05% TFA in water to 0.04% TFA in acetonitrile. Fractions containing the reduced and alkylated protein were concentrated under vacuum and an aliquot was reserved to determine the molecular weight of RCM XL35 prior to N-glycanase treatment. The remainder of RCM XL35 was re-suspended in TCS containing 0.5% SDS to denature the protein for N-glycanase treatment. The protein was boiled at 95^{o}C for 10 minutes and after cooling, a 5-fold excess of NP40 was added followed by the addition of 240 ng of native N-glycanase. The reaction was incubated at 37^{o}C overnight and was terminated by heating to 95^{o}C. XL35 was precipitated from the reaction mixture using 9 volumes of cold ethanol and was re-suspended in 0.1% TFA for MALDI analysis. Crystalline BSA (Sigma A0281) was used as the calibration standard and the M+H, M+2H, and M+3H peaks were selected as calibrants prior to the analysis of XL35.

Chemical Modification Studies

Control and treated XL35 (approximately 10 μg/mL) were pretreated for 1 hour at room temperature with DTT, SDS, iodoacetamide urea or the solvents listed in Figure 3-9 prior to use in the ELISA inhibition assay described later in this section. Briefly, microplates were coated with total JCP and blocked as described, but a fixed concentration of XL35 was employed to compare treated and untreated material. The chemical additive remained in the microplate wells during the incubation step to ensure that any observable binding was not a result of renaturation following removal of the chemical

additive. Unbound material was washed away and bound XL35 quantitated using a Streptavidin-HRP conjugate with an *ortho*-phenylene diamine substrate.

Samples treated with Koshland's reagent were treated for an abbreviated time (5 minutes) and both the control and the treated sample were dialyzed against TCS to remove excess reagents. EDC-mediated amidation was performed for 1 hour, but both the control and treated sample were dialyzed against TCS to remove excess reagents. Immediately following treatement and dialysis, the control and treated samples were used in the ELISA as described.

Preparation of JCP-Alkaline Phosphatase Conjugate - Thiolation of JCP

Approximately 10 milligrams JCP were dissolved in 4 M Guanidine HCl, 0.1 M Tris, pH 8 and was reduced for 1 hour at 37^{o}C using 10 mM DTT. After reduction for 1 hour, iodoacetamide was added to the reduced JCP at a final concentration of 50 mM and the sample was alkylated for another hour at 37^{o}C. The reduced and carboxymethylated (RCM) JCP was centrifuged at 15,000 g for 1 hour to remove particulates and desalted twice against PBS with 5 mM EDTA, pH 8.0 in preparation for thiolating the sample with S-acetylmercaptosuccinic anhydride (SATA). The SATA (3.1 milligrams) was dissolved into 100 μL of DMSO, and 30 μL of the SATA mixture was added to 3 mL of RCM JCP in PBS with 5 mM EDTA, pH 8 (final concentration SATA=1.3 mM). After reacting for 2 hours at 25^{o}C, the excess SATA was removed by dialyzing three times against PBS with 5 mM EDTA. One milliliter of the JCP-SATA conjugate (2.6 milligrams protein) was deacetylated using 0.5 M hydroxylamine in PBS with 25 mM EDTA, pH 7.5 for 2 hours. The deacetylated JCP-SATA was desalted against PBS with 25 mM EDTA, pH 7.2 in preparation for conjugation with derivatized BAP.

Preparation of JCP-Alkaline Phosphatase Conjugate - Derivatization of BAP

Five milligrams of Bacterial Alkaline Phosphatase (BAP) was obtained from Worthington and was desalted three times against PBS+5 mM EDTA, pH 8 prior to reaction with

succinimidyl 4-(N-maleimidomethyl)cyclohexane-1-carboxylate (SMCC). To the solution containing BAP, 50 μL of a 60 mM solution of SMCC in DMSO was added and the reaction proceeded for 1 hour at 25°C. The BAP-SMCC mixture was desalted twice against PBS with 5 mM EDTA, pH 7.2 and added to the deacetylated JCP-SATA conjugate. The reaction was allowed to proceed for 2 hours at 25°C, then overnight at 4°C. The final conjugate was dialyzed against two buffer changes of TBS with 1mM $MgCl_2$ and alkaline phosphatase activity was confirmed using saturation binding assays.

Biotinylation of XL35

Purified XL35 (250 micrograms) was dialyzed against HCS (10 mM Hepes, 10 mM $CaCl_2$, 150 mM NaCl, pH 8.0), and biotinylated using NHS-Biotin (Pierce) according to the manufacturer's instructions. One milligram of NHS-Biotin was dissolved in 75 μL DMSO and 25 μL of the NHS-Biotin solution was added to 250 micrograms of purified XL35 in HCS, pH 8.0. The reaction proceeded for 2 hours at 25°C, and the biotinylated XL35 (bXL35) was then dialyzed against TCS, pH 7.2 with 0.02% azide to remove unreacted reagents.

ELISA Inhibition Assay

Approximately 10 nanograms of total JCP in 50 mM sodium bicarbonate, pH 9.4, was coated onto each well of Corning Half Area ELISA plates for 1 hour at 25°C or overnight at 4°C. Following coating, the plates were washed three times with water and nonspecific sites blocked for one hour using blocking buffer (TCS with 1%BSA and 0.1%Tween 20). After blocking was complete, the blocking buffer was discarded and 20 μL of blocking buffer was added to each well. Inhibitors were dissolved in blocking buffer, added to the first column of wells and serially diluted across the microplate. Twenty microliters of biotinylated XL35 (0.5 ug/mL in blocking buffer) were then added to each well and allowed to incubate for 1 hour at 25°C. After an hour incubation, the

plates were washed three times with TCS and 40 µL of Streptavidin-HRP (0.2 ug/mL in blocking buffer) was added. After incubating for 45 minutes, the plates were again washed three times and a colorimetric reaction initiated by the addition of *ortho*-phenylene diamine (0.3 mg/mL in 50 mM sodium citrate/50 mM sodium phosphate, pH 4.5 and 0.003% H_2O_2). After the reaction was stopped using 2 M H_2SO_4 the absorbance for each well was recorded at 495 nm.

Capture Inhibition Assay

Approximately 20 micrograms of XL35 in 50 mM sodium bicarbonate, pH 9.4 were coated onto Corning Half Area ELISA plates for 1 hour at 25°C, and the plates were blocked using TCS with 1% BSA and 0.1% Tween 20 as described previously. After blocking was complete, the blocking buffer was discarded and 20 µL of blocking buffer was added to each well. Inhibitors were dissolved in blocking buffer, added to the first column and serially diluted across the microplate. Twenty microliters of JCP-BAP conjugate (1:2500 in blocking buffer) were added to each well and allowed to incubate overnight at 4°C. The plates were washed three times using TCS and developed at 37°C using 120 µL per well of *para*-nitrophenol in 0.2 M Tris, pH 10.2. Following development, the absorbance for each well was recorded at 405 nm.

Saturation Binding Assays

Assays were performed in a similar fashion to their corresponding inhibition assays with the exception that no inhibitor was added. Instead, saturating concentrations of primary conjugates (biotinylated XL35 or JCP-BAP) were added to the first column of wells and serially diluted across the microplate. Following incubation of the primary conjugate, the plates were washed three times. For biotinylated XL35, the plates were incubated with 0.2 ug/mL streptavidin-HRP in blocking buffer for 45 minutes prior to washing and development. For the JCP-BAP conjugate, the plates were simply washed three times

and developed. For each concentration of conjugate, a three blank wells were used to assess non-specific binding. Results are expressed in terms of specific binding, which is the difference between the quantity of conjugate bound minus the quantity of nonspecific binding observed at that concentration of labelled conjugate.

Surface Plasmon Resonance (SPR) Analyses

XL35 was coupled to a CM5 chip using the manufacturer's instructions. Briefly, 100 μg of purified XL35 were dialyzed against 50 mM sodium acetate, pH 5 for 2 hours. Immediately before coupling, the dialyzed XL35 was diluted 10-fold in 10 mM sodium acetate, pH 4. 1-Ethyl-3-(3-Dimethylaminopropyl)-Carbodiimide Hydrochloride (EDC) and N-Hydroxysuccinimide (NHS) were weighed out and suspended in water immediately before use at final concentrations of 400 and 100 mM, respectively. The coupling reaction was carried out using the Biacore control software and 15,000 Resonance Units (RU) were selected as the target level using the "Aim for Immobilization Level" program. Samples of a trimer derivitized with Gal(α1,3)Gal, glycopolymers derivitized with melibiose and N-acetylglucosamine (negative control) were dissolved at a concentration of 0.625 mg/mL in running buffer (10 mM Hepes, 10 mM $CaCl_2$, 150 mM NaCl with 0.005% Tween 20, pH 7.2). The flow rate was set to 15 μL/min and 50 μL of each sample was injected using the "Kinject" command.

Kinetic and equilibrium analyses were performed by injecting serial dilutions of the 17% melibiose glycopolymer over a surface containing 5000 RU of XL35 prepared as described above. Kinetic analyses were conducted as a flow rate of 15 μL/min to minimize mass transport effects; however, mass transport limitations were not observed even at lower flow rates. Equilibrium analyses were performed using the same surface, but at a flow rate of 4 μL/min.

Aminopropyl melibiose was biotinylated using Sulfo-NHS-LC-biotin (Pierce). The biotinlyated sugar was isolated using preparative reverse-phase chromatography, and its structure confirmed using NMR. 10000 RU of streptavidin was coupled to a CM5 chip using the NHS and EDC as described above, but the coupling was carried out by manually injecting the NHS/EDC mixture for 40 minutes followed by a 40-minute injection of streptavidin (25 μg/mL in 10 mM sodium acetate, pH 4.0). Unreacted NHS esters on the chip were blocked using an injection of 1 M ethanolamine, pH 8. Biotinylated aminopropyl melibiose was then injected over the surface and was immobilized by the coupled streptavidin. A calibration curve for XL35 was generated using serial dilutions of XL35 (200 μg/mL starting concentration), and a concentration of 75 μg/mL was used for solution competition experiments. Increasing concentrations of melibiose (up to 10 mM final concentration) were used to compete XL35 from the streptavidin-melibiose surface.

Characterization of the Glycopolymers and JCP

The molecular weight of the glycopolymers were determined using gel filtration on a Sephacryl S-400 column (1.5 $\times$ 50 cm) equilibrated in 200 mM NaCl with 10 mM H_3PO_4 titrated to pH 6.0 using NaOH. The flow rate for all analyses was 2.5 mL/min and detection was performed at 206 nm. The system was calibrated using a combination of commercially available polyacid (Fluka) and dextran (Sigma) standards.

Phenol-Sulfuric Assay

Using the molar composition of the JCP obtained by compositional analysis, standards were prepared by using the appropriate molar combination of monosaccharides suspended in blocking buffer (TCS with 1%BSA and 0.1%Tween 20) as previously described[160]. Briefly, 10 μL of a 5% phenol (w/w) solution in deionized water was

added to individual wells of a microtiter plate followed by the addition of 10 μL of sample or standard. 150 μL of concentrated H_2SO_4 was quickly added to each of the wells and immediately mixed 5 times. Microplates were then placed on a shaker for 10 minutes prior to the absorbance being read at 495 nm.

CHAPTER 3 - RESULTS

Structural Studies – Mechanism of XL35 Oligomerization

The predicted secondary structure of XL35 (Figure 3-1) is consistent with that of many lectins[89] in that it shows very few regions of the polypeptide predicted to have defined structure, with the exception of the C-terminus, which contains relatively high levels of hydrophobic residues and is predicted to contain a short α-helical segment. To gain insight into oligomerization characteristics of XL35, a series of experiments using SDS-PAGE after various treatments were performed.

Results using SDS-PAGE indicated that hydrophobic contacts are partly responsible for the formation of XL35 oligomers, since XL35 that was heat-denatured without a reducing agent showed a characteristic ladder pattern corresponding to a mixed population of oligomers (Figure 3-2, lane 2). The pattern shows oligomers from N=2 to N=10-12, suggesting that the higher-order oligomers are composed of predominantly of dimers formed by interchain disulfide bonds that then associate via hydrophobic contacts to form higher-order structures. Prior addition of β-mercaptoethanol or DTT to the same sample before electrophoresis yielded a single band corresponding to the glycosylated monomer, suggesting that interchain disulfide bonds were responsible for the ladder-pattern of oligomers observed in the previous sample.

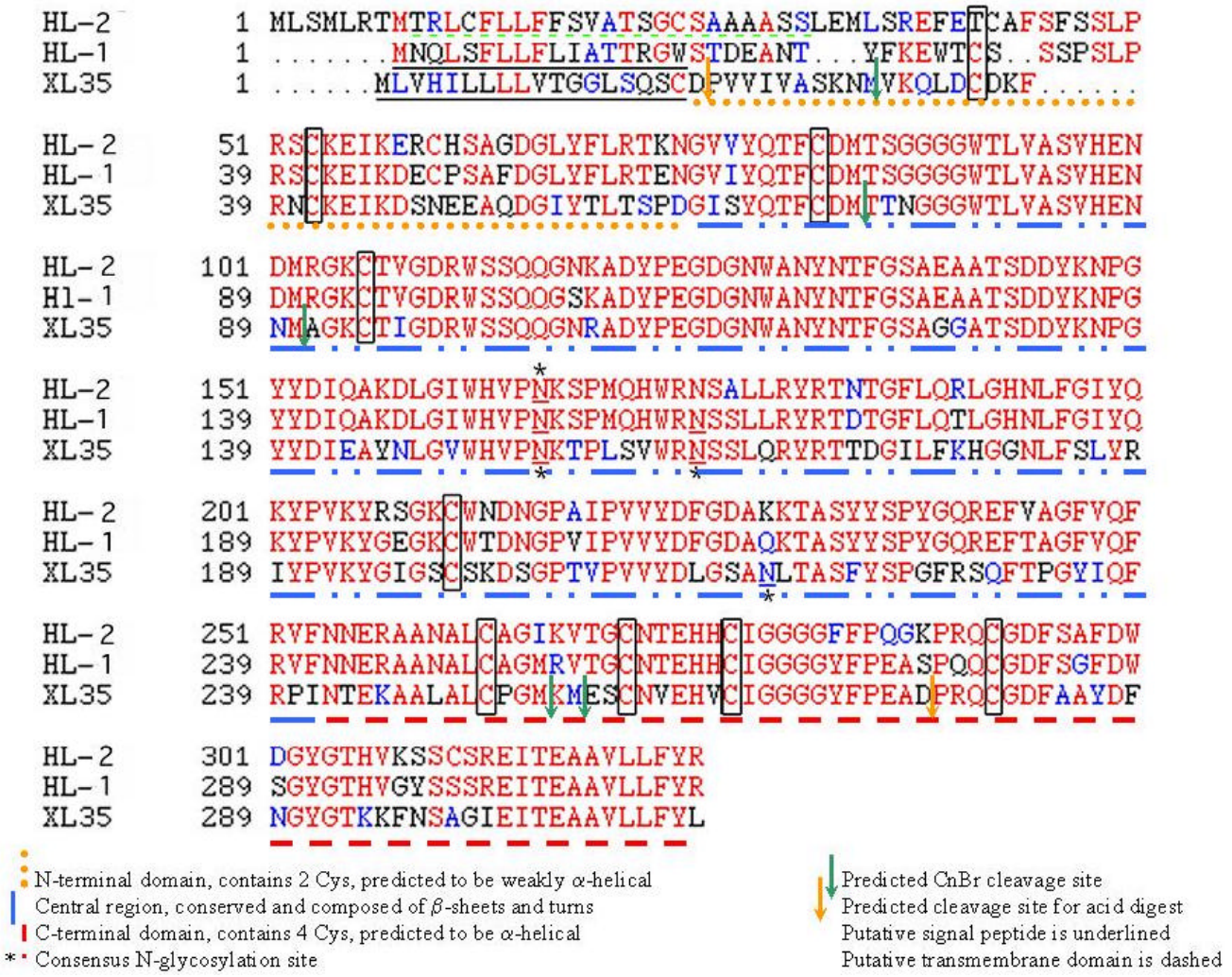

Figure 3-1: Primary Sequence and Domains of XL35

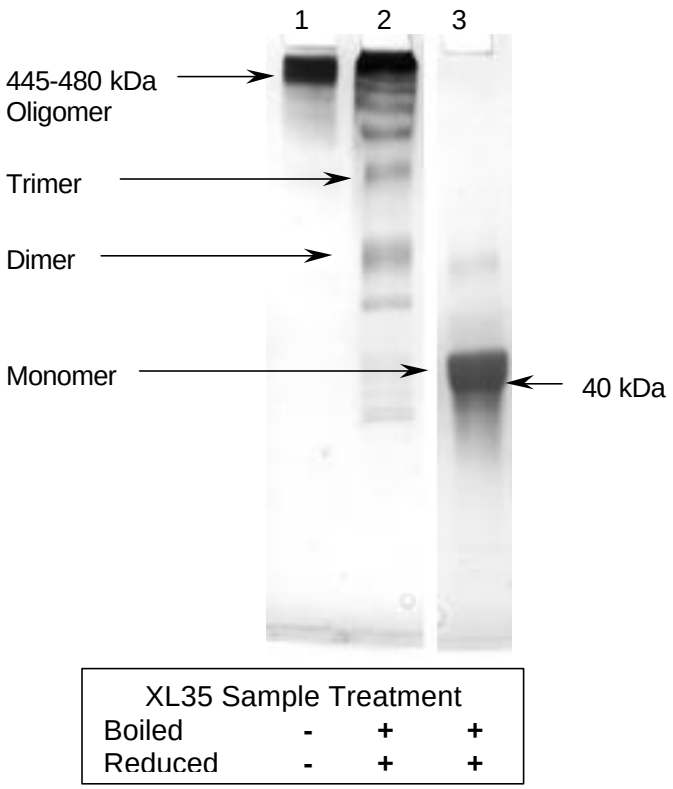

Different sample treatments show the mechanisms of XL35 oligomerization:
Lane 1: XL35 that has not been heat denatured or reduced
Lane 2: denatured but not reduced XL35
Lane 3: XL35 that has been denatured and reduced
Electrophoresis was performed using a Bio-Rad 4-20% polyacrylamide Tris-glycine gel.

Figure 3-2: XL35 Oligomerizes Through a Combination of Hydrophobic Contacts and Disulfide Bonds

Additional evidence that suggests the C-terminal domain of XL35 is responsible for oligomerization comes from limited acid digests of XL35 that cleave the peptide selectively at Asp-Pro peptide bonds. From the primary sequence there is only one combination of Asp and Pro that will yield detectable products (cleaves between residues 276-277, shown in Figure 3-1) and acid treatment of XL35 eliminates higher-order oligomers without the use of reducing agents. Although this reaction is reported to only be approximately 70% efficient, acid treatment appeared to remove the oligomerization domain from XL35, since the high molecular-weight oligomers that are typically seen by nonreducing SDS-PAGE were eliminated by acid-cleavage. These

data, along with the hydrophobicity of the XL35 C-terminus suggest that the region responsible for forming oligomers lies in the C-terminal section of the polypeptide.

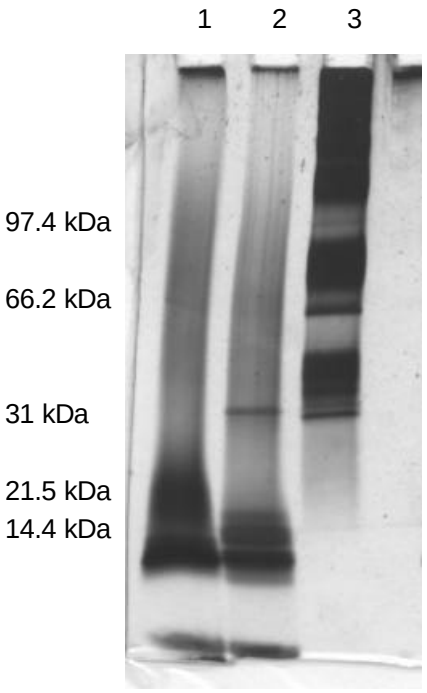

Limited acid digestion of XL35 eliminates oligomers.
Lane 1: Acid-digested XL35
Lane 2: Acid-digested XL35 subsequently treated with N-glycanase (without reducing agents)
Lane 3: XL35 treated with N-glycanase (no acid digest)
Samples were electrophoresed on a 4-20% polyacrylamide Tris-glycine gel without reducing agents.

Figure 3-3: XL35 Subjected to a Limited Acid Digest is not an Oligomer

Structural Studies – Size of Oligomer as Determined by Sedimentation Equilibrium

The molecular weight of the XL35 oligomer was determined using sedimentation equilibrium analysis. Three aliquots of purified XL35 at concentrations ranging from 3.33 to 10.0 μM were loaded into a Beckman Optima XLA analytical ultracentrifuge and centrifuged until equilibrium was attained. The absorbance was then taken along the

radius of each cell and the molecular weight determined by fitting the data to the following nonlinear equation:

$$C_r = C_0 \exp\left\{H \times M\left(r^2 - r_0^2\right)\right\} + E$$

where:

r_0 = initial radial position (cm)

C_0 = concentration at initial radial position (absorbance at 280 nm)

C_r = concentration at radial position r (absorbance at 280 nm)

H = $\frac{w^2(1-\nabla r)}{2RT}$

E = baseline offset

M = molecular weight

Analytical data from each of the cells are shown in Figure 3-4, along with the residuals from the fit to the equation shown above. Based on the results from the three concentrations of XL35 analyzed, the protein did not show concentration-based aggregation. The partial specific molar volume (∇) of XL35 was calculated using the full-length sequence (although the N-terminus shows some heterogeneity). Using the calculated value of ∇ = 0.71 mL/g, the molecular weight of XL35 was determined to be 466.5 kDa based on an average of the apparent molecular weight for the three concentrations analyzed.

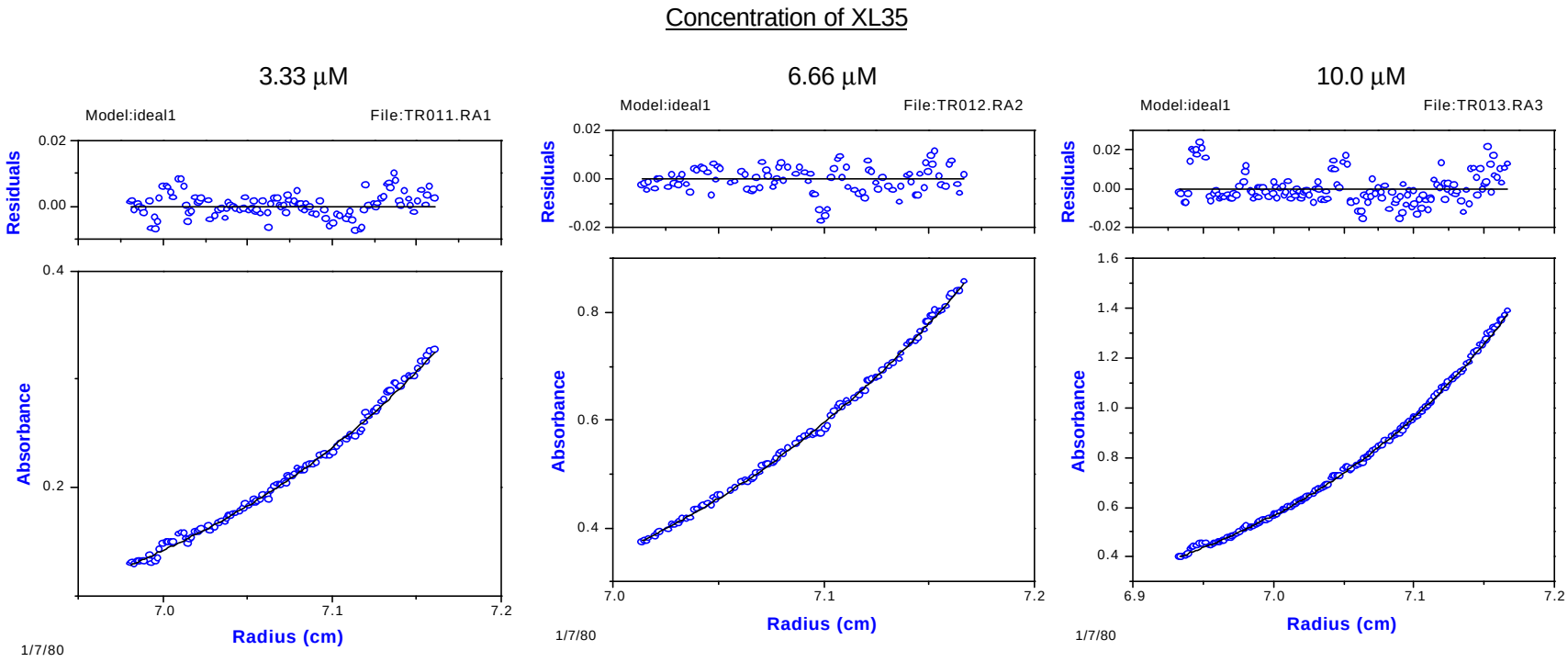

Figure 3-4: Sedimentation Equilibrium Analysis of XL35

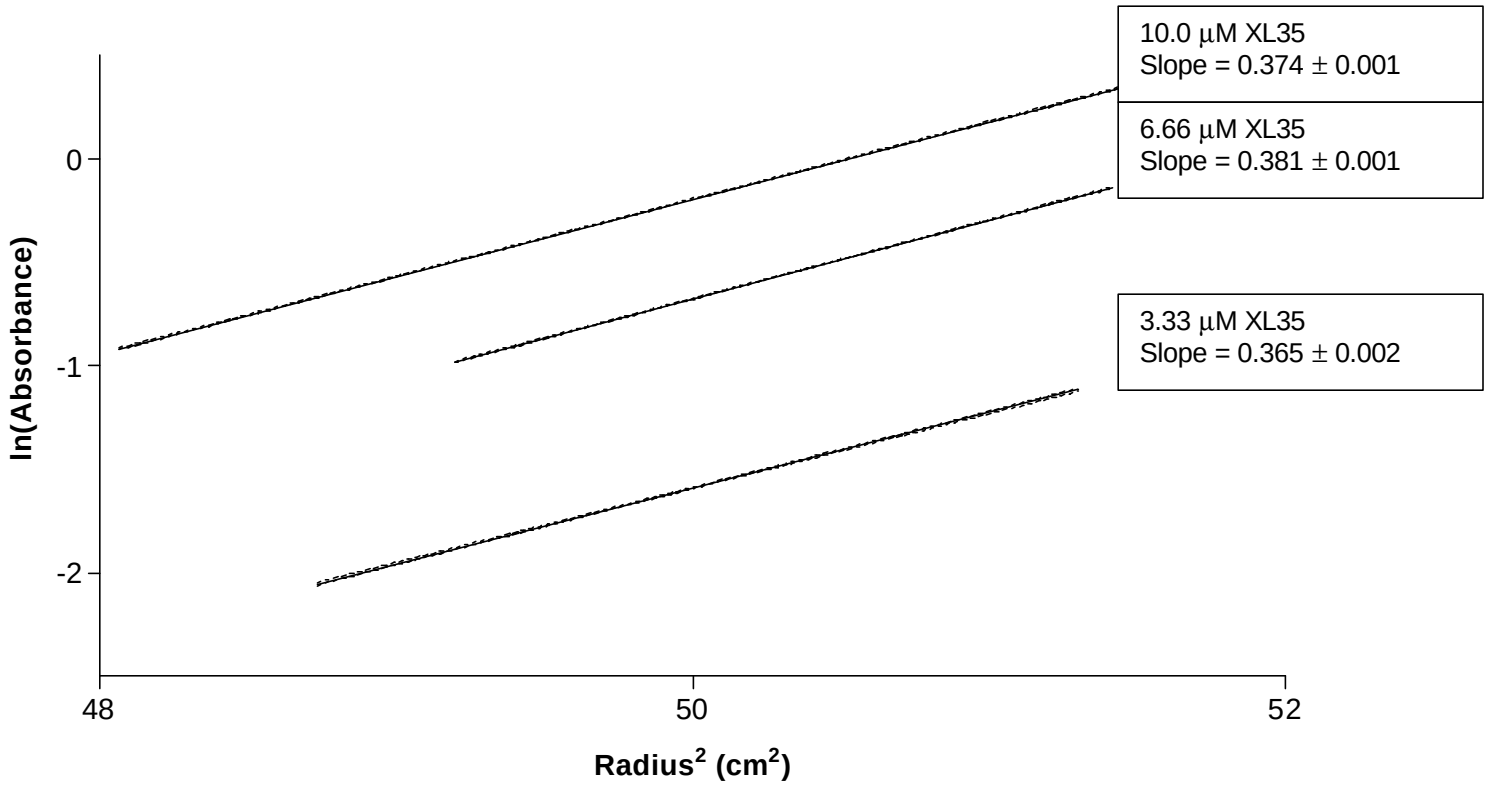

Since molecular weight ∝ slope of $\frac{\ln C}{r^2}$, macromolecules that do not associate would be expected to have a similar slope regardless of protein concentration. This is observed, suggesting that XL35 does not associate in a concentration-dependant fashion.

Figure 3-5: Apparent Molecular Weight of XL35 at Different Concentrations

Structural Studies – Size of Oligomer as Determined by Light Scattering

Dynamic light scattering using a Protein Solutions DynaPro dynamic light scattering system was also performed on intact XL35, since it is an orthogonal technique for determining the molecular weight of macromolecules, and when used in conjunction with sedimentation equilibrium experiments, can provide information on the shape of the macromolecule. Using XL35 that had been centrifuged to remove particulates, the light scattering measurements were consistent over 20-30 readings. The diffusion coefficient was determined to 289.5×10^{-9} cm^2/s and the hydrodynamic radius was calculated to be 7.2 nm based on the Stokes-Einstein equation. The data for two separate experiments are summarized in Table 3-1 along with a description of each of the parameters listed:

Table 3-1: Dynamic Light Scattering Results for XL35

Parameter	Experiment 1	Experiment 2
D ($\times 10^{-9}$ cm^2/s)	291.0	289.5
R_H (nm)	7.18	7.22
C_P/R_H (%)	7.6	10.3
Baseline	1.000	1.001
Sum of Squares (SOS) error	0.277	0.310
No. of measurements	30	32

D ($\times 10^{-9}$ cm^2/s): the measured diffusion coefficient in cm^2/sec.

R_H (nm): hydrodynamic radius given in nm. This calculation assumes a hard sphere in a viscous medium but is calculated from the measured diffusion coefficient.

C_P/R_H (%): a measure of the polydispersity of the solution; values <15% suggest that the protein solution is likely to crystallize

Baseline: values between 0.977-1.002 suggest a monomodal distribution

SOS error: values less than 5.000 indicate low noise

The description of parameters is adapted from Habel et al.[161]

Based on the mass of XL35 determined by sedimentation equilibrium (and confirmed by SDS-PAGE analysis), along with the diffusion coefficient (D) and calculated hydrodynamic radius (R_H), it is possible to calculate the shape factor (F) for the XL35 oligomer. The shape factor is given by:

$$F = \frac{f}{f_0} = \frac{R_H}{R_{sph}}$$

where:

f = the measured frictional coefficient,

f_0 = hypothetical frictional coefficient of a sphere with the same molecular weight

R_H = measured hydrodynamic radius

R_{sph} = the hydrodynamic radius for a perfect sphere of identical molecular weight.

Given that $R_{sph} = \sqrt[3]{\left(\frac{3M_W\nabla}{4p\ N_A}\right)}$

where:

M_W = mass (determined to be 466,500 Da by sedimentation equilibrium)

∇ = partial specific molar volume (0.71 mL/g)

N_A = Avogadro's number

The value for R_{sph} is calculated to be 5.08 nm, which yields a shape factor of 1.42 for the XL35 oligomer and axial ratios of 7.72 and 9.01 (prolate and oblate). The observed shape factor is within the range of values typically observed for globular proteins and

does not suggest that XL35 contains long linear structures such as the collagenous domain on collectins or the Fc region of antibodies.

The shape factor can then be used to back-calculate the apparent molecular weight of XL35 using a model that incorporates factors for the partial specific volume and shape of the protein. Based on average hydrodynamic radii of 7.18 and 7.22 nm for two separate experiments, the molecular weight of the XL35 oligomer is determined to be 460 and 467 kDa respectively. This is in excellent agreement with the molecular weight determined by sedimentation equilibrium, which was 466.5 kDa.

Studies on Monomer - Signal Sequence and Molecular Weight of XL35 Monomer

Based on signal peptide prediction algorithms,[162] both Ser15 and Ser17 have a high probability of serving as the cleavage site for secreted XL35. MALDI-TOF data of reduced and carboxymethylated (RCM) XL35 after exhaustive treatment with N-glycanase (Figure 3-8) showed two forms of XL35, one of which appeared to be present at higher abundance than the other was. The mass of the primary M+H peak in the spectra was 34,531 Da, and the mass of secondary peak, which appears as a shoulder off of the main peak, was 33,385 Da. Taking into account the combined mass of the alkylating groups, the predicted mass of full-length XL35 after carboxymethylation is 34,826 Da, which is within 0.8% of the experimentally determined mass of 34,531 for the larger form. Subsequent MALDI analyses of N-glycanase-treated RCM XL35 confirmed the initial mass value for the higher-mass species and consistantly showed it to be the predominant species within the preparation which indicates that the bulk of XL35 is secreted intact. The predicted mass for deglycosylated XL35, after processing by the signal peptidase (assuming cleavage between Ser15 and Gln16 and adding the mass of the alkylating groups), is 33,265 Da, which is within 0.4% of the experimentally determined value of 33,385 Da for the smaller form of XL35. Previous results[123] have shown that XL35 treated with N-glycanase migrates as a protein with an apparent

molecular weight of 35 kDa, and the present mass spectrometry data suggests that the earlier SDS-PAGE results are surprisingly accurate. It is likely that the form of the XL35 polypeptide processed by the signal peptidase was not observed by SDS-PAGE because it is present in low quantities relative to the intact polypeptide. The N-terminal heterogeneity of XL35 does not permit the use of N-terminal sequencing data to identify accurately the N-terminus but sequencing results corroborate the MALDI data that showed the existence of more than one form of the XL35 polypeptide. Additional N-terminal sequencing analyses were performed using larger amounts of XL35, which had the effect of increasing the overall signal but did not lessen the heterogeneity of the sequencing data. These results confirmed that the observed heterogeneity was not simply a result of insufficient material.

The size of the XL35 monomer (with N-glycans) was also determined by MALDI-TOF analysis and the data are shown in Figure 3-7. The molecular mass and heterogeneity of RCM XL35 prior to treatment with N-glycanase confirmed that XL35 is N-glycosylated and the difference of 5298 Da between the glycosylated and treated forms of RCM XL35 suggests that at least 2-3 putative N-glycosylation sites are utilized. RCM XL35 prior to treatment with N-glycanase shows a broad peak indicative of glycan heterogeneity. The observed molecular weight (39,829 Da) obtained using MALDI-TOF correlated well with reducing SDS-PAGE analysis, which indicated that reduced XL35 containing glycans has a molecular weight of approximately 40 kDa.

In conclusion, mass spectrometric studies demonstrated that as purified from oocytes, the majority of the XL35 polypeptide does not show secretion signal sequence cleavage although a limited amount of XL35 shows removal of the signal peptide as would be expected for secretory proteins. Other peptides and proteins known to transit the regulated secretory pathway, as discussed in Chapter 4; have been shown to be packaged in secretory granules as pro-forms of the mature polypeptide. Processing of

these full-length polypeptides then occurs in secretory granules to produce the mature protein or peptide. Given XL35's localization to a set of regulated secretory granules in the oocyte, this pathway is the most likely one utilized to package XL35 into the cortical granules, which then undergo the regulated secretion of their contents at fertilization.

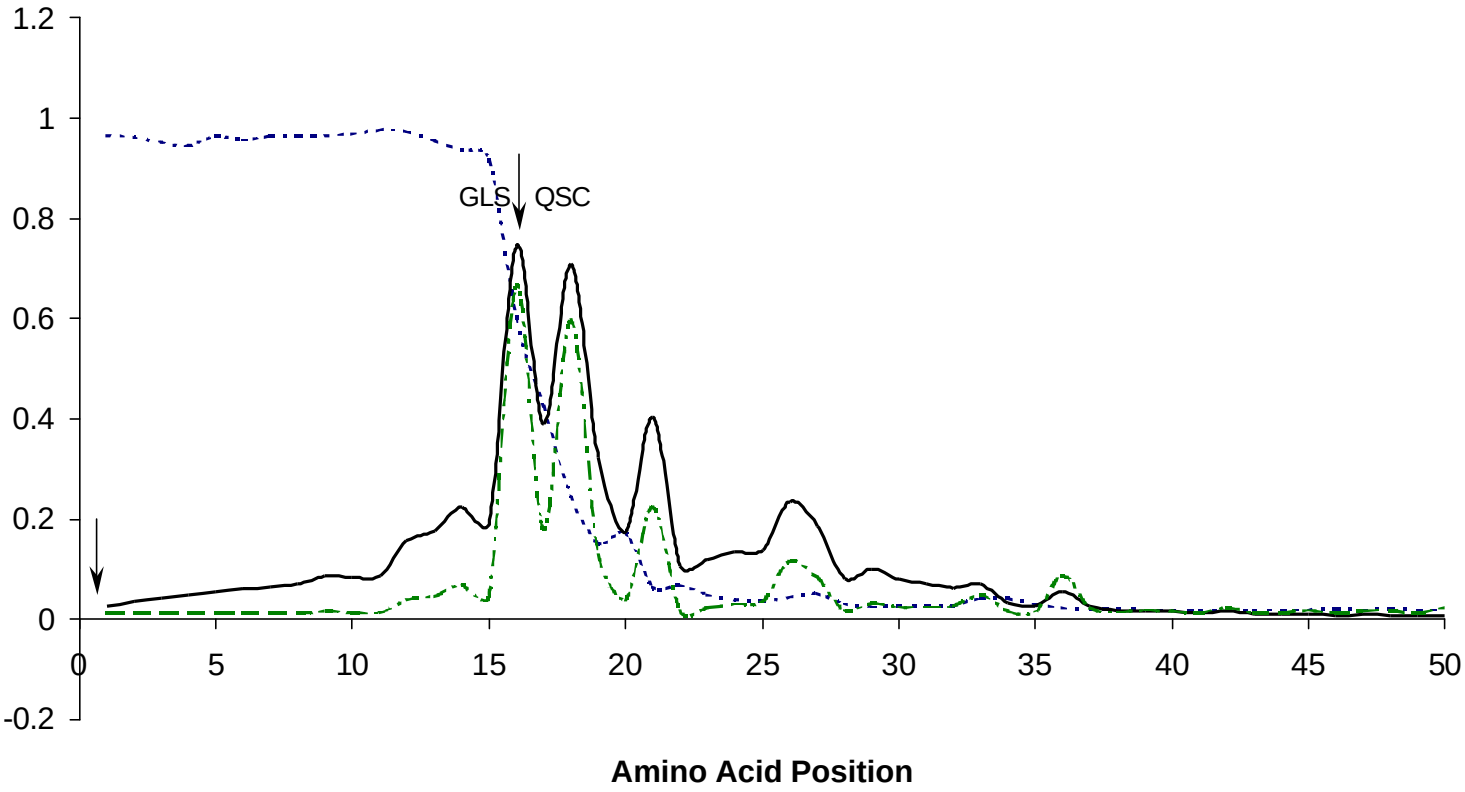

Predicted signal peptide for XL35. The predominant forms of XL35 are shown by the arrows and correspond to the intact polypeptide (major species) and a smaller population of the peptide that is processed by the signal peptidase.

Predicted sesults generated using SignalP [162]

Figure 3-6: Predicted Signal Sequence for XL35

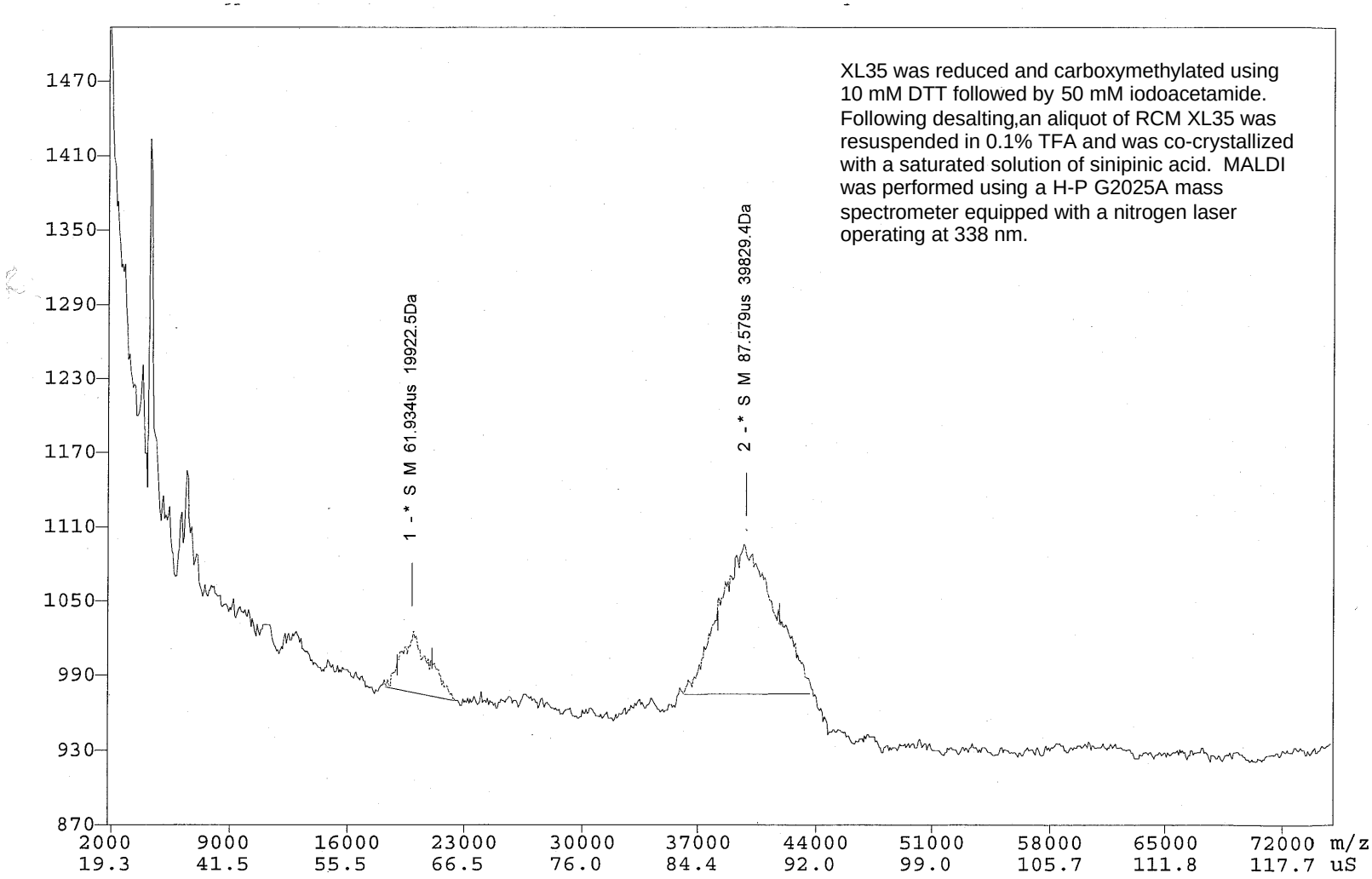

Figure 3-7: MALDI-TOF of Reduced and Carboxymethylated (RCM) XL35

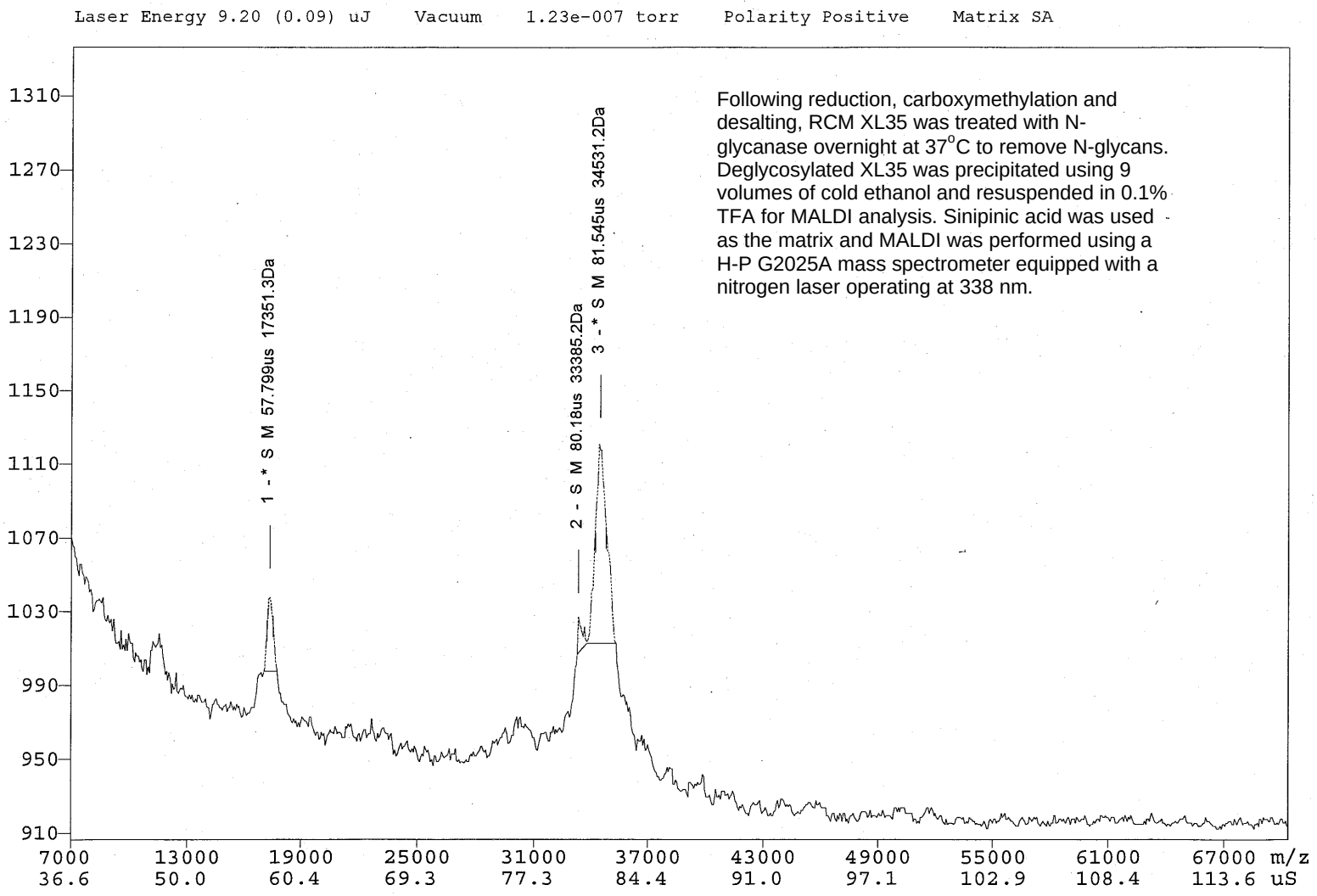

Figure 3-8: MALDI of RCM XL35 Treated with N-glycanase

Ligand Binding Properties of XL35 - Residues involved in ligand binding

A wide variety of buffers and additives that had been shown to partially disrupt oligomerization were assessed for their impact on XL35's ability to bind its native ligand. Surprisingly, XL35 binding activity was found to be very robust despite the addition of 0.1% SDS, 10-200 mM DTT, 2 M urea or 10% organic solvents. XL35 was treated with the additive to be tested and then the activity was assessed in the ELISA-based binding assay and compared to untreated XL35 analyzed under the same conditions. Briefly, total JCP was coated onto the wells of a microtiter plate, and after blocking, both treated and untreated XL35 was added to individual wells. After incubation for one hour, unbound XL35 was washed away and bound XL35 was detected by a streptavidin-HRP conjugate. These results are summarized in Figure 3-9 and show that XL35 retained a substantial amount of its ligand binding activity in the presence of a variety of chaotropes, surfactants, and reducing agents. It was surprising that the addition of both DTT and SDS did not have a greater effect on ligand binding activity. The ligand binding site is presumed to be composed of loops and turns that are in part stabilized by intramolecular disulfide bonds; therefore DTT would be expected to destabilize those regions in which the disulfides that act as tethers. Additionally, had the combination of surfactant and reducing agent been able to significantly disrupt the oligomeric structure of XL35, ligand binding would not have been detectable because the dissociation rates for the millimolar monovalent interactions are very rapid, as discussed below. The retention of approximately 40% of native (untreated) ligand binding activity suggests that both ligand-binding and oligomerization domains are substantially intact after these treatments.

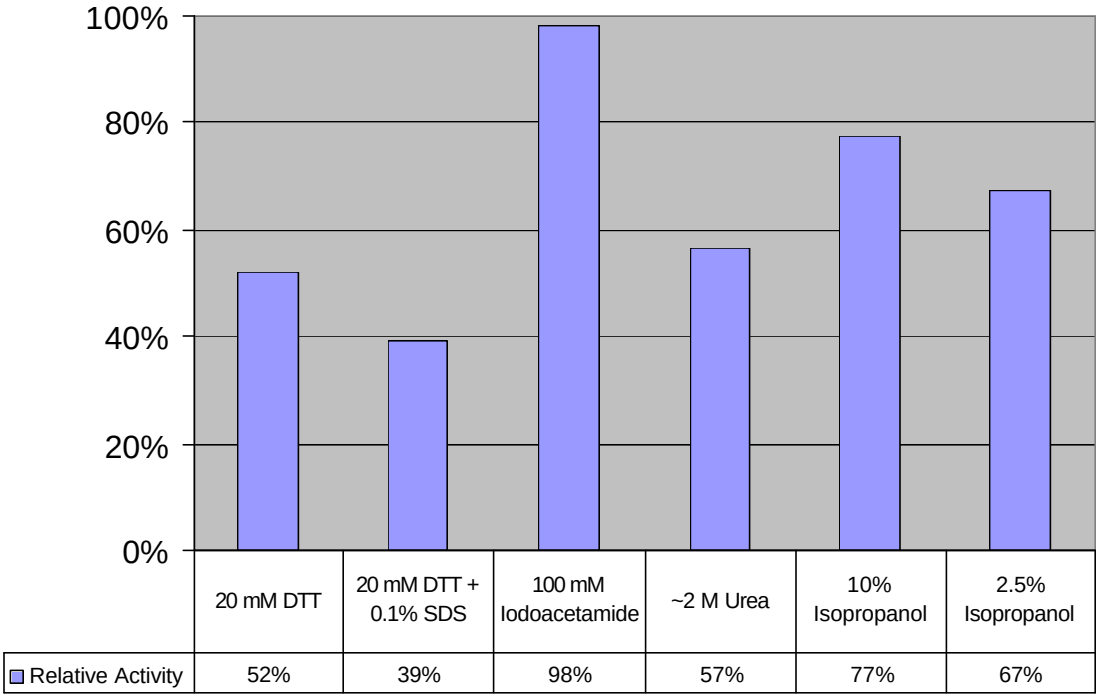

Figure 3-9: A Wide Variety of Chemical Treatments Do Not Eliminate XL35 Binding

Given that XL35 had been shown to be relatively insensitive to a wide range of chemical treatments, it was surprising to discover that two mild chemical treatments that modify tryptophan or the carboxylic acids on aspartate or glutamate completely abrogated ligand binding. The binding sites of almost all known galactose-binding lectins have been shown to contain a tryptophan and an acid-amide pair that are important in ligand binding. Alkylation of tryptophan using Koshland's reagent (2-Hydroxy-5-nitrobenzyl Bromide, HNBB) or the amidation of carboxylic acids using EDC and glycine ethyl ester completely eliminated XL35's ability to bind ligand, suggesting that these residues are critical for ligand binding. Although it is possible that the selected chemical treatments act by denaturing XL35 rather than by modifying residues in or near the ligand binding site, XL35's ability to bind ligand in the presence of several chemicals used to denature proteins tends to argue against that possibility.

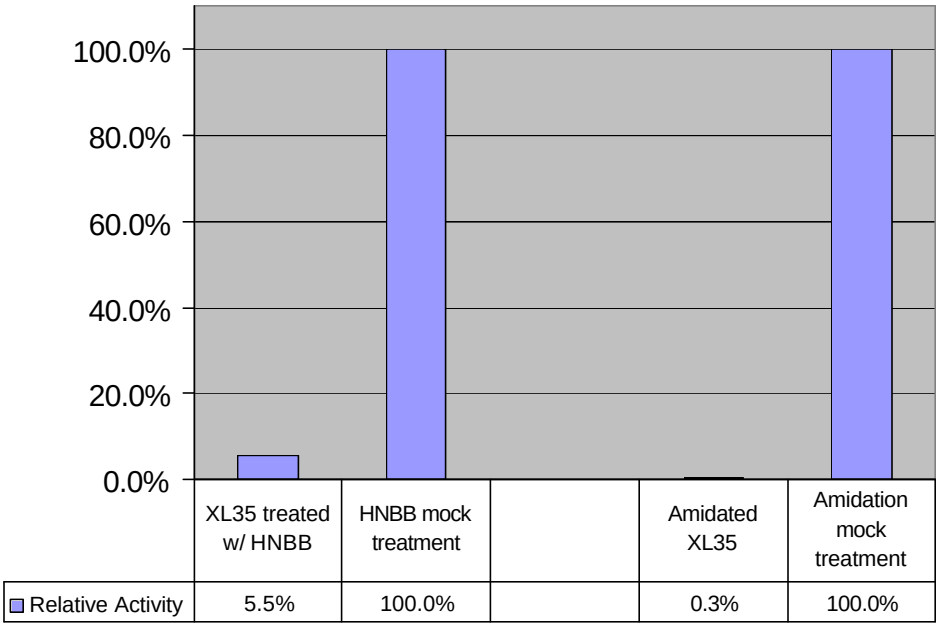

Figure 3-11: Chemical Treatments That Modify Trp or Asp/Glu Eliminate Binding Activity

Ligand Binding – ELISA Assay Development and Characterization

Several ELISA assay formats were initially explored to characterize in detail the ligand-binding properties of XL35. The initial inhibition assay involved coating microplates with JCP and then incubating the JCP-coated microplate with biotinylated XL35 in the presence or absence of commercially available mono- or oligosaccharides. Although the inhibition curves (a typical inhibition curve is shown in Figure 3-12) and IC_{50} values obtained from this assay correlated well with previous studies that measured the inhibition of agglutination of trypsinized rabbit erythrocytes (TRE), saturation isotherms for this assay were not reproducible. The JCP-BAP conjugate was developed to address the initial problems with reproducibility in the ELISA assay which were attributed to the multiple washing and incubation steps required for the initial assay format.

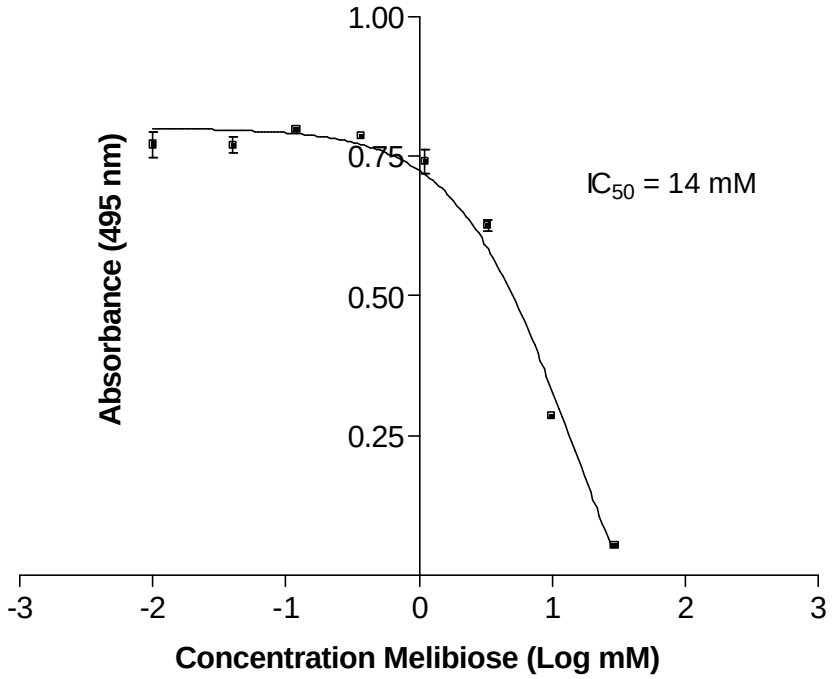

Figure 3-12: Effect of Melibiose on Binding of XL35 to JCP

Initial inhibtion ELISA used to map the selectivity of XL35. Total JCP was coated onto the wells of a microplate and after blocking, a fixed concentration of biotinylated XL35 was added in the presence of increasing amounts of a soluble ligand and allowed to incubate for one hour. Unbound biotin-XL35 was washed away and bound biotin-XL35 was quantitated through the addition of Streptavidin-HRP followed by color development using *ortho*-phenylene diamine.

Several alternative conjugates and assay formats were examined but the most reproducible results were obtained by coating XL35 onto a microtiter plate and incubating the bound XL35 with a fixed concentration of the JCP-BAP conjugate in the presence or absence of commercial and synthetic sugars. In order to verify that the assay was reporting on a specific (and saturable) interaction and to establish the midpoint of the saturation isotherm, saturation binding studies were conducted and were found to be reproducible (data are presented in Figure 3-13). Homologous inhibition experiments using an alkylated form of the JCP conjugate yielded an IC_{50} value of 11 μM

(Figure 3-14) which is in excellent agreement with the apparent K_D of 6.0 μM obtained from the saturation binding experiments shown in . The agreement between the K_D obtained from saturation binding studies and IC_{50} from homologous inhibition experiments demonstrated that the JCP-BAP conjugate was at the proper concentration to conduct inhibition studes. Additionally, the favorable comparison between these experiments also suggests that the conjugation of the alkaline phosphatase to the JCP did not lower the apparent affinity for the enzyme conjugate through a steric effect. Inhibition studies using negative controls such as mannose and N-acetylgalactosamine showed that the specificity of XL35 had not been significantly altered by immobilizing it on the microtiter plate (See inset, Figure 3-14).

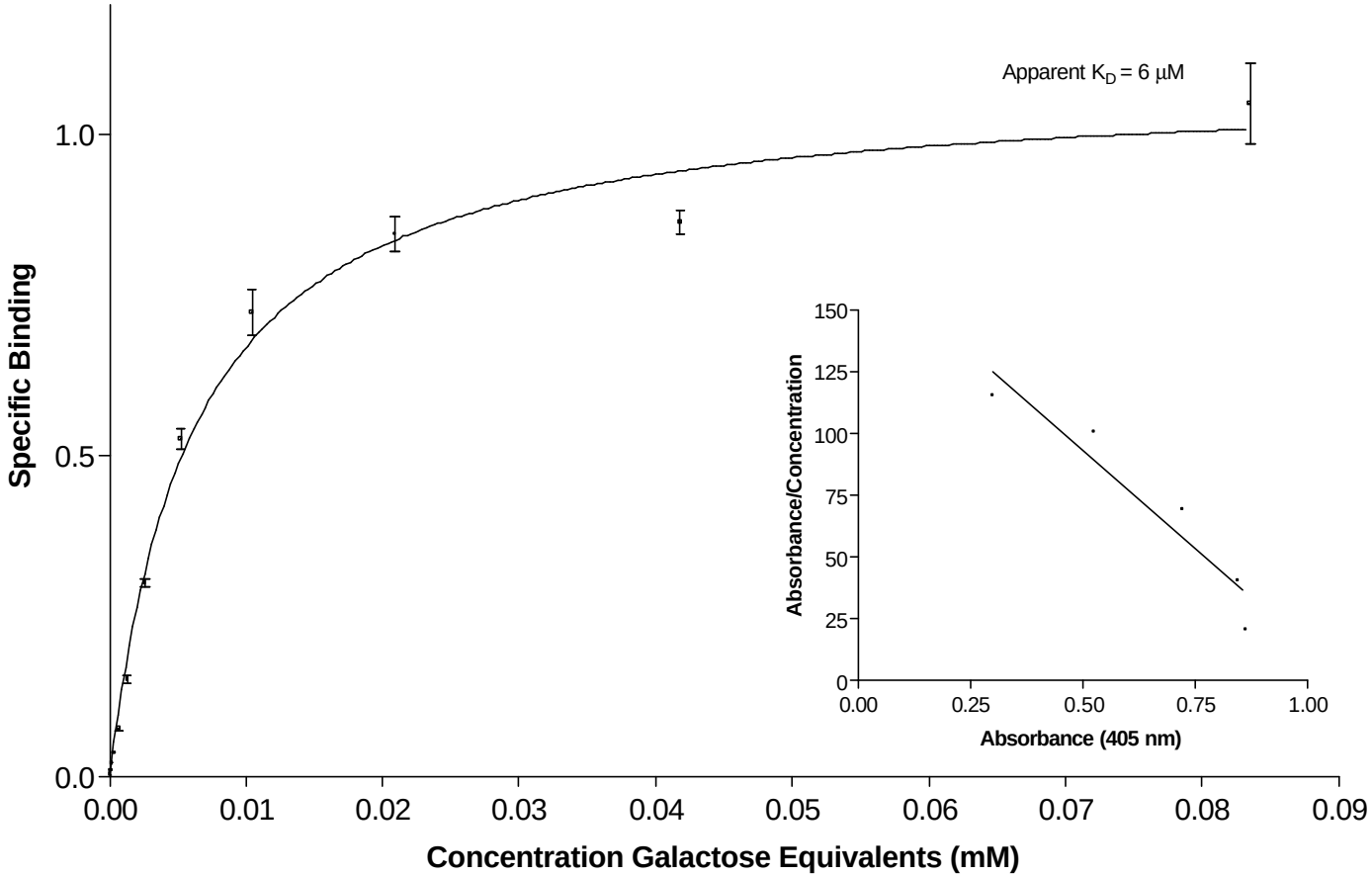

A fixed amount of XL35 was coated onto the wells of microtiter plates and nonspecific sites were blocked by adding 1% bovine serum albumin in TCS + 0.1% Tween 20. Increasing amounts of JCP-BAP conjugate was added and the quantity bound was determined through the addition of pNPP.

Figure 3-13: Saturation Binding Curve Using JCP-BAP Conjugate

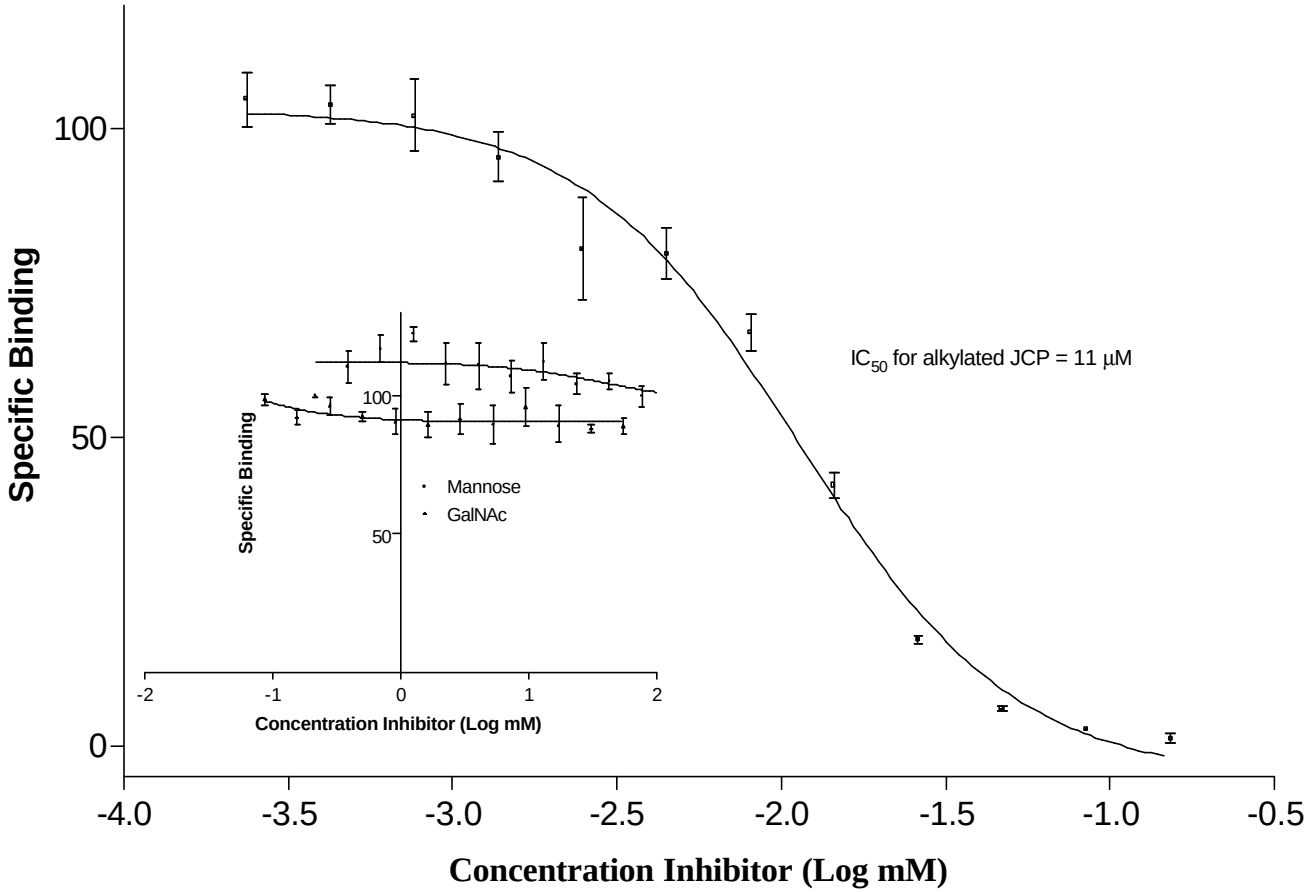

A fixed amount of XL35 was coated onto the wells of microtiter plates and nonspecific sites were blocked by adding 1% bovine serum albumin in TCS + 0.1% Tween 20. Increasing amounts of alkylated JCP (JCP-BAP lacking enzyme conjugate, homologous competitor) was added along with a fixed amount of JCP-BAP and the quantity bound was determined through the addition of pNPP. Inset shows negative controls using mannose and N-acetylgalactosamine.

Figure 3-14: Homologous Inhibition and Negative Controls

Monovalent Interactions

Table 3-2 summarizes the inhibition data for monovalent ligands using the inhibition ELISA with XL35 coated onto the plate. Although the IC_{50} values listed in the table do not represent true dissociation constants, they illustrate the weakness of the monovalent interaction, as well as the broad specificity that XL35 exhibits for galactose-containing oligosaccharides. XL35 is capable of recognizing both the α- and β-anomers of galactose and sulfation does not appear to affect binding, provided the sulfation occurs in the 6' position. Interestingly, galactose-containing saccharides with substitutions at the 2'-position are poor ligands, since neither galactosamine nor N-acetylgalactosamine can inhibit XL35 binding. Structurally distinct carbohydrates such as mannose and fucose are also not recognized, which is consistent with structural data on other lectins that has indicated that the geometry of the binding site for galactose-binding lectins tends to exclude ligands such as mannose or fucose[89].

Table 3-2: Inhibition Data for Monovalent Compounds

Compound	IC_{50} ($\times 10^{-3}$ M)	95% Confidence Interval ($\times 10^{-3}$ M)
Galactose	29	23-36
α-Methyl Galactose	27	24-31
β-Methyl Galactose	29	22-38
Galactose-6-sulfate	14	9.8-21
Galactose-4-sulfate	88	55-140
Galactose-6-phosphate	65	55-77
Galacturonic acid	48	41-55
Thiodigalactoside	2.8	2.2-3.5

Compound	IC_{50} ($\times 10^{-3}$ M)	95% Confidence Interval ($\times 10^{-3}$ M)
Melibiose	11	6.7-17
Lactose	14	12-17
α-Galactose-R	8.0	6.2-10
β-Galactose-R	26	21-31
(α-1,2Fucose)β-Galactose-R	21	16-28
Galactose(α-1,4)Galactose-R	8.4	6.6-11
Galactose(α 1,4)((α 1,2) Fucose)Galactose-R	3.1	2.2-4.4

R = aminopropyl group

Multi- and Polyvalent Interactions

Using inhibition ELISA, the strength of multivalent interactions between XL35 and several natural and synthetic ligands were also assessed. A series of small-molecule inhibitors with ligand valencies of 3 to 18 were synthesized in collaboration with Dr. Esther Arranz-Plaza of the Complex Carbohydrate Research Center, along with a series of multivalent glycopolymers that were constructed using a common 156 kDa polyacrylamide backbone that was synthesized by Dr. Aloysius Siriwardena.

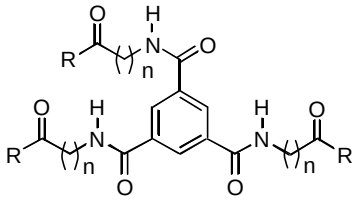

a) n = 3; b) n= 4; c) n=5

where R represents synthetic aminopropyl glycans

Figure 3-15: Synthetic Core for Trimeric Clusters

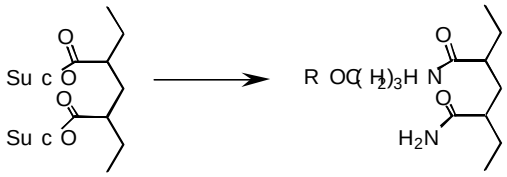

where R represents synthetic aminopropyl glycans

Figure 3-16: Polyacrylamide Backbone Used for Glycopolymer

To these scaffolds were conjugated synthetic mono- and disaccharides that had been tested previously as monovalent ligands. The ligand density was varied according to the type of ligand being synthesized. For the small-molecule inhibitors (valencies from 3-18), all available sites were derivatized with saccharides, while the polymers were designed so the synthetic mono- or disaccharides were conjugated to a fixed proportion (4, 8 or 17%) of the total number of sites available on the polymer backbone. This strategy permitted the direct comparison of identical ligands; one group presented monovalently, the other presented multivalently but as a well-defined synthetic species. The inhibition profile of the trimeric compounds was not significantly different than their monovalent counterparts, implying that the small molecule trimers and dendrimers were

incapable of spanning multiple sites on XL35. For that reason, further work with these small-molecule inhibitors was not attempted. The synthetic glycopolymers, however, did show an enhanced inhibition profile that was typically 10- to 20-fold better than that of the corresponding monovalent hapten when the data are corrected for valency (Table 3-3 and Figure 3-17). The enhanced inhibition profile for multivalent inhibitors that are capable of spanning multiple ligand-binding sites on XL35 is an example of the "cluster glycoside effect," which has been described as an enhancement in avidity that is larger than would be anticipated based on the valency of the inhibitor[163].

Table 3-3: Inhibition Data for Multivalent Ligands

Compound	IC_{50} ($\times 10^{-5}$ M) (Based on Glycopolymer concentration)	IC_{50} ($\times 10^{-3}$ M) (Valence adjusted for qty of glycan)
Melibiose (4% load)	1.6	0.4 (0.2-0.7)
Melibiose (8% load)	1.6	0.7 (0.4-1.2)
Melibiose (17% load)	0.7	0.6 (0.4-0.9)
All subsequent polymers had 17% loading		
α-Galactose	1.8	2.5 (1.9-3.3)
β-Galactose	0.9	0.4 (0.2-0.6)
Galactose(α-1,4)Galactose	1.9	1.2 (1.1-2.5)
β-Galactose((α-1,2)Fucose)	2.4	1.7 (1.1-2.5)
Galactose(α-1,4) Galactose((α-1,2)Fucose	0.5	0.4 (0.3-0.5)

Inhibition ELISA using XL35 coated onto microplates. A fixed amount of XL35 was passively coated onto microplates and nonspecific sites were blocking using 1% bovine serum albumin/0.1% Tween 20 in TCS. Increasing amounts of glycopolymer were added to a fixed amount of JCP-BAP conjugate and incubated in the microplates overnight at 4°C. Unbound material was washed away and bound material was quantitated using pNPP. Results shown are either valence-corrected (based on the quantity of mono- or oligosaccharide) or are based on the molar quantity of polymer (not valence-corrected).

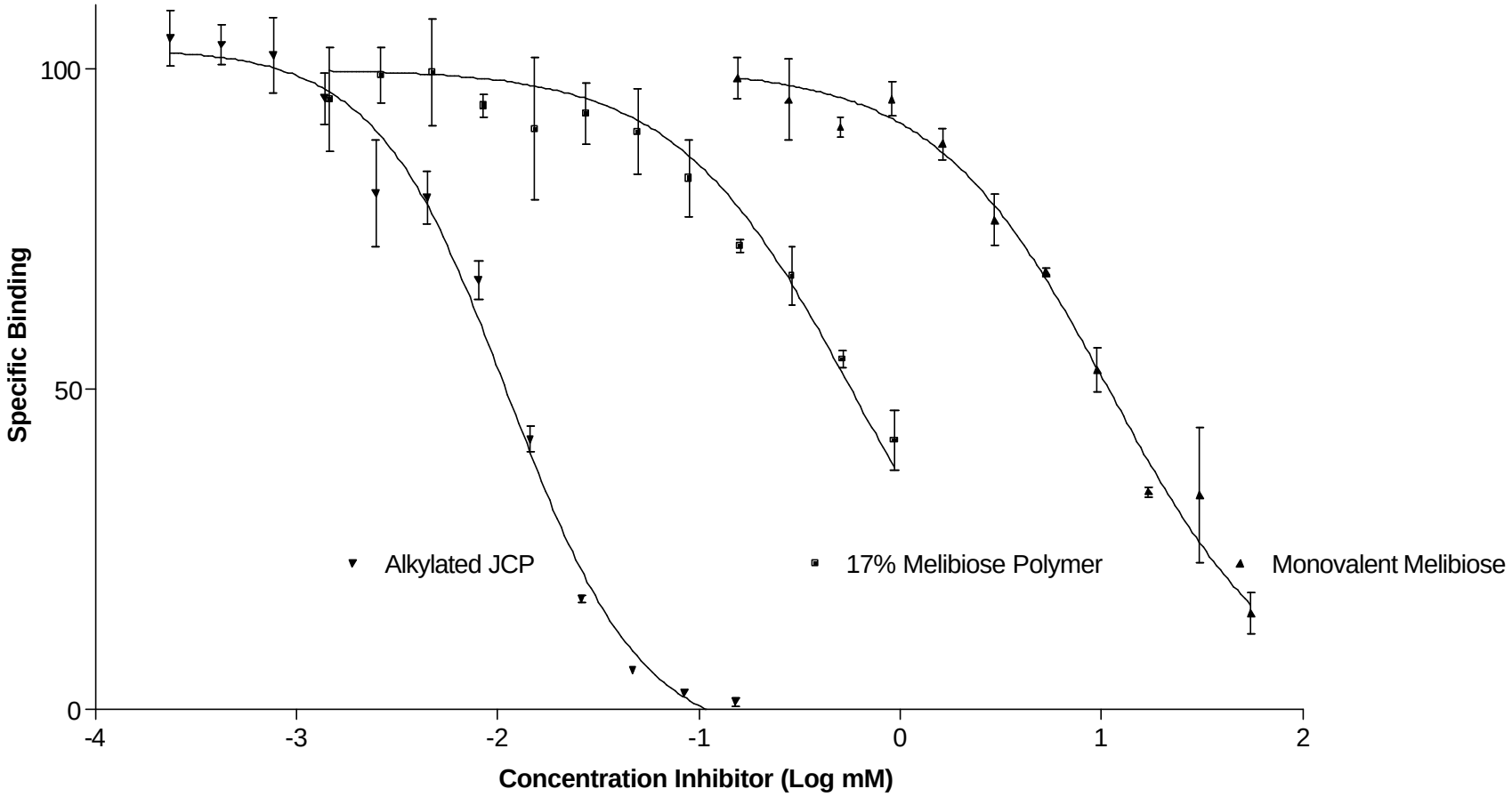

A comparison of the valence-corrected inhibition ELISA curves for a series of monovalent and multivalent ligands showing the enhancement in avidity observed with increasingly multivalent ligands.

Figure 3-17: Comparison of Monovalent and Multivalent Ligands for XL35

Ligand Binding – Surface Plasmon Resonance Analysis

Surface plasmon resonance (SPR)[164-167] was used to study the kinetic and equilibrium binding characteristics between XL35 and mono- and multivalent ligands. A series of sensorgrams of XL35 using several concentrations of lactose as a ligand is shown in Figure 3-18. The association and dissociation profiles reveal the very fast kinetics which typify the weak interaction characteristic of a lectin binding to a monovalent ligand. Attempts were made to generate a saturation binding curve using SPR in conjunction with monovalent ligands; however, the high concentrations of monovalent ligands required to saturate the system caused large baseline shifts that made it impossible to determine the K_D accurately using this approach.

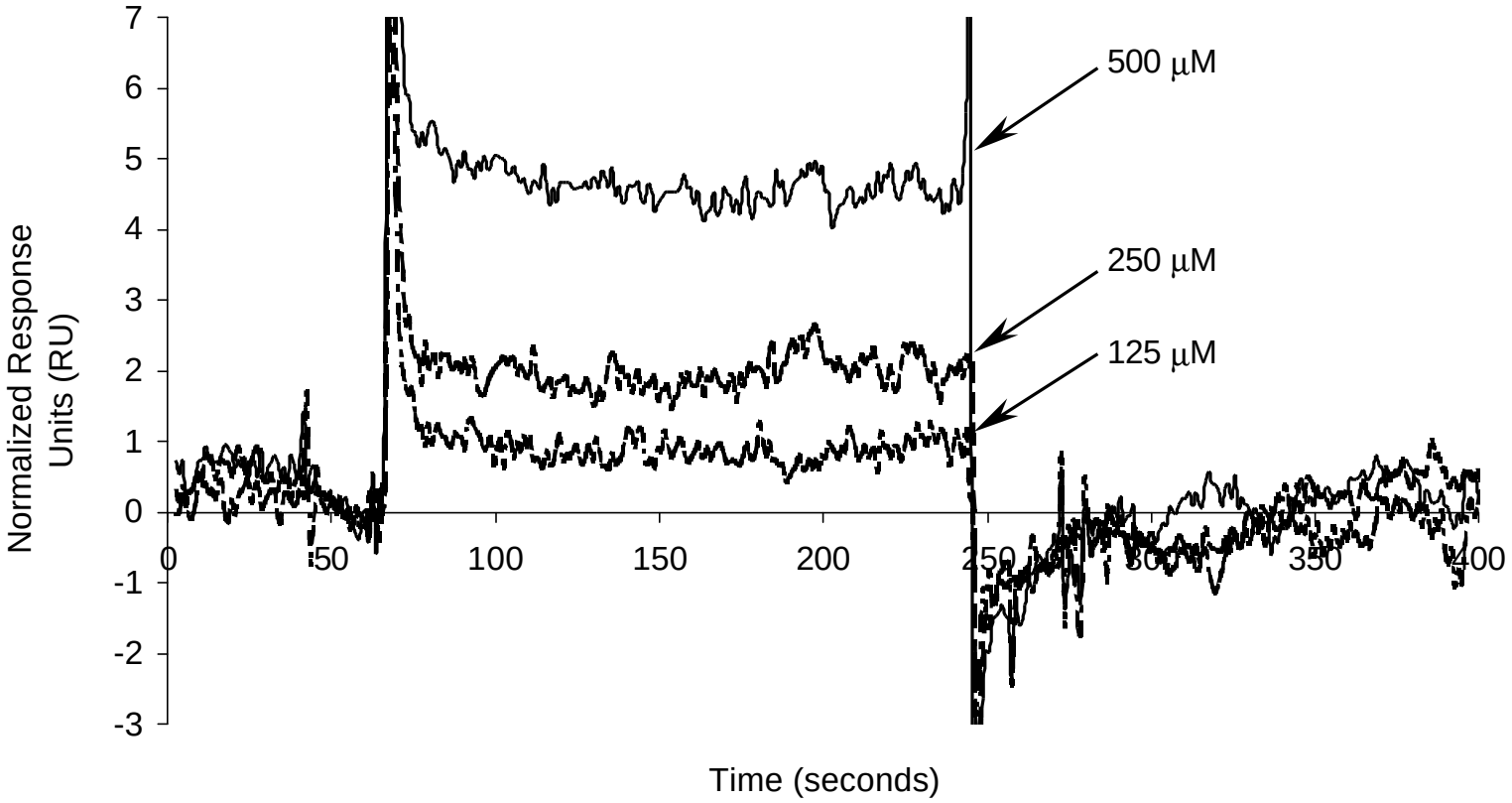

Figure 3-18: Sensorgram of Monovalent Ligand (Lactose)

Multivalent Interactions by SPR

ELISA results had suggested that the small-molecule inhibitors could not span multiple binding sites, and to directly test this hypothesis, surface plasmon resonance (SPR) studies using both small-molecule and polymeric inhibitors were employed. Initial experiments focused on comparing the association and dissociation profiles of a trimeric glycocluster and a glycopolymer derivatized with melibiose. If either ligand were capable of interacting with multiple sites on XL35, then the observed SPR dissociation profile would differ significantly from that of a monovalent ligand, since the apparent off-rate (k_d apparent) would be the microscopic k_d raised to the valency of the interaction (k_d apparent = k_d^n, where n is the valency of the interaction). Qualitatively, this may be thought of as the decreased probability that a multivalent ligand can dissociate from n sites simultaneously, a condition that is required for multivalent ligands to dissociate completely from XL35. Estimates of half-lives for lectin-ligand complexes, when calculated in this fashion, are seen to increase dramatically with valency.

The comparison of the trimer and melibiose glycopolymer is shown in Figure 3-19, along with an N-acetylglucosamine-derivatized glycopolymer that served as a negative control. The trimeric compound cannot span multiple XL35 binding sites and behaves as a monomeric inhibitor (similar to the sensorgrams shown in Figure 3-18), while the melibiose glycopolymer shows a rapid but measurable association phase, followed by a slow dissociation phase that indicates a multivalent interaction. The observed k_d is the product of the off-rate for several independent sites.

In the absence of the regeneration pulse at approximately 1000 seconds, the sensorgram does not return to baseline even under conditions of flow that would be expected to prevent or at least greatly limit rebinding of the glycopolymer, had it been able to dissociate from XL35. In a control experiment, an identical concentration of the N-acetylglucosamine-derivatized glycopolymer was injected over the same XL35 derivatized surface but gave no detectable response, confirming that the interactions of the glycocluster and melibiose glycopolymer were indeed selective.

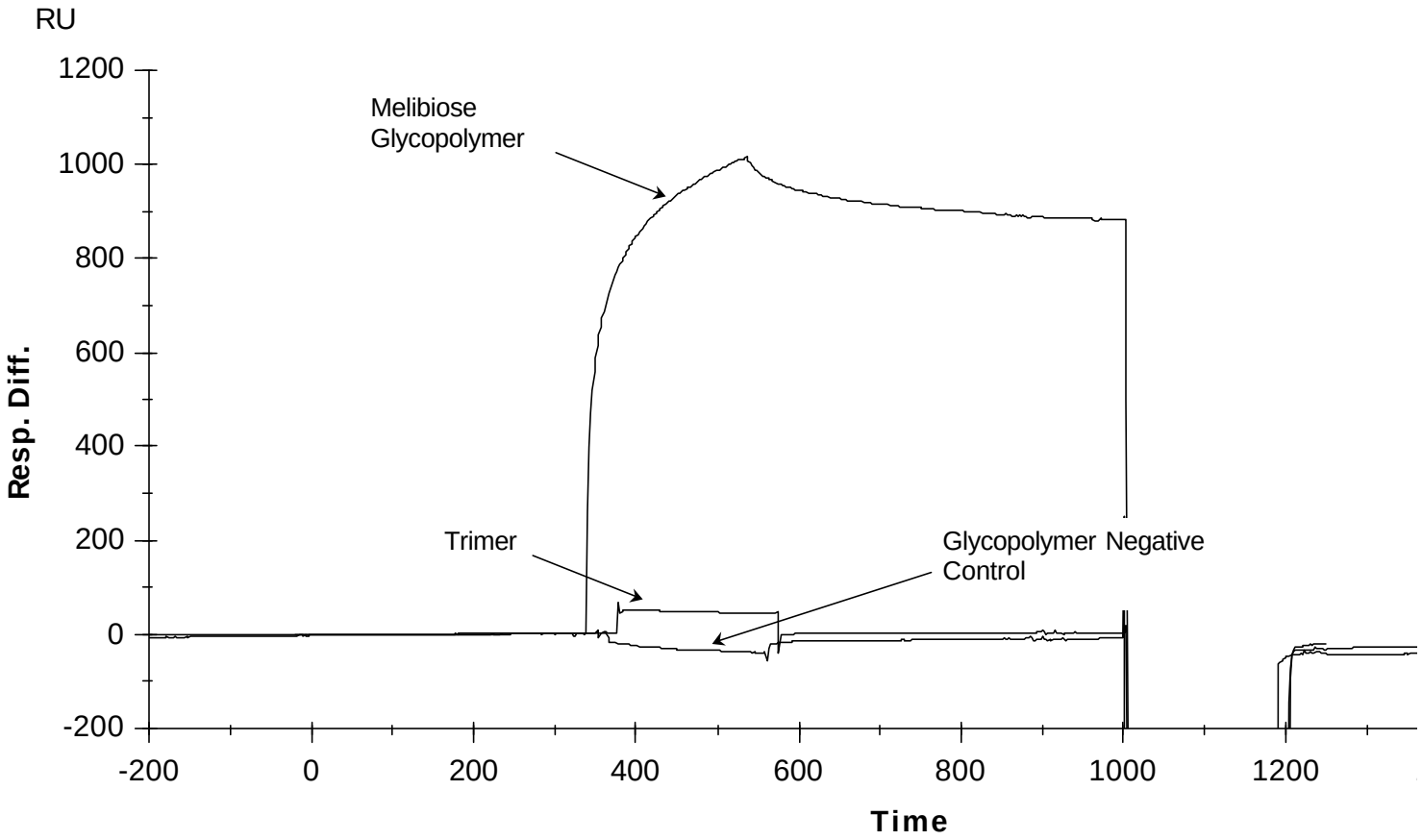

Figure 3-19: Overlay of SPR Analyses Showing the Effect Multivalency Has on the Kinetics of the Interaction

Having established that the interaction between XL35 and the glycopolymers was indeed multivalent, a series of kinetic and equilibrium SPR experiments was used to probe the binding event in more depth. The kinetic experiments were designed to study the avidity of the multivalent interaction by determining the dissociation constants for the melibiose glycopolymers, and they were performed using an SPR chip to which 5000 RU of XL35 had been coupled. A series of concentrations of the 17% melibiose polymer was injected over the chip using the Kinject command with an association time of 120 seconds and a dissociation time of 1800 seconds. The particularly long dissociation time was chosen in an attempt to maximize the chances that bound polymer could dissociate. At a flow rate of 15 μL/min, the XL35:glycopolymer complex was washed with 7500 flow-cell volumes of buffer during the 30-minute dissociation phase. Analysis of the group of sensorgrams obtained under these conditions indicated that the dissociation profile was biphasic, with an initial dissociation phase that was relatively rapid, and permitted 15% of bound glycopolymer to dissociate after 120 seconds, which corresponded to a rate of dissociation of 7.5%/min. The population of glycopolymer capable of dissociating quickly presumably represented the fraction that interacted with a minimal number of XL35 binding sites and was consequently able to dissociate rapidly. After the initial 120 seconds, however, the rate of dissociation dropped sharply to 0.43%/min. After 30 minutes of dissociation under flow, only 27% of the bound polymer was able to dissociate. The apparent off-rate for the entire 30-minute dissociation phase was estimated to be 1.75×10^{-4} sec^{-1}, but if the initial 120 seconds containing the weakly bound polymer were to be excluded, the apparent off-rate dropped substantially to 7.85×10^{-5} sec^{-1}. Based on these calculations, the difference between observed off-rates for monovalent and multivalent interactions was approximately 1000-fold.

Control experiments were conducted using identical concentrations of the melibiose polymer at flow rates of 5, 15 and 75 μL/min to demonstrate that the results were not affected by mass transport limitations. Additionally, although the dissociation profile indicates a very stable complex between XL35 and the synthetic polymer, the dissociation profiles do not appear to show the formation of an irreversible complex since variations in injection time do not significantly change the dissociation profile.

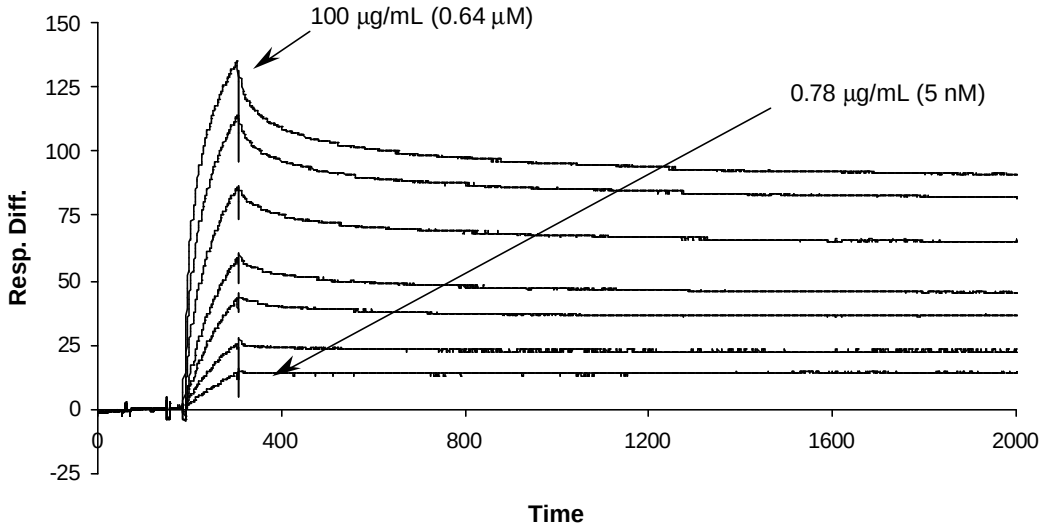

Serial dilutions of melibiose glycopolymer were injected over 5000 RU of XL35 that had been covalently coupled to an SPR chip. Even after 1800 seconds, the sensorgrams fail to return to baseline, indicating the stability of the multivalent interaction between XL35 and multivalent ligands.

Figure 3-20: A Series of Kinetic Sensorgrams Using Melibiose Polymer

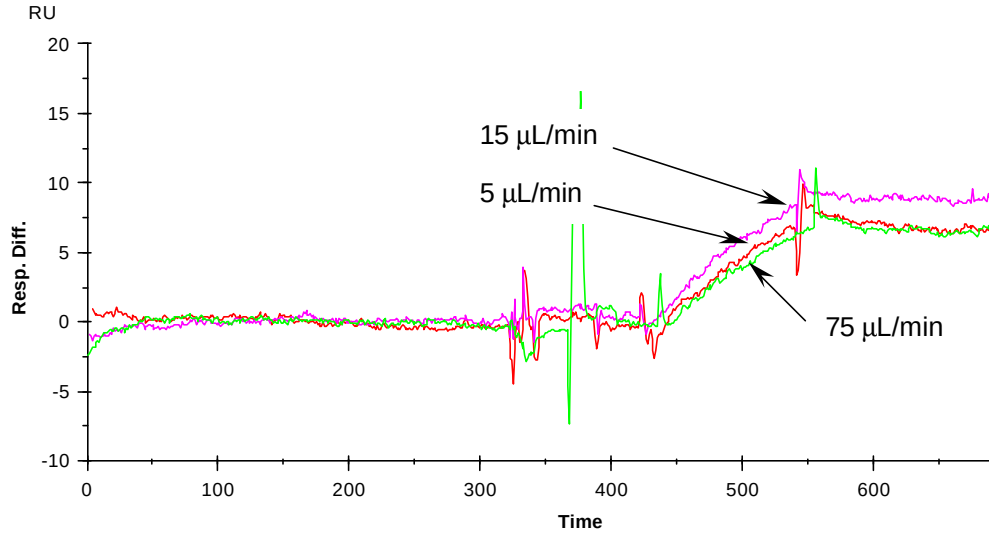

Identical concentrations of melibiose glycopolymer were injected at different flow rates to determine whether the previous kinetic results were affected by mass-transport limitations. Despite the large size (156 kDa) and extended structure of the glycopolymers, no effect was observed.

Figure 3-21: Evaluation of Mass Transport at Low Concentrations of Melibiose Polymer

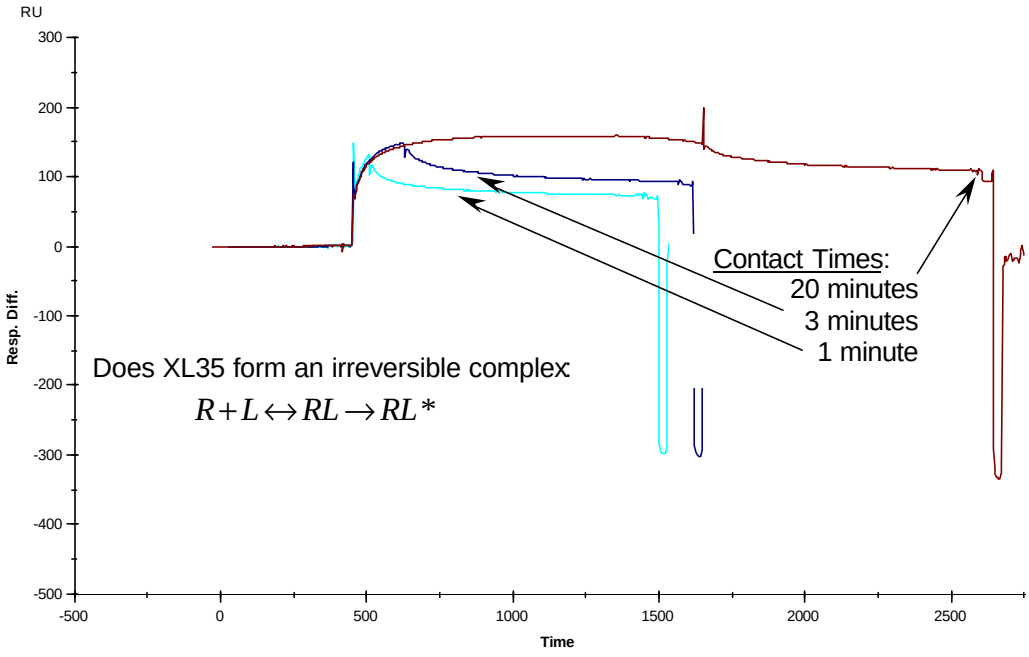

Identical concentrations of melibiose glycopolymer were injected using increasing contact times. Analysis of the dissociation profile as a function of association time did not suggest the formation of a irrerversible complex, although the apparent k_{off} does get smaller as the contact time is increased.

Figure 3-22: Using SPR to Assess the Formation of a Irreversible Complex

After analyzing the data from Figure 3-22, however, it was apparent that the dissociation constant varied as a function of contact (association) time: as the contact time increased, the apparent k_{off} decreased (Table 3-4). By increasing the contact time, the experimental conditions selected for glycopolymers that were tethered at many points, while those multivalent ligands that were only weakly associated through one or two binding sites could be competed away by the large excess of ligand flowing over the surface of the chip. This experiment is analogous to a hybridization experiment where the probe:target complex is washed with a series of buffers of increasing stringency: by the final wash, only those sequences that hybridize very tightly to the probe can be detected.

Table 3-4 : Differences in Apparent k_{off} as a Function of Association Time

	Association Time		
	20 minutes	3 minutes	1 minute
k_{off} (sec^{-1})	3.341×10^{-3}	5.171×10^{-3}	6.482×10^{-3}
Half-life (sec)	207.5	134.1	106.9
Maximum Response	147	98	65
Plateau	119	70	44
Ligand remaining*	81%	71%	67%

*Defined as the percent ligand still bound after 1000 second dissociation phase at 5 µL/min.

The dissociation of a typical ligand from its receptor (one that does not form a irreversible complex) would be expected to follow the following equation:

$$R = R_0 e^{-k_{off} t}$$

where:

R_0 = the initial response at T=0 (when the injection of ligand ends)

R = the response after some time interval T

k_{off} = the apparent dissociation rate constant (sec^{-1})

t = time in seconds

Based on control experiments, the kinetic data obtained using the melibiose glycopolymer were valid and could potentially be used to determine the equilibrium K_D. The stability of a multivalent interaction, however, renders its evaluation by a kinetic approach complex, since the data cannot be fitted to any simple mono- or bivalent model. An alternative approach would be to employ equilibrium SPR analysis to obtain the dissociation constant, although multivalency and the resulting stability require modification of typical experimental procedures employed. If the rate equation of a receptor-ligand interaction is considered:

$$d[RL]/dt = k_a[R][L] - k_d[RL]$$

where [R] = concentration of receptor

[L] = concentration of ligand

[k_a] = association constant

[k_d] = dissociation constant

and $d[RL]/dt$ represents the change in the extent of binding with respect to time, equilibrium will be reached when $d[RL]/dt = 0$, but this is only true as t approaches infinity. After 5 half-lives, however, the measured binding is within 3% of the true equilibrium value, and Motulsky and Mahan[168] have demonstrated that the time to reach 5 half-lives is given by:

$$t = \frac{5 \times 0.69}{k_a L + k_d}$$

Unless the concentration of ligand [L] is very high, a ligand with a small k_d will require a very long contact time in order to reach equilibrium. This result can be rationalized in a physical sense, since under conditions of equilibrium, for every receptor-ligand complex formed another must dissociate (which is statistically unlikely for multivalent interactions). Additionally, since a concentration of ligand approximately 10 times that of the K_D is required to generate a saturation binding isotherm, this type of experiment requires not only long contact times but also injections of large amounts of ligand.

The saturation binding experiments shown in Figure 3-23 were designed to strike a balance between the long injection times required to reach equilibrium and the large quantities of material required to saturate the immobilized XL35. The data showed that despite the long contact times employed, the system had not come to complete equilibrium. Nevertheless, using this approach a non-valence corrected K_D (apparent) of 1.67×10^{-6} M can be calculated from the saturation binding isotherm, which is in excellent agreement with apparent K_I of 3.7×10^{-6} M determined by the inhibition ELISA assay.

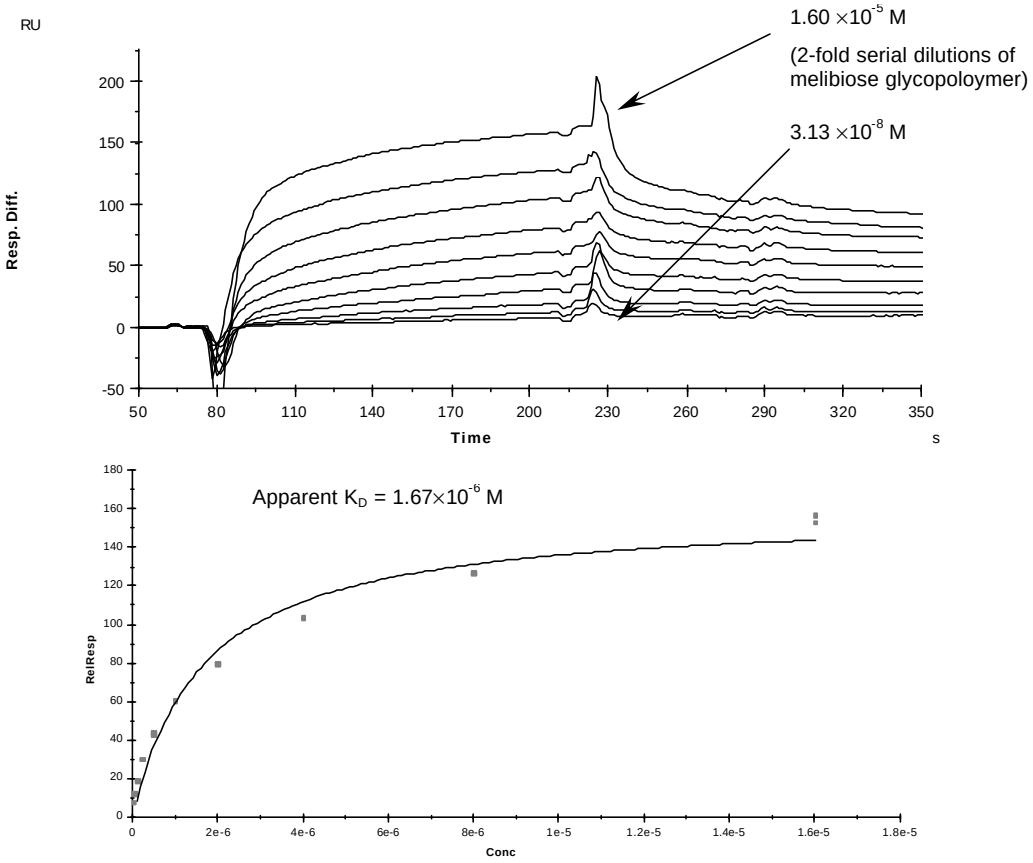

Figure 3-23: Equilibrium SPR Analysis Using Melibiose Glycopolymer

Similar SPR analyses of ligand binding were also conducted using the native JCP ligand (Figure 3-24). Although the nature of the interaction precludes quantitative analysis, there are striking differences between the interaction of XL35 and its native ligand as compared to either monovalent interactions or even the interaction between XL35 and the synthetic glycopolymers. While the monovalent sensorgrams showed extremely rapid off-rates and the glycopolymers showed very slow but measurable dissociation, the binding profiles between XL35 and the JCP showed *no dissociation over a 30-minute experiment*. The apparent off-rate is so low that it cannot be measured by SPR. In that respect, the binding event between XL35 and its ligand is similar to the interaction between biotin and streptavidin, which is one of the strongest non-covalent interactions known.

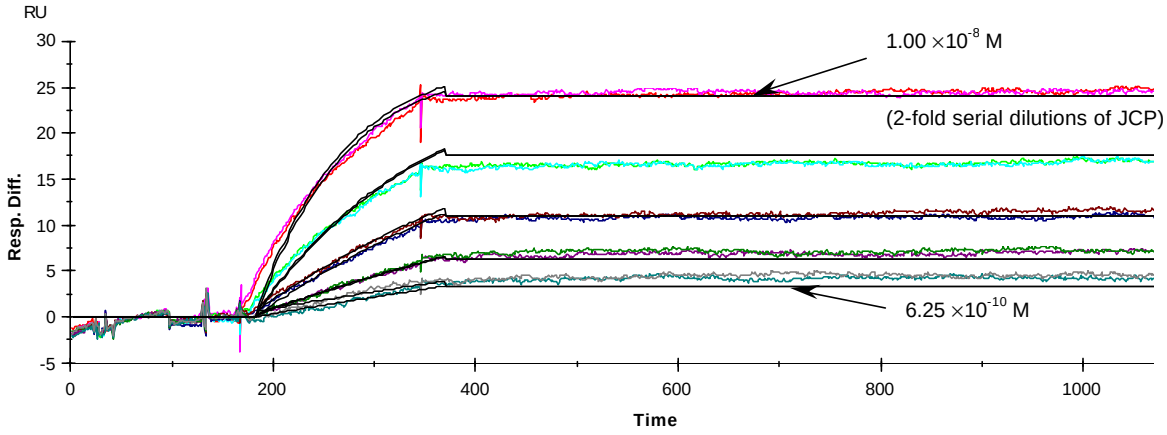

Figure 3-24: Sensorgram of Interaction Between XL35 and Solubilized JCP

While it is possible to attempt either kinetic or equilibrium experiments to quantitate the interaction between XL35 and the JCP using SPR, the inability to dissociate bound JCP would require prohibitively long injections to achieve equilibrium. The data presented in Figure 3-13 and 3-14, which were obtained from microplate-based assays that can be incubated overnight, represent the best way to determine the apparent K_D for the interaction between XL35 and JCP because the difficulties associated with using a flow-based system to study multivalent interactions are avoided.

In summary, oligomerization plays an important role in the biochemical function of XL35 because the formation of oligomers rendered the ligand binding event multivalent and therefore highly stable. The process of oligomerization appears to use a combination of hydrophobic contacts and disulfide bonds to form a macromolecule that is a 12-mer and appears to be globular in shape. Ligand binding results showed that XL35 has a broad specificity for galactose-terminated oligosaccharides although the β-anomers of galactose were bound with measurably lower affinity.

Chemical modification experiments potentially implicated tryptophan residues and a carboxylic acid moiety in ligand binding which is consistent with crystallographic structures of lectins. XL35 appeared to bind monovalent ligands with millimolar dissociation constansts but kinetic SPR measurements showed little to no dissociation of multivalent ligands, even under conditions of flow.

CHAPTER 4 - DISCUSSION

One focus of this dissertation was to gain an understanding of the structural elements of XL35 that contribute to its biological function. A series of detailed ligand binding experiments were designed to map the selectivity, affinity and avidity of the lectin-carbohydrate interaction in detail. Additionally, a set of complementary macromolecular characterization studies were used to determine the size and shape of the XL35 oligomer as well as to predict some of the regions and residues involved both in oligomerization and ligand binding.

Structure and Organization of XL35

The identification of the N-terminus of XL35 and the determination of the molecular mass of monomeric XL35 were important components of the structural studies on XL35, since these data provided information on the precise mass of the XL35 monomer and permitted an accurate determination of ∇, the partial specific volume. It was surprising, however, to find that majority of reduced and carboxymethylated (RCM) XL35 that had been exhaustively digested with N-glycanase displayed a molecular mass of 34,531 Da, which corresponds to the molecular weight of full-length XL35 based on its deduced amino acid sequence. A smaller form of the full-length polypeptide was also observed that lacked the N-terminal 15 amino acids, corresponding to the predicted signal peptidase cleavage site between Ser15 and Gln16. The presence of both forms results in heterogeneity of mass, determined both by MALDI-TOF as well as by N-terminal sequencing. MALDI data also provided information on the mass of the glycans

present on XL35, since the difference in mass between RCM XL35 and the deglycosylated form of this sample was approximately 5300 Da. Based on the average molecular weight of a complex N-glycan, which is 2221 Da for a disialylated biantennary structure, these data suggest that 2-3 of the putative N-glycosylation sites are occupied. Additional evidence suggesting multiple N-glycosylation sites are occupied can be inferred from the degree of micro-heterogeneity observed in the MALDI data for glycosylated RCM XL35, which showed a an exceptionally broad peak.

XL35's presence in the cortical granules demonstrates that it most likely entered into and transited through the regulated secretory pathway as opposed to the constitutive secretory pathway. This observation could explain why the N-terminal region of XL35 is largely full-length, and shows only minimal proteolysis. It is particularly interesting that the bulk of the polypeptide is not cleaved while a relatively small portion of secreted XL35 is processed by the signal peptidase. Perhaps XL35 oligomers are formed post-translationally in the ER and a single polypeptide containing a cleaved signal sequence is sufficient to direct the entire oligomer towards the secretory granules. The regulated secretory pathway that ultimately terminates in specialized secretory granules is typically used by proteins that undergo secretion in response to a cellular stimulus,[169, 170] as is the case for many hormones, bioactive peptides, and XL35. Although many of the specific events and factors involved in the regulation of this pathway are poorly understood, it appears that proteins destined for this pathway are specifically sorted in the *trans*-Golgi network (TGN) and are packaged into immature granules which then condense to form mature secretory vesicles. The prototypical chaperones involved in the regulated secretory pathway appear to be a class of acidic proteins known as the granins[171-175], which have specific N- and C-terminal sequences that appear to target them to these immature secretory granules. The granins have been shown to undergo Ca^{2+} and pH-dependent aggregation[176]. Attempts to

secrete recombinantly expressed XL35 into cell culture medium have been unsuccessful using a variety of expression systems and host cell types. Evidence from these expression studies with recombinant XL35 could also be interpreted to suggest that XL35 could require specialized packaging or recognition by a specific chaperone.

Hormones such as prolactin packaged into regulated secretory granules are known to form aggregates that serve to concentrate the proteins up to 200-fold during the condensation process[177]. By SDS-PAGE and by sedimentation equilibrium analysis, XL35 forms oligomers that appear to be composed of approximately 12 monomers. The shape factor (R_H / R_{sph}) for XL35, which is a measure of how closely the macromolecule's shape approximates a perfect sphere, is 1.42, suggesting that the XL35 oligomer is essentially globular. Although the techniques used to obtain the shape factor are incapable of providing detailed structural information, the difference between the shape factors obtained for XL35 and conglutinin (shape factor of 2.7)[178] indicate that XL35 does not contain extended linear structures such as the collagenous domains found in MBP and conglutinin. SDS-PAGE analysis indicates that the majority of the higher-order oligomers of XL35 are formed via hydrophobic contacts rather than through intermolecular disulfide bonds, and once formed, these oligomers appeared to be relatively stable, since treatment of the oligomer with 0.1 % SDS and glycerol did not disrupt oligomerization unless the protein was heat-denatured.

SDS-PAGE analysis of XL35 that had been denatured but not reduced suggests that XL35 monomers associate to form dimers through interchain disulfide bonds since the smallest oligomer seen in Lane 2 of Figure 3-2 is a dimer. XL35 that had been denatured using heat and surfactants prior to SDS-PAGE shows a mixed population of oligomers from N=2 to 12 (Figure 3-2, Lane 2), suggesting that the higher-order

oligomers are formed through a combination of hydrophobic contacts and disulifide bonds that are resistant to heat treatment.

Although it is possible to partially disrupt oligomerization using surfactants and reducing agents, data presented here and in earlier studies[115] show that XL35 can remain biologically active despite a wide variety of chemical treatments, including the use of chaotropes, surfactants, organic solvents and reducing agents. While these general treatments that tend to denature proteins did not eliminate XL35 ligand binding activity, the chemical modification of certain amino acids was effective and suggests that the specific amino acid residues in or near the binding site of XL35 are conserved between other galactose-binding lectins. Koshland's reagent, which specifically alkylates tryptophan at neutral pH eliminated XL35 binding activity, similar to the effects seen by this reagent on other lectins[179-184]. Additional control experiments where the JCP was treated with Koshland's reagent showed no effect on binding activity, demonstrating that this treatment exerted an effect only on XL35. Alignments of several galactose-binding lectins based on the bound galactose ligand show a similar pattern of hydrophobic packing between the plane of the C3-C6 atoms on the galactose moiety and the indole ring of the tryptophan[89]. Provided that the alkylation reaction is completely specific for tryptophan, the introduction of a bulky benzyl group onto the C3 of the indole ring[185] would be expected to significantly perturb the native conformation of the modified tryptophan. Based on the crystal structures of galactose-binding lectins and the chemical modification data presented here, it follows that treatment with Koshland's reagent would prevent XL35 from binding to its ligand.

An additional structural motif employed by Ca^{2+}-dependent lectins is the use of an acid-amide pair within the binding pocket that chelates Ca^{2+} and properly orients the sugar for binding via hydrogen bonding to vicinal hydroxyls on the glycan. By using EDC, a zero-length cross-linker, it is possible to selectively conjugate a blocking group

(in this case, glycine ethyl ester) to any available carboxylic acid moeities, including the putative group involved in XL35 ligand binding. As is the case with Koshland's reagent, the reaction conditions were very mild but XL35 that had been amidated using glycine ethyl ester lost all measurable ligand-binding activity. It is possible that the selected chemical treatments simply denatured XL35 or modified additional amino acid residues required for ligand binding but XL35's apparent stability in the presence of more non-specific protein denaturing agents tends to argue against that possibility. Instead, the data presented here suggest a specific role in binding ligand for the specific amino acids modified by amidation, most likely carboxylic acids, or the amino acids modified by treatment with Koshland's reagent, tryptophan. These results with XL35 are corroborated by crystallographic data on a wide variety of galactose-binding lectins[89].

Although amidation experiments demonstrated that a carboxylic acid functionality is likely involved in ligand binding, the large number of aspartic and glutamic acid residues in the deduced XL35 sequence makes it difficult to use these data to infer the location of the binding site. Tryptophan is a considerably rarer amino acid as compared to aspartate and glutamate, so data from experiments using Koshland's reagent provided more information on the potential location of the carbohydrate recognition domain (CRD). There are five tryptophan residues in the XL35 sequence and all are located within the central portion of the polypeptide that had previously been predicted to contain the CRD based on the prevalance of extended structures, including loops and turns, found in that region. Additionally, all five tryptophan residues are conserved between XL35, HL-1 and HL-2, suggesting a conservation of residues involved in ligand binding.

In summary, these chemical modification data correlate well with previous studies[88] that have shown that the combination of Ca^{2+} chelation and the use of a correctly positioned hydrophobic residue is critical for ligand binding and contributes to

the specificity of lectin-sugar interactions. In most galactose-binding lectins, that residue is Trp, although there is one structure of a bacterial lectin that employs Phe rather than Trp[88]. Despite the absence of a C-type lectin domain as defined by Drickamer (Figure 1-4), XL35 ligand binding does appear to use several of the same amino acid residues previously identified as being important for ligand binding in C-type lectins.

XL35 Ligand Binding Properties

The ELISA assay used to characterize the selectivity and affinity of XL35 was carefully developed and the final assay format reflected the need to design a reproducible assay that could be performed using only 25 μL of ligand, since many of the synthetic glycans were in short supply. Although many of the glycans tested were of synthetic origin, all of the structures were based on core epitopes found repeatedly in the JCP. The ability of these glycans to inhibit binding between XL35 and its native ligand demonstrates that XL35 does not require both protein and carbohydrate epitopes as is clearly the case with P-selectin[186]. Control experiments using mannose and fucose, two ligands that should serve as negative controls for XL35 based on previous reports, showed that irrelevant monosaccharides were unable to inhibit XL35 binding even at concentrations that were five-fold higher than those used in the inhibition ELISA. The inability of irrelevant ligands to show any measurable inhibition by ELISA demonstrated that the results obtained here represent a specific carbohydrate-protein interaction and that the assay format did not affect XL35's ligand binding properties.

Selectivity

Based on the inhibition ELISA using the JCP-BAP conjugate, the two most potent monovalent ligands for XL35 were thiodigalactoside, which is a divalent β-galactoside and the synthetic trisaccharide containing the complete core epitope Gal(α,1-4)Gal(Fuc(α,1-3)) that is found on many of the JCP glycans[150, 155, 157]. When the

inhibition data were adjusted for valency, the synthetic trisaccharide does appear to be a marginally better inhibitor. Since thiodigalactoside is a divalent hapten, when its inhibition data are corrected for valency, its IC_{50} becomes 5.6 mM. XL35 has broad selectivity for oligosaccharides terminated with either the α- and β-anomers of galactose, but the β-anomers of galactose-containing mono- and disaccharides were consistently poorer inhibitors than their corresponding α-anomers. Inhibition studies using galactosamine or N-acetylgalactosamine showed that these monosaccharides are not recognized by XL35, suggesting that either a 2' amino or N-acetyl functionality is inhibitory or that a 2' hydroxyl is required for binding.

Although XL35 appears to tolerate sulfation at the 6' position, sulfation does not appear to enhance the affinity of XL35 for galactosides. Monosaccharides that are sulfated at other positions (4'-OH) or phosphorylated at the 6' position are not good ligands, suggesting that the ability to tolerate sulfate at selected positions is specific for that particular modification and does not represent a simple charge-charge interaction between XL35 and acidic glycans. XL35's ability to bind properly sulfated glycans is relevant because many mucins have been shown to contain sulfate esters on their glycans, and recent studies[150] have identified 6 sulfated glycans in the *Xenopus* JCP. Despite the microheterogeneity that typifies glycosylation, the sulfation observed on the JCP glycans showed a much more restricted pattern, since sulfate esters were only found on either the 3' or 6' positions of galactose and N-acetylglucosamine.

The broad selectivity of XL35 is uncommon among lectins, but has been previously seen in the "pattern recognition" lectins such as MBP that function in innate immunity and are required to recognize a wide variety of potential ligands. Within the context of fertilization, recent studies by Guerardel et al.[150] on the JCP of *Xenopus* eggs provide a biological requirement for XL35's ability to function as a pattern-

recognition lectin for a wide variety of oligosaccharides terminated in galactose as opposed to recognizing a very limited set of glycans. The oligosaccharide structures from six individual *Xenopii* were determined and several of the specimens were found to lack oligosaccharides terminated with an α-galactose moiety[150]. Since α-galactose had long been considered the putative ligand for XL35, the authors expected to find fewer viable embryos from those specimens lacking terminal α-galactosides because it was presumed that the formation of the fertilization layer would be impaired. Despite the apparent lack of α-galactose-terminated oligosaccharides, no significant biological effect was found: approximately 90% of oocytes could be fertilized regardless of the quantity of α-galactosides found in their jellycoat. All of the fertilized eggs showed normal development. The presence of oligosaccharides terminated in β-galactose in the JCP from frogs lacking terminal α-galactose was apparently sufficient to permit the formation of the fertilization layer between XL35 and the JCP. Since the experiments in this dissertation have demonstrated that XL35 has the ability to recognize both α- and β-anomers of galactose, it is possible to reconcile the results of earlier studies that suggested that XL35 only recognizes α-galactose with the more recent results that demonstrate that the lack of α-galacose-terminated oligosaccharides has no effect on the formation of the fertilization layer.

Experiments presented here also demonstrate that the broad selectivity observed for monovalent ligands is also observed when those ligands are presented in a multivalent fashion on the glycopolymers. This result is particularly striking because previous reports demonstrated that while glucose and mannose could be recognized by Concanavalin A with approximately equal affinity, when those ligands were presented in a multivalent fashion, a clear preference for mannose-containing polymers emerged. Small differences in affinity between the two ligands that could not be observed when

the ligands were presented monovalently were magnified by making the ligands multivalent. By contrast to results obtained using Concanavilin A, the lack of discrimination that XL35 exhibits for both mono- and multivalent ligands suggests that XL35 recognizes a wide variety of galactose-containing glycans with only minimal differences in affinity.

Affinity

A fundamental question raised at the outset of this study is how a protein that binds to monovalent oligosaccharides with millimolar dissociation constants can mediate the formation of a permanent protective layer around the fertilized egg. Using SPR surface competition experiments, the K_D for XL35 and melibiose is estimated to be approximately 2-5 mM. Given the weakness of the interaction, the kinetic constants were too rapid to determine by SPR but the SPR profiles of ligand-binding proved very diagnostic and were capable of indicating whether the interaction between XL35 and a given ligand was mono- or multivalent.

Initial attempts to define the role of multivalency in the strength of the interaction between XL35 and its ligand employed a set of defined glycoclusters or dendrimers containing synthetic sugars previously tested as monovalent ligands. When conjugated to the core molecules for the clusters or dendrimers, these sugars were now presented multivalently, although on relatively small molecules. Inhibition results using one of the trimeric glycoclusters showed only a minimal enhancement in affinity. After correcting the IC_{50} value for valency, these glycoclusters did not appear to be capable of spanning multiple binding sites on XL35 since the valence-corrected IC_{50} was no better than the corresponding monovalent data. Although there are some examples[187-190] of low-molecular weight glycoclusters that function as efficient inhibitors of lectin binding, most are only slightly better than their monovalent counterparts when the data are corrected for valency[191, 192]. To confirm that these low molecular-weight inhibitors were only

interacting with individual binding sites on XL35, SPR was employed. The kinetics of the profiles generated using the glycoclusters (Figure 3-19) were identical to the kinetics observed for monovalent glycans (Figure 3-18). Both ELISA data and SPR profiles indicated that these low-molecular weight compounds were incapable of spanning multiple binding sites on XL35 and were, therefore, no more efficient than a monovalent oligosaccharide.

Although the equilibrium inhibition results using the glycoclusters showed no enhancement of binding affinity as compared to their monovalent counterparts, they suggest that XL35 must exhibit a relatively slow association constant, which also explains the absence of mass transport-limited behavior in subsequent SPR experiments. If the association constant for XL35 had approached that of P-selectin ($k_{on}=10^6$ $M^{-1}s^{-1}$), one would have expected the glycoclusters to function as more efficient inhibitors than the corresponding monovalent compounds. After a glycocluster was bound by XL35, rather than simply diffusing away from the XL35 binding site, the glycoclusters would have had an enhanced probability of being re-bound by XL35 by one of their free arms. *In vivo*, however, were XL35 to demonstrate such a rapid k_{on}, it might have a deleterious effect on the formation of the fertilization layer. It would be expected that a lectin with a rapid k_{on} would exhibit mass-transport limited behavior and would tend to cross-link regions immediately adjacent to the point of exocytosis rather than forming a complete layer around the fertilized egg which is necessary for the viability of the developing embryo.

Unlike the smaller ligands, the glycopolymers do show IC_{50} values that are ten- to twenty-fold better than their monovalent counterparts even when the data are normalized to take into account the valency of the polymer. If the data are reported based on the molar quantity of glycopolymer (not valence-corrected), the enhancement is roughly 800-fold. Assaying highly multivalent systems for ligand binding activity can be

difficult and although there are reports[193] of multivalent ligands demonstrating greater efficacy, many of these previous results have been shown to be highly assay-dependent[194]. Gratifyingly, the results presented in this dissertation, which were obtained using different ligand-binding assays, correlate very well with one another, suggesting that the results represent a specific biological interaction rather than an entropically driven aggregation event. The physical basis for the more potent IC_{50} values observed using the glycopolymers suggested that the glycopolymers were capable of interacting with multiple binding sites on XL35, and SPR sensorgrams confirmed this to be the case (Figure 3-19).

In principle, the highly stable complex between XL35 and multivalent ligands could suggest the formation of a irreversible complex that would account for the extremely slow dissociation profiles. Several control experiments using SPR were conducted that employed an identical concentration of glycopolymer injected for 1, 3, or 20 minutes. The dissociation profiles were analyzed as a function of the different association times to determine whether XL35 forms a irreversible complex with its multivalent ligand. The minimal change observed in the apparent dissociation constant even when the association time was extended significantly argues against the formation of a irreversible complex. Additionally, the ability to abrogate binding with EDTA alone indicated that the interaction was reversible.

Although the dissociation profile of XL35 and the glycopolymers did not show the dramatic changes that might suggest the formation of a irreversible complex, there were subtle quantitative changes in the dissociation profile that provided clues into the stability of the fertilization layer and the mechanics of its formation. As the contact time between XL35 and its ligands was increased, the apparent dissociation constant decreased, which had the effect of increasing the half-life of the complex and decreasing the amount of ligand that could dissociate through simple diffusion. This trend towards a more stable

complex as the association time was increased suggested that XL35 could sample different regions of its multivalent ligand during the binding process. Since the monovalent affinity was fairly weak, interactions that only involved 1-2 binding sites on XL35 could be broken easily through diffusion or by direct competition from the additional ligand flowing over the XL35 surface. With increasing contact times, the experimental conditions selected for a population of complexes that were tethered at multiple points and were therefore increasingly stable.

By ELISA, the valence-adjusted IC_{50} for the JCP obtained by compositional analysis is 11 μM, which is approximately 40-fold lower than the best value obtained using the synthetic glycopolymers. The 40-fold difference in apparent affinity is not sufficiently large to suggest that the glycopolymers do not approximate the JCP in terms of their efficacy but they also highlight the challenges inherent in inhibiting highly multivalent interactions. The most obvious difference in ligand binding between the glycopolymers and the JCP is observed in the dissociation profiles obtained using SPR. While the glycopolymers serve as reasonable mimics for XL35's mucin ligand in an equilibrium setting, the kinetic profiles do not approach those obtained for the native ligand. The XL35:glycopolymer complex is very stable, with only 27% of the bound glycopolymer dissociating from immobilized XL35 after 30 minutes of flow. By contrast, the XL35:JCP complex is so stable that the *dissociation is not measurable over an identical 30-minute period*.

The differences in potency can be rationalized because of the differences in size and ligand density between the JCP and the glycopolymers: the JCP mucin has an apparent molecular weight >2 MDa by size exclusion chromatography while the molecular weight of the glycopolymer is estimated at 156 kDa. Structurally, mucins are known to be arranged as tandem repeats of Ser/Thr-rich regions that are heavily glycosylated and are separated by short regions of peptide which often contain cysteines

and mediate intermolecular disulfide bonds. [153] Compared to the glycopolymer, the overall level of glycosylation is substantially higher on the mucin and the clustering of the glycans on the Ser/Thr-rich domains also provides a much higher ligand density. The combined effect of this larger size and increased ligand density substantially alters the kinetic profiles of the interaction as assessed by SPR.

The lack of dissociation observed using the JCP clearly demonstrates XL35's ability to form what is essentially a permanent layer of matrix based on an intrinsically weak protein-carbohydrate interaction. *In vivo*, XL35 diffuses through the extracellular matrix (ECM) before forming a very stable protective layer. The ability to form this layer is linked to its low monovalent affinity that permits it to sample several regions of the ECM before selecting a location that allows the maximum number of binding sites to be occupied. It is possible that a lectin containing fewer binding sites but capable of a very strong monovalent interaction could perhaps mimic the stability of the multivalent interaction between XL35 and the JCP, but it is likely that the resulting fertilization layer would contain gaps that would compromise its integrity as a barrier to polyspermy. It is the combination of low affinity and high avidity through multivalency that uniquely suits XL35 to perform its biological function.

The characteristics of the highly multivalent interaction between XL35 and its native ligand show that efficiently inhibiting multivalent binding events in an equilibrium setting presents a formidable challenge. The results presented here suggest that it may be more appropriate to attempt to inhibit interactions between multivalent partners that have a limited amount of time to interact before being cleared from the circulatory system. Within the context of fertilization, the weakness of XL35's monovalent interactions apparently gives it the ability to sample multiple regions within the jellycoat matrix and to create a complex that is very thermodynamically favorable and can completely envelop and protect the fertilized egg.

It is interesting to speculate whether the same characteristics that permit XL35 to efficiently form a permanent layer through the sum of many weak monovalent interactions could permit it to function as an efficient anti-microbial, given its localization to the epidermis in *Xenopus*. Amphibian skin has been recognized as a potent source of antimicrobial peptides,[128-132] and the most well-characterized family of peptides with antimicrobial activity are termed the magainins, whch are amphipathic structures that form pores in the cell walls of various pathogens[128, 133-136]. In addition to their localization to Xenopus epidermis, the magainins have also been found in a Paneth cell analogue in Xenopus small intestine, which provides additional support for their role in host defense[138]. It is noteworthy that both of the human homologues of XL35 were isolated from a human small intestine cDNA library and that subsequent to its identification, HL-2 has been localized to human Paneth cells whose function is defined as microbial surveillance. HL-1 has been identified in a range of epithelial cells in various organs, and its amino acid sequence similiarity to HL-2 and XL35 suggest that it may also function in innate immunity. The results presented in this dissertation demonstrate that the highly stable type of interaction observed between XL35 and multivalent ligands could function to inhibit bacterial or fungal infections, either through prophylaxis of the invading organism or through a series of binding and signaling events that target the organism for destruction. The localization of XL35 mRNA to a secretory organ involved in innate immunity as well as the tissue and cellular distribution observed for the human lectins offers intriguing new insights into potential functions for XL35 in addition to its previously documented role during fertilization.

REFERENCES

1. Van Den Hamer, C.J., A.G. Morell, I.H. Scheinberg, J. Hickman, and G. Ashwell, *Physical and chemical studies on ceruloplasmin. IX. The role of galactosyl residues in the clearance of ceruloplasmin from the circulation.* J Biol Chem, 1970. **245**: p. 4397-4402.
2. Morell, A.G., G. Gregoriadis, I.H. Scheinberg, J. Hickman, and G. Ashwell, *The role of sialic acid in determining the survival of glycoproteins in the circulation.* J Biol Chem, 1971. **246**: p. 1461-1467.
3. Ashwell, G. and J. Harford, *Carbohydrate-specific receptors of the liver.* Annu. Rev. Biochem., 1982. **51**: p. 531-554.
4. Morell, A.G., R.A. Irvine, I. Sternlieb, I.M. Schinberg, and G. Ashwell, *Physical and chemical studies on ceruloplasmin. V. Metabolic studies on sialic acid-free ceruloplasmin in vivo.* J Biol Chem, 1968. **243**: p. 155-159.
5. Hudgin, R.L., W.E.J. Pricer, G. Ashwell, R.J. Stockert, and A.G. Morell, *The isolation and properties of a rabbit liver binding protein specific for asialoglycoproteins.* J Biol Chem, 1974. **249**: p. 5536-5543.
6. Novogrodsky, A. and G. Ashwell, *Lymphocyte mitogenesis induced by a mammalian liver protein that specifically binds desialytated glycoproteins.* Proc Natl Acad Sci U S A, 1977. **74**: p. 676-678.
7. Cooper, D.N. and S.H. Barondes, *Evidence for export of a muscle lectin from cytosol to extracellular matrix and for a novel secretory mechanism.* J. Cell. Biol., 1990. **110**: p. 1681-1691.

8. Mehul, B. and R.C. Hughes, *Plasma membrane targetting, vesicular budding and release of galectin 3 from the cytoplasm of mammalian cells during secretion.* J. Cell. Sci., 1997. **110**: p. 1169-1178.

9. Cho, M. and R.D. Cummings, *Galectin-1, a b-galactoside-binding lectin in Chinese hamster ovary cells. II. Localization and biosynthesis.* J Biol Chem, 1995. **270**: p. 5207-5212.

10. Cleves, A.E., D.N. Cooper, S.H. Barondes, and R.B. Kelly, *A new pathway for protein export in Saccharomyces cerevisiae.* J. Cell. Biol., 1996. **133**: p. 1017-1026.

11. Kuchler, K. and J. Thorner, *Secretion of peptides and proteins lacking hydrophobic signal sequences: The role of adenosine triphosphate-driven membrane translocators.* Endocr. Rev., 1992. **13**: p. 499-514.

12. Sato, S., I. Burdett, and R.C. Hughes, *Secretion of the baby hamster kidney 30-kDa galactose-binding lectin from polarized and nonpolarized cells: A pathway independent of the endoplasmic reticulum-Golgi complex.* J. Exp. Cell. Res., 1993. **207**: p. 8-18.

13. Zhou, Q. and R.D. Cummings, *L-14 lectin recognition of laminin and its promotion of in vitro cell adhesion.* Arch Biochem Biophys, 1993. **300**: p. 6-17.

14. Wagner-Hulsmann, C., N. Bachinski, B. Diehl-Seifert, B. Blumbach, R. Steffen, Z. Pancer, and W.E. Muller, *A galectin links the aggregation factor to cells in the sponge (Geodia cydonium) system.* Glycobiology, 1996. **6**: p. 785-793.

15. Perillo, N.L., K.E. Pace, J.J. Seilhamer, and L.G. Baum, *Apoptosis of T cells mediated by galectin-1.* Nature, 1995. **378**: p. 736-739.

16. Perillo, N.L., C.H. Uittenbogaart, J.T. Nguyen, and L.G. Baum, *Galectin-1, an endogenous lectin produced by thymic epithelial cells, induces apoptosis of human thymocytes.* J. Exp. Med., 1997. **185**: p. 1851-1858.

17. Hickman, S., L.J. Shapiro, and E.F. Neufeld, *A recognition marker required for uptake of a lysosomal enzyme by cultured fibroblasts.* Biochem. Biophys. Res. Commun., 1974. **57**: p. 55-61.

18. Leroy, J.G., M.W. Ho, M.C. MacBrinn, K. Zielke, J. Jacob, and J.S. OBrien, *I-cell disease: Biochemical studies.* Pediatr. Res., 1972. **6**: p. 752-757.

19. Glaser, J.H., K.J. Roozen, F.E. Brot, and W.S. Sly, *Multiple isoelectric and recognitions forms of human b-glucuronidase activity.* Arch Biochem Biophys, 1975. **166**: p. 526-542.

20. Sando, G.N. and E.F. Neufeld, *Recognition and receptor-mediated uptake of a lysosomal enzyme, a-1-iduronidase, by cultured human fibroblasts.* Cell, 1977. **12**: p. 619-627.

21. Sahagian, G.G., J. Distler, and G.W. Jourdian, *Characterization of a membrane-associated receptor from bovine liver that binds phosphomannosyl residues of bovine testicular b-galactosidase.* Proc Natl Acad Sci U S A, 1981. **78**: p. 4289-4293.

22. Varki, A. and S. Kornfield, *The spectrum of anionic oligosaccharides released by endo-b-N-acetylglucosaminidase H from glycoproteins. Structural studies and interactions with the phosphomannosyl receptor.* J Biol Chem, 1983. **258**: p. 2808-2818.

23. Hoflack, B. and S. Kornfield, *Purification and characterization of a cation-dependent mannose-6-phosphate receptor from murine P388D1 macrophages and bovine liver.* J Biol Chem, 1985. **260**: p. 12008-12014.

24. Kornfield, S., *Structure and function of the mannose-6-phosphate/insulin-like growth factor II receptors.* Annu. Rev. Biochem., 1992. **61**: p. 307-330.

25. Ludwig, T., R. Le Borgne, and B. Hoflack, *Roles for mannose-6-phosphate receptors in lysosomal enzyme sorting, IGF-II binding and clathrin-coat assembly.* Trends Cell Biol., 1995. **5**: p. 202-206.

26. Kornfield, S., *Lysosomal enzyme targeting.* Biochem. Soc. Trans., 1990. **18**: p. 367-374.

27. Kornfield, S. and I. Mellman, *The biogenesis of lysosomes.* Annu. Rev. Cell Biol., 1989. **5**: p. 483-525.

28. Kornfield, S., *Trafficking of lysosomal enzymes.* FASEB J., 1987. **1**: p. 462-468.

29. Dahms, N.M., P. Lobel, and S. Kornfield, *Mannose-6-phospate receptors and lysosomal enzyme targeting.* J Biol Chem, 1989. **264**: p. 12115-12118.

30. von Figura, K. and A. Hasilik, *Lysosomal enzymes and their receptors.* Annu. Rev. Biochem., 1986. **55**: p. 167-193.

31. Traub, L.M. and S. Kornfield, *The trans-Golgi network: A late secretory sorting station.* Curr. Opin. Cell Biol., 1997. **9**: p. 527-533.

32. Chao, H.H.-J., A. Waheed, R. Pohlmann, A. Hille, and K. von Figura, *Mannose 6-phosphate receptor dependent secretion of lysosomal enzymes.* EMBO J., 1990. **9**: p. 3507-3513.

33. Munier-Lehmann, H., F. Mauxion, U. Bauer, P. Lobel, and B. Hoflack, *Re-expression of the mannose 6-phosphate receptors in receptor-deficient fibroblasts-Complementary function of the two mannose 6-phosphate receptors in lysosomal enzyme targeting.* J Biol Chem, 1996. **271**: p. 15166-15174.

34. Kasper, D., F. Dittmer, K. von Figura, and R. Pohlmann, *Neither type of mannose 6-phosphate receptor is sufficient for targeting of lysosomal enzymes along intracellular routes.* J. Cell. Biol., 1996. **134**: p. 615-623.

35. Pohlmann, R., M.W.C. Boeker, and K. von Figura, *The two mannose 6-phosphate receptors transport distinct complements of lysosomal proteins.* J Biol Chem, 1995. **270**: p. 27311-27318.

36. Collins, B.E., M. Kiso, A. Hasegawa, M.B. Tropak, J.C. Roder, P.R. Crocker, and R.L. Schnaar, *Binding specificities of the sialoadhesin family of I-type lectins. Sialic acid linkage and substructure requirements for binding of myelin-associated glycoprotein, Schwann cell myelin protein, and sialoadhesin.* J Biol Chem, 1997. **272**: p. 16889-16895.

37. Crocker, P.R., S. Kelm, C. Dubois, B. Martin, A.S. McWilliam, D.M. Shotton, J.C. Paulson, and S. Gordon, *Purification and properties of sialoadhesin, a sialic acid-binding receptor of murine tissue macrophages.* EMBO J., 1991. **10**: p. 1661-1669.

38. Crocker, P.R., S. Mucklow, V. Bouckson, A.S. McWilliam, A.C. Willis, S. Gordon, G. Milon, S. Kelm, and P. Bradfield, *Sialoadhesin, a macrophage sialic acid binding receptor for haemopoietic cells with 17 immunoglobulin-like domains.* EMBO J., 1994. **13**: p. 4490-4503.

39. Crocker, P.R., S. Freeman, S. Gordon, and S. Kelm, *Sialoadhesin binds preferentially to cells of the granulocytic lineage.* J. Clin. Invest., 1995. **95**: p. 635-643.

40. Crocker, P.R., S. Kelm, A. Hartnell, S. Freeman, D. Nath, M. Vinson, and S. Mucklow, *Sialoadhesin and related cellular recognition molecules of the immunoglobulin superfamily.* Biochem Soc Trans, 1996. **24**: p. 150-156.

41. Crocker, P.R., A. Hartnell, J. Munday, and D. Nath, *the potential role of sialoadhesin as a macrophage recognition molecule in health and disease.* Glycoconj. J., 1997. **14**(601-609).

42. Kelm, S., R. Schauer, and P.R. Crocker, *The Sialoadhesins - A family of sialic acid-dependent cellular recognition molecules within the immunoglobulin superfamily.* Glyconj. J., 1996. **13**: p. 913-926.

43. Steiniger, B., P. Barth, B. Herbst, A. Hartnell, and P.R. Crocker, *The species-specific structure of microanatomical compartments in the human spleen: Strongly sialoadhesin-positive macrophages occur in the perifollicular zone, but not in the marginal zone.* Immunology, 1997. **92**: p. 307-316.

44. van den Berg, T.K., J.J. Breve, J.G. Damoiseaux, E.A. Dopp, S. Kelm, P.R. Crocker, C.D. Dijkstra, and G. Kraal, *Sialoadhesin on macrophages: Its identification as a lymphocyte adhesion molecule.* J. Exp. Med., 1992. **176**: p. 647-655.

45. Vinson, M., P.A. van der Merwe, S. Kelm, A. May, E.Y. Jones, and P.R. Crocker, *Characterization of the sialic acid-binding site in sialoadhesin by site-directed mutagenesis.* J Biol Chem, 1996. **271**(9267-9272).

46. Leprince, C., K.E. Draves, R.L. Geahlen, J.A. Ledbetter, and E.A. Clark, Proc Natl Acad Sci U S A, 1993. **90**: p. 3236-3240.

47. Schulte, R.J., M.A. Campbell, W.H. Fischer, and B.M. Sefton, *Tyrosine phosphorylation of CD22 during B cell activation.* Science, 1992. **258**: p. 1001-1004.

48. Campbell, M.A. and N.R. Klinman, *Phosphotyrosine-dependent association between CD22 and protein tyrosine phosphatase IC.* Eur J Immunol, 1995. **25**: p. 1573-1579.

49. Doody, G.M., L.B. Justement, C.C. Delibrias, R.J. Matthews, J. Lin, M.I. Thomas, and D.T. Fearon, *A role in B cell activation for CD22 and the protein tyrosine phosphatase SHP.* Science, 1995. **269**: p. 242-244.

50. Lankester, A.C., G.M. van Schijndel, and R.A. van Lier, *Hematopoietic cell phosphatase is recruited to CD22 following B cell antigen receptor ligation.* J Biol Chem, 1995. **270**: p. 20305-20308.

51. O'Keefe, T.L., G.T. Williams, S.L. Davies, and M.S. Neuberger, *Hyperresponsive B cells in CD22-deficient mice.* Science, 1996. **274**: p. 798-801.

52. Drickamer, K., *Two distinct classes of carbohydrate-recognition domains in animal lectins.* J Biol Chem, 1988. **263**: p. 9557-9560.

53. Drickamer, K., *Complete amino acid sequence of a membrane receptor for glycoproteins. Sequence of the chicken hepatic lectin.* J Biol Chem, 1981. **256**: p. 5827-5839.

54. Drickamer, K. and M.E. Taylor, *Biology of animal lectins.* Annu. Rev. Cell Biol., 1993. **9**: p. 237-264.

55. Komiya, T., Y. Tanigawa, and S. Hirohashi, *Cloning of the novel gene intelectin, which is expressed in intestinal paneth cells in mice.* Biochem. Biophys. Res. Commun., 1998. **251**: p. 759-762.

56. Lee, J.-K., J. Schnee, M. Pang, M. Wolfert, L.G. Baum, K.W. Moremen, and M. Pierce, *Human homologs of the Xenopus oocyte cortical granule lectin XL35.* Glycobiology, 2001. **11**(1): p. 65-73.

57. Drickamer, K., *Ca^{2+}-dependent carbohydrate-recognitions domains in animal proteins.* Curr. Opin. Struct. Biol., 1993. **3**: p. 393-400.

58. Drickamer, K., M.S. Dordal, and L. Reynolds, *Mannose-binding proteins isolated from rat liver contain carbohydrate-recognition domains linked to collagenous tails.* J. Biol. Chem., 1986. **261**: p. 6878-6887.

59. Kawai, T., Y. Suzuki, S. Eda, K. Ohtani, T. Kase, Y. Fujinaga, T. Sakamoto, T. Kurimura, and N. Wakamiya, *Cloning and characterization of a cDNA encoding bovine mannan-binding protein.* Gene, 1997. **186**: p. 161-165.

60. Kawai, T., Y. Suzuki, S. Eda, K. Ohtani, T. Kase, T. Sakamoto, H. Uemura, and N. Wakamiya, *Molecular and biological characterization of rabbit mannan-binding protein.* Glycobiology, 1998. **8**: p. 237-244.

61. Laursen, S.B., T.S. Dalgaard, S. Thiel, B.L. Lim, T.V. Jensen, H.R. Juul-Madsen, A. Takahashi, T. Hamana, M. Kawakami, and J.C. Jensenius, *Cloning and sequencing of a cDNA encoding chicken mannan-binding lectin (MBL) and comparison with mammalian analogues.* Immunology, 1998. **93**: p. 421-430.

62. Mogues, T., T. Ota, A.I. Tauber, and K.N. Sastry, *Characterization of two mannose-binding protein cDNAs from rhesus monkey (Macaca mulatta): structure and evolutionary implications.* Glycobiology, 1996. **6**: p. 543-550.

63. Sastry, K., G.A. Herman, L. Day, E. Deignan, G. Bruns, C.C. Morton, and R.A. Ezekowitz, *The human mannose-binding protein gene. Exon structure reveals its evolutionary relationship to a human pulmonary surfactant gene and localization to chromosome 10.* J. Exp. Med., 1989. **170**: p. 1175-1189.

64. Sastry, K., K. Zahedi, J.M. Lelias, A.S. Whitehead, and R.A. Ezekowitz, *Molecular characterization of the mouse mannose-binding proteins. The mannose-binding protein A but not C is an acute phase reactant.* J. Immunol., 1991. **147**: p. 692-697.

65. Taylor, M.E., P.M. Brickell, R.K. Craig, and J.A. Summerfield, *Structure and evolutionary origin of the gene encoding a human serum mannose-binding protein.* Biochem. J., 1989. **262**: p. 763-771.

66. Ikeda, K., T. Sannoh, N. Kawasaki, T. Kawasaki, and I. Yamashima, J. Biol. Chem., 1987. **262**: p. 7451-7554.

67. Lu, J., S. Thiel, H. Wiedemann, R. Timpl, and K.B.M. Reid, J. Immunol., 1990. **144**: p. 2287-2294.

68. Ohta, M., M. Okada, I. Yamashima, and T. Kawasaki, J. Biol. Chem., 1990. **265**: p. 1980-1984.

69. Tenner, A., S. Robinson, and R.A. Ezekowitz, *Mannose binding protein (MBP) enhances mononuclear phagocyte function via a receptor that contains the 126,000 M(r) component of the C1q receptor.* Immunity, 1995. **3**: p. 485-493.

70. Kuhlman, M., K. Joiner, and R.A. Ezekowitz, *The human mannose-binding protein functions as an opsonin.* J. Exp. Med., 1989. **169**: p. 1733-1745.

71. Turner, M.W. and R.M.J. Hamvas, *Mannose-binding lectin: structure, function, genetics and disease associations.* Rev Immunogenetics, 2000. **2**: p. 305-322.

72. Drickamer, K., Nature, 1992. **360**: p. 183-186.

73. Weis, W.I., K. Drickamer, and W.A. Hendrickson, *Structure of a C-type mannose-binding protein complexed with an oligosaccharide.* Nature, 1992. **360**(12): p. 127-134.

74. Sheriff, S., C.Y.Y. Chang, and R.A.B. Ezekowitz, *Human mannose-binding protein carbohydrate recognition domain trimerizes through a triple α-helical coiled-coil.* Struct. Biol., 1994. **1**(11): p. 789-793.

75. Schweinle, J.E., M. Nishiyasu, T.Q. Ding, K. Sastry, S.D. Gillies, and R.A.B. Ezekowitz, *Truncated forms of mannose-binding protein multimerize and bind to mannose-rich Salmonella montevideo but fail to activate complement in vitro.* J. Biol. Chem., 1993. **268**(1): p. 364-370.

76. Wallis, R. and K. Drickamer, *Molecular determinants of oligomer formation and complement fixation in mannose-binding proteins.* J. Biol. Chem., 1999. **274**(6): p. 3580-3589.

77. Weis, W.I., R. Kahn, R. Fourme, K. Drickamer, and W.A. Hendrickson, *Structure of the calcium-dependent lectin domain from a rat mannose-binding protein determined by MAD phasing.* Science, 1991. **254**: p. 1608-1615.

78. Mullin, N.P., K.T. Hall, and M.E. Taylor, J. Biol. Chem., 1994. **269**: p. 28405-28413.

79. Ewart, K.V., D.S.C. Yang, V.S. Ananthanarayanan, G.L. Fletcher, and C.L. Hew, J. Biol. Chem., 1996. **271**: p. 16627-16632.

80. Anostario, M.J. and K.-S. Huang, J. Biol. Chem., 1995. **270**: p. 8138-8144.

81. Geng, J.-G., K.L. Moore, A.E. Johnson, and R.P. McEver, J. Biol. Chem., 1991. **266**: p. 22313-22318.

82. Andersen, T.T., J.W. Freytag, and R.L. Hill, J. Biol. Chem., 1982. **257**: p. 8036-8041.

83. Loeb, J.A. and K. Drickamer, J. Biol. Chem., 1988. **263**: p. 9752-9760.

84. Haagsman, H.P., T. Sargeant, P.V. Hauschka, B.J. Benson, and S. Hawgood, Biochemistry, 1990. **29**: p. 8894-8900.

85. Weis, W.I., G.W. Crichlow, H.M.K. Murthy, W.A. Hendrickson, and K. Drickamer, J. Biol. Chem., 1991. **266**: p. 20678-20686.

86. Ng, K.-S., S. Park-Snyder, and W.I. Weis, *Ca^{2+}-Dependent structural changes in C-type mannose-binding proteins.* Biochemistry, 1998. **37**: p. 17965-17976.

87. Bourne, Y., P. Rougé, and C. Cambillau, J. Biol. Chem., 1990. **265**: p. 18161-65.

88. Weis, W.I. and K. Drickamer, *Structural basis of lectin-carbohydrate recognition.* Annu. Rev. Biochem., 1996. **65**: p. 441-473.

89. Rini, J.M., *Lectin Structure.* Annu. Rev. Biophys. Biomol. Struct., 1995. **24**: p. 551-77.

90. Iobst, S.T. and K. Drickamer, *Binding of sugar ligands to Ca^{2+}-dependent animal lectins II. Generation of high-affinity galactose binding by site-directed mutagenesis.* J Biol Chem, 1994. **269**(22): p. 15512-15519.

91. Iobst, S.T., M.R. Wormald, W.I. Weis, R.A. Dwek, and K. Drickamer, J Biol Chem, 1994. **269**(22): p. 15505-15511.

92. Kolatkar, A.R. and W.I. Weis, *Structural basis of galactose recognition by C-type animal lectins.* J Biol Chem, 1996. **271**(12): p. 6679-6685.

93. Kozutsumi, Y., T. Kawasaki, and I. Yamashima, Biochem. Biophys. Res. Commun., 1980. **95**: p. 658-664.

94. Chang, C.Y.Y., K. Sastry, S.D. Gillies, R.A. Ezekowitz, and S. Sheriff, *Crystallization and preliminary X-ray analysis of a trimeric form of human mannose binding protein.* Crystallization Notes, 1994: p. 125-127.

95. Sumiya, M., M. Super, P. Tabona, R.J. Levinsky, T. Arai, M.W. Turner, and J.A. Summerfield, *Molecular basis of the opsonic defect in immunodeficient children.* Lancet, 1991. **337**: p. 1569-1570.

96. Super, M., J. Lu, S. Thiel, R.J. Levinsky, and M.W. Turner, *Association of low levels of mannan-binding protein with a common defect of opsonisation.* Lancet, 1989. **2**: p. 1236-1239.

97. Miller, M.E., J. Seals, R. Kaye, and L.C. Levitsky, Lancet, 1968. **ii**: p. 60-63.

98. Soothill, J.F. and B.A.M. Harvey, Arch. Dis. Child, 1976. **51**: p. 91-99.

99. Candy, D.C.A., V.F. Larcher, J.H. Tripp, J.T. Harries, B.A.M. Harvey, and J.F. Soothill, Arch. Dis. Child, 1980. **55**: p. 189-193.

100. Richardson, V.F., V.F. Larcher, and J.F. Price, Arch. Dis. Child, 1983. **58**: p. 799-802.

101. Lipscombe, R.J., D.W. Beatty, M. Ganczakowski, E.A. Goddard, T. Jenkins, Y.L. Lau, A.B. Spurdle, M. Sumiya, J.A. Summerfield, and M.W. Turner, *High frequencies in African and non-African populations of independent mutations in the mannose-binding protein gene.* Hum. Mol. Gen., 1992. **1**: p. 709-715.

102. Madsen, H.O., P. Garred, J.A. Kurtzhals, L.U. Lamm, L.P. Ryder, S. Thiel, and A. Svejgaard, *A new frequent allele is the missing link in the structural*

polymorphism of the human mannan-binding protein. Immunogenetics, 1994. **40**: p. 37-44.

103. Garred, P., S. Thiel, H.O. Madsen, L.P. Ryder, J.C. Jensenius, and A. Svejgaard, *Gene frequency and partial protein characterization of an allelic variant of mannan binding protein associated with low serum concentrations.* Clin. Exp. Immunol., 1992. **90**: p. 517-520.
104. Heise, C.T., J.R. Nichols, C.E. Leamy, and R. Wallis, *Impaired secretion of rat mannose-binding protein resulting from mutations in the collagen-like domain.* J. Immunol., 2000. **165**: p. 1403-1409.
105. Wallis, R. and J.Y.T. Cheng, *Molecular defects in variant forms of mannose-binding protein associated with immunodeficiency.* J. Immunol., 1999. **163**: p. 4953-4958.
106. Super, M., S.D. Gillies, S. Foley, K. Sastry, J.E. Schweinle, V.J. Silverman, and R.A. Ezekowitz, *Distinct and overlapping functions of allelic forms of human mannose-binding protein.* Nature Genet., 1992. **2**: p. 50-55.
107. Kurata, H., H.M. Cheng, Y. Kozutsumi, Y. Yokota, and T. Kawasaki, *Role of the collagen-like domain of the human serum mannan-binding protein in the activation of complement and the secretion of this lectin.* Biochem. Biophys. Res. Commun., 1993. **191**: p. 1204-1210.
108. Lipscombe, R.J., Y.L. Lau, R.J. Levinsky, M. Sumiya, J.A. Summerfield, and M.W. Turner, Immunol. Lett., 1992. **32**: p. 253-258.
109. Matsushita, M. and T. Fujita, J. Exp. Med., 1992. **176**: p. 1497-1502.
110. Busa, W.B. and R. Nuccitelli, *An elevated free cytosolic calcium wave follows fertilization in the eggs of the frog Xenopus laevis.* J. Cell. Biol., 1985. **100**: p. 1325-1329.

111. Vacquier, V.D. and J.E. Payne, *Methods for quantitating sea urchin sperm in egg binding.* Exp. Cell Res., 1973. **82**: p. 227-235.

112. Wyrick, R.E., T. Nishihara, and J.L. Hedrick, *Agglutination of jelly coat and cortical granule components and the block to polyspermy in the amphibian Xenopus laevis.* Proc Natl Acad Sci U S A, 1974. **71**(5): p. 2067-71.

113. Greve, L.C. and J.L. Hedrick, *Immunocytochemical Localization of Cortical Granule Lectin in Fertilized and Unfertilized Eggs of Xenopus-Laevis.* Gamete Research, 1978. **1**(1): p. 13-18.

114. Nishihara, T. and J.L. Hedrick, *A molecular mechanism for envelope elevation at fertilization.* Fed. Proc., 1977. **36**: p. 811-814.

115. Nishihara, T., R.E. Wyrick, P.K. Working, Y.H. Chen, and J.L. Hedrick, *Isolation and characterization of a lectin from the cortical granules of Xenopus laevis eggs.* Biochemistry, 1986. **25**(20): p. 6013-20.

116. Prody, G.A., L.C. Greve, and J.L. Hedrick, J Exp Zool, 1985. **235**: p. 335-340.

117. Greve, L.C., G.A. Prody, and J.L. Hedrick, Gemete Res, 1985. **12**: p. 305-312.

118. Lindsay, L.L. and J.L. Hedrick, Dev Biol, 1989. **135**: p. 202-211.

119. Roberson, M.M. and S.H. Barondes, *Lectin from embryos and oocytes of Xenopus laevis. Purification and properties.* J Biol Chem, 1982. **257**(13): p. 7520-4.

120. Chamow, S.M. and J.L. Hedrick, *Subunit structure of a cortical granule lectin involved in the block to polyspermy in Xenopus laevis eggs.* FEBS Lett, 1986. **206**(2): p. 353-7.

121. Roberson, M.M. and S.H. Barondes, *Xenopus-Laevis Lectin Is Localized at Several Sites in Xenopus Oocytes, Eggs, and Embryos.* Journal of Cell Biology, 1983. **97**(6): p. 1875-1881.

122. Outenreath, R.L., M.M. Roberson, and S.H. Barondes, *Endogenous lectin secretion into the extracellular matrix of early embryos of Xenopus laevis.* Dev Biol, 1988. **125**(1): p. 187-94.

123. Lee, J.-K., P. Buckhaults, C. Wilkes, M. Teilhet, M.L. King, K.W. Moremen, and M. Pierce, *Cloning and expression of a Xenopus laevis oocyte lectin and characterization of its mRNA levels during early development.* Glycobiology, 1997. **7**(3): p. 367-372.

124. Austin, C.R., *Fertilization*. 1965, Englewood Cliffs, New Jersey: Prentice-Hall.

125. Chandler, D.E. and J. Heuser, *Membrane fusion during secretion: Cortical granule exocytosis in sea urchin eggs as studied by quick-freezing and freeze fracture.* J. Cell. Biol., 1979. **83**: p. 91-108.

126. Nomura, K., N. Nakajo, J. Hidari, H. Nomura, M. Murata, M. Suzuki, K. Yamana, and Y. Hirabayashi, *Occurence of a novel fucose-containing pentaglycosylceramide with blood-group-B active determinant in Xenopus blastula cells: its possible involvement in cell-cell adhesion.* Biochem. J., 1995. **306**: p. 821-827.

127. Gawantka, V., N. Pollet, H. Delius, M. Vingron, R. Pfister, R. Nitsch, C. Blumenstock, and C. Niehrs, *Gene expression screening in Xenopus identifes molecular pathways, predicts gene function and provides a global view of embryonic patterning.* Mech. Dev., 1998. **77**: p. 95-141.

128. Jacob, L. and M. Zasloff, *Potential therapeutic applications of magainins and other antimicrobial agents of animal origin.* Ciba Found Symp, 1994. **186**: p. 197-216; discussion 216-23.

129. Barra, D. and M. Simmaco, *Amphibian skin: a promising resource for antimicrobial peptides.* Trends Biotechnol, 1995. **13**(6): p. 205-9.

130. Kreil, G., *Antimicrobial peptides from amphibian skin: an overview.* Ciba Found Symp, 1994. **186**: p. 77-85; discussion 85-90.

131. Spencer, J.H., *Antimicrobial peptides of frog skin.* Adv Enzyme Regul, 1992. **32**: p. 117-29.

132. Soravia, E., G. Martini, and M. Zasloff, *Antimicrobial properties of peptides from Xenopus granular gland secretions.* FEBS Lett, 1988. **228**(2): p. 337-40.

133. Ali, M.F., A. Soto, F.C. Knoop, and J.M. Conlon, *Antimicrobial peptides isolated from skin secretions of the diploid frog, Xenopus tropicalis (Pipidae).* Biochim Biophys Acta, 2001. **1550**(1): p. 81-9.

134. Chopra, I., *The magainins: antimicrobial peptides with potential for topical application.* J Antimicrob Chemother, 1993. **32**(3): p. 351-3.

135. Zasloff, M., *Magainins, a class of antimicrobial peptides from Xenopus skin: isolation, characterization of two active forms, and partial cDNA sequence of a precursor.* Proc Natl Acad Sci U S A, 1987. **84**(15): p. 5449-53.

136. Zasloff, M., B. Martin, and H.C. Chen, *Antimicrobial activity of synthetic magainin peptides and several analogues.* Proc Natl Acad Sci U S A, 1988. **85**(3): p. 910-3.

137. Moore, K.S., C.L. Bevins, N. Tomassini, K.M. Huttner, K. Sadler, J.E. Moreira, J. Reynolds, and M. Zasloff, *A novel peptide-producing cell in Xenopus: multinucleated gastric mucosal cell strikingly similar to the granular gland of the skin.* J Histochem Cytochem, 1992. **40**(3): p. 367-78.

138. Reilly, D.S., N. Tomassini, C.L. Bevins, and M. Zasloff, *A Paneth cell analogue in Xenopus small intestine expresses antimicrobial peptide genes: conservation of an intestinal host-defense system.* J Histochem Cytochem, 1994. **42**(6): p. 697-704.

139. Moore, K.S., C.L. Bevins, M.M. Brasseur, N. Tomassini, K. Turner, H. Eck, and M. Zasloff, *Antimicrobial peptides in the stomach of Xenopus laevis.* J Biol Chem, 1991. **266**(29): p. 19851-7.

140. Reilly, D.S., N. Tomassini, and M. Zasloff, *Expression of magainin antimicrobial peptide genes in the developing granular glands of Xenopus skin and induction by thyroid hormone.* Dev Biol, 1994. **162**(1): p. 123-33.

141. Baum, L.G., M. Pierce, and J.-K. Lee. 2002.

142. Abou-Zeid, C., A. Voiland, G. Michel, and C. Cocito, *Structure of the wall polysaccharide isolated from a group of corynebacteria.* Eur J Biochem, 1982. **128**(2-3): p. 363-70.

143. Voiland, A. and G. Michel, *Structural studies of the cell wall polysaccharide of Nocardia asteroides R 399.* Can. J. Microbiol., 1985. **31**(11): p. 1011-1018.

144. Stewart-Savage, J. and R.D. Grey, *Fertilization of investment-free Xenopus eggs.* Exp. Cell Res., 1984. **154**: p. 639-642.

145. Hedrick, J.L. and T. Nishihara, *Structure and function of the extracellular matrix of anuran eggs.* J. Elect. Microsc. Tech., 1991. **17**: p. 319-335.

146. Epel, D., *The program of fertilization.* Sci. Am., 1977. **237**(5): p. 128-138.

147. Quill, T.A. and J.L. Hedrick, *Oviductal Localization of the Cortical Granule Lectin Ligand Involved in the Block to Polyspermy of Xenopus-Laevis.* Development Growth & Differentiation, 1994. **36**(6): p. 615-620.

148. Mozingo, N.M. and J.L. Hedrick, *Localization of cortical granule lectin ligand in Xenopus laevis egg jelly.* Develop. Growth Differ., 1996. **38**: p. 647-652.

149. Yurewicz, E.C., G. Oliphant, and J.L. Hedrick, *The macromolecular composition of Xenopus laevis egg jelly coat.* Biochemistry, 1975. **14**(14): p. 3101-3107.

150. Guerardel, Y., O. Kol, E. Maes, T. Lefebvre, B. Boilly, M. Davril, and G. Strecker, *O-glycan variability of egg-jelly mucins from Xenopus laevis: characterization of*

four phenotypes that differ by the terminal glycosylation of their mucins. Biochem. J., 2000. **352**: p. 449-463.

151. Yurewicz, E.C. and J.L. Hedrick, *Macromolecular Composition of Xenopus-Laevis Egg Jelly Coats.* Biology of Reproduction, 1973. **9**(1): p. 72-73.

152. Bonnell, B.S., D. Reinhart, and D.E. Chandler, *Xenopus laevis egg jelly coats consist of small diffusible proteins bound to a complex system of structurally stable networks composed of high-molecular-weight glycoconjugates.* Dev Biol, 1996. **174**: p. 32-42.

153. Perez-Vilar, J. and R.L. Hill, *The structure and assembly of secreted mucins.* J. Biol. Chem., 1999. **274**(45): p. 31751-31754.

154. Jentoft, N., Trends Biochem. Sci., 1991. **15**: p. 291-294.

155. Strecker, G., J.M. Wieruszeski, Y. Plancke, and B. Boilly, *Primary structure of 12 neutral oligosaccharide-alditols released from the jelly coats of the anuran Xenopus laevis by reductive beta- elimination.* Glycobiology, 1995. **5**(1): p. 137-46.

156. Tseng, K., L.L. Lindsay, S. Penn, J.L. Hedrick, and C.B. Lebrilla, *Characterization of Neutral Oligosaccharide-Alditols from Xenopus laevis Egg Jelly Coats by Matrix-Assisted Laser Desorption Fourier Transform Mass Spectrometry.* Anal. Biochem., 1997. **250**: p. 18-28.

157. Plancke, Y., J.M. Wieruszeski, C. Alonso, B. Boilly, and G. Strecker, *Structure of four acidic oligosaccharides from the jelly coat surrounding the eggs of Xenopus laevis.* Eur. J. Biochem., 1995. **231**(2): p. 434-9.

158. Ishihara, K., J. Hosona, H. Kanatani, and C. Katagiri, *Toad egg-jelly as a source of divalent cations essential for fertilization.* Dev. Biol., 1984. **105**: p. 435-442.

159. Watson, M.L., S.F. Kingsmore, G.I. Johnston, M.H. Siegelman, M.M. Le Beau, R.S. Lemons, N.S. Bora, T.A. Howard, L.L. Weissman, and R.P. McEver,

Genomic organization of the selectin family of leukocyte adhesion molecules on human and mouse chromosome 1. J. Exp. Med., 1990. **172**: p. 263-272.

160. Saha, S.K. and C.F. Brewer, Carbohydrate Research, 1994. **254**: p. 157-167.

161. Habel, J.E., J.F. Ohren, and G.E.O. Borgstahl, *Dynamic light-scattering analysis of full-length human RPA14/32 dimer: purification, crystallization and self-association.* Acta Crystallographica, 2001. **D57**: p. 254-259.

162. Nielsen, H., J. Engelbrecht, S. Brunak, and G.v. Heijne, *Identification of prokaryotic and eukaryotic signal peptides and prediction of their cleavage sites.* Protein Engineering, 1997. **10**: p. 1-6.

163. Lee, Y.C., *Biochemistry of carbohydrate-protein interactions.* FASEB J., 1992. **6**: p. 319-320.

164. Szabo, A., L. Stolz, and R. Granzow, *Surface plasmon resonance and its use in biomolecular interaction analysis (BIA).* Curr Opin Struct Biol, 1995. **5**(5): p. 699-705.

165. Garland, P.B., *Optical evanescent wave methods for the study of biomolecular interactions.* Q Rev Biophys, 1996. **29**(1): p. 91-117.

166. Malmqvist, M., *Surface plasmon resonance for detection and measurement of antibody-antigen affinity and kinetics.* Curr Opin Immunol, 1993. **5**(2): p. 282-6.

167. McDonnell, J.M., *Surface plasmon resonance: towards an understanding of the mechanisms of biological molecular recognition.* Curr Opin Chem Biol, 2001. **5**(5): p. 572-7.

168. Motulsky, H.J. and L.C. Mahan, Mol. Pharmacol., 1984. **25**: p. 1-9.

169. Arvan, P. and D. Castle, *Sorting and storage during secretory granule biogenesis: looking backward and looking forward.* Biochem J, 1998. **332**: p. 593-610.

170. Dannies, P.S., *Protein hormone storage in secretory granules: mechanisms for concentration and sorting.* Endocrine Rev, 1999. **20**(1): p. 3-21.

171. Aunis, D. and M.H. Metz-Boutigue, *Chromogranins: current concepts. Structural and functional aspects.* Adv Exp Med Biol, 2000. **482**: p. 21-38.

172. Fischer-Colbrie, R., A. Laslop, and R. Kirchmair, *Secretogranin II: molecular properties, regulation of biosynthesis and processing to the neuropeptide secretoneurin.* Prog Neurobiol, 1995. **46**(1): p. 49-70.

173. Huttner, W.B., H.H. Gerdes, and P. Rosa, *The granin (chromogranin/secretogranin) family.* Trends Biochem Sci, 1991. **16**(1): p. 27-30.

174. Huttner, W.B. and S. Natori, *Regulated secretion. Helper proteins for neuroendocrine secretion.* Curr Biol, 1995. **5**(3): p. 242-5.

175. Ozawa, H. and K. Takata, *The granin family--its role in sorting and secretory granule formation.* Cell Struct Funct, 1995. **20**(6): p. 415-20.

176. Park, H.Y., S.H. So, W.B. Lee, S.H. You, and S.H. Yoo, *Purification, pH-dependent conformational change, aggregation, and secretory granule membrane binding property of Secretogranin II (Chromogranin C).* Biochemistry, 2002. **41**: p. 1259-1266.

177. Farquhar, M.G., J.J. Reid, and L.W. Daniell, *Intracellular transport and packaging of prolactin: a quantitative electron microscope autoradiographic study of mammotrophs dissociated from rat pituitaries.* Endocrinology, 1978. **102**: p. 296-311.

178. Holmskov, U., S.B. Laursen, R. Malhotra, H. Wiedemann, R. Timpl, G.R. Stuart, I. Tornoe, P.S. Madsen, K.B.M. Reid, and J.C. Jensenius, *Comparative study of the structural and functional properties of a bovine plasma C-type lectin, collectin-43, with other collectins.* Biochem J, 1995. **305**: p. 889-896.

179. Nadimpalli, S.K., *Chemical modification studies on the glucose/mannose specific lectins from field and lablab beans.* Biochem Mol Biol Int, 1999. **47**(5): p. 825-34.

180. Chowdhury, S., H. Ahmed, and B.P. Chatterjee, *Chemical modification studies of Artocarpus lakoocha lectin artocarpin.* Biochimie, 1991. **73**(5): p. 563-71.

181. Patanjali, S.R., M.J. Swamy, V. Anantharam, M.I. Khan, and A. Surolia, *Chemical modification studies on Abrus agglutinin. Involvement of tryptophan residues in sugar binding.* Biochem J, 1984. **217**(3): p. 773-81.

182. Oda, Y., S. Ichida, S. Aonuma, and T. Shibahara, *Studies on chemical modification of Tulipa gesneriana lectin.* Chem Pharm Bull (Tokyo), 1989. **37**(8): p. 2170-3.

183. Basu, S., C. Mandal, and A.K. Allen, *Chemical-modification studies of a unique sialic acid-binding lectin from the snail Achatina fulica. Involvement of tryptophan and histidine residues in biological activity.* Biochem J, 1988. **254**(1): p. 195-202.

184. Maranville, E., A. Zhu, and S.K. Nadimpalli, *Assessment of amino-acid substitutions at tryptophan 16 in alpha-galactosidase.* Eur J Biochem, 2000. **267**(5): p. 1495-501.

185. Barman, T.E. and D.E. Koshland, J Biol Chem, 1967. **242**: p. 5771.

186. Sako, D., K.M. Comess, K.M. Barone, R.T. Camphausen, D.A. Cumming, and G.D. Shaw, *A sulfated peptide segment at the amino terminus of PSGL-1 is critical for P-selectin binding.* Cell, 1995. **83**(2): p. 323-331.

187. Kitov, P.I.S., J.M.; Mulvey, G.; Armstrong, G.D.; Ling, H.; Pannu, N.S.; Read, R.J.; Bundle, D.R., Nature, 2000. **403**(669-672).

188. Fan, E.Z., Z.; Minke, W.E.; Hou, Z.; Verlinde, C.L.M.J.; Hol, W.G.J., J. Am. Chem. Soc., 2000. **122**.

189. Biessen, E.A.L.N., F.; vanTeijlingen, M.E.; Kuiper, J.; BarretBergshoeff, M.; Bijsterbosch, M.K.; Rijken, D.C.; vanBerkel, T.J.C., J. Biol. Chem., 1996. **271**: p. 28024-28030.

190. Lee, Y.C. and R.T. Lee, Acc. Chem. Res., 1995. **28**: p. 321-327.

191. Mann, D.A. and L.L. Kiessling, *The Chemistry and Biology of Multivalent Saccharide Displays*, in *Glycochemistry*, P.G. Wang and C.R. Bertozzi, Editors. 2001. p. 221-275.

192. Burkhalter, N.F., S.M. Kimick, and E.J. Toone, *Protein-Carbohydrate Interactions: Fundamental Considerations*, in *Carbohydrates in Chemistry and Biology*, G.W.H.B. Ernst and P. Sinnay, Editors. 2000, Wiley-VCH. p. 865-914.

193. Signal, G.B., M. Mammen, G. Dahmann, and G.M. Whitesides, *Polyacrylamides bearing pendant a-sialoside groups strongly inhibit agglutination of erythrocytes by influenze virus: the strong inhibition reflects enhanced binding through cooperative polyvalent interactions.* J. Am. Chem. Soc., 1996. **118**(16): p. 3789-3800.

194. Corbell, J.B., J.J. Lundquist, and E.J. Toone, *A comparison of biological and calorimetric analyses of multivalent glycodendrimer ligands for concanavalin A.* Tetrahedron: *Assymetry*, 2000. **11**: p. 95-111.